NLRP3 protects the alveolar barrier by an inflammasome-independent increase of epithelial cell adherence

Inaugural-Dissertation

to obtain the academic degree

Doctor rerum naturalium (Dr. rer. nat.)

submitted to the Department of Biology, Chemistry and Pharmacy

of Freie Universität Berlin

by

Elena Ivaylova Kostadinova, Msc

Place of Birth: Sofia, Bulgaria

Berlin

2017

Time period: 01.11.2011 – 31.08.2016

Supervisor: Prof. Dr. Bastian Opitz

Institute: Medizinische Klinik m.S. Infektiologie und Pneumologie
Charitè-Universitätsmedizin, Berlin

1st Reviewer: Prof. Dr. Bastian Opitz
Medizinische Klinik m.S. Infektiologie und Pneumologie
Charitè-Universitätsmedizin, Berlin

2nd Reviewer: Prof. Dr. Rupert Mutzel
Institut für Biologie - Microbiologie
Freie Universität, Berlin

Date of defence: 19.06.2017

ACKNOWLEDGEMENTS

First of all, I want to express my gratitude to my supervisor Prof. Bastian Opitz for giving me the opportunity to work on this fascinating project in such a stimulating environment. Moreover, I am very grateful to Prof. Rupert Mutzel for accepting to be my second referee. I would also like to thank Prof. Martin Witzenrath and Dr. Birgitt Gutbier for all their support and valuable advice throughout this work and Prof. Norbert Suttorp for giving me the chance to perform my PhD in the Department of Infectious Diseases and Pulmonary Medicine.

Furthermore, I am thankful to the International Max Planck Research School for Infectious Diseases and Immunology as part of the ZIBI graduate school for funding me and enabling me to attend numerous lectures, seminars and international conferences. I also would like to thank the former and current coordinators Dr. Susanne Beetz, Dr. Martina Sick, Dr. Andreas Schmidt and Dr. Juliane Kofer, as well as my colleagues and friends from the ZIBI Graduate School.

I am particularly grateful to Dr. Catherine Chaput who always motivated me in the hard times and worked by my side no matter what. I also thank Dr. Juliane Lippmann who supported me with the final parts of my project and Dr. Thomas Korte for his technical assistance. Moreover, I would like to thank Prof. Dr. Leif Sander and Dr. Janine Zahlten for their readiness to help in every situation. I am also grateful to all the current and former members of the Opitz lab for being there for me and for providing a friendly atmosphere inside and outside the lab: Anne, Claudia, Jan, Juan, Laura, Oliver, Philip, Sandra, Uwe. Also, many special thanks to all current and alumni members of the DDDC, to my other colleagues from the Department of Infectious Diseases and Pulmonary Medicine and especially to my Matteo.

Finally, I would like to express my enormous gratitude to the most amazing family in the world, Glúmur and my awesome friends in Berlin and all over the world for their support and encouragement during the past years. Thank you for your endless love, trust and support. I am nothing without you and I owe it all to you.

Table of Contents

II - Results 40

III – Discussion 58

IV – Materials and Methods 76

I – Introduction

1. LUNG ALVEOLAR MEMBRANE MAINTENANCE

The human body is constantly exposed to microorganisms present in the surrounding environment. Very generally, the absolute first line of defense against external infectious and non-infectious agents is the structurally intact physical barrier of the body – the internal/external epithelial surfaces. Most of the time, these are extremely effective due to the plethora of mechanisms which ensure that most breaches are kept under control or eliminated[1]. Yet, depending on their positioning in the body and the type of threats encountered, the physical barriers are equipped with various defense mechanisms. The air-blood barrier created by the alveolar membrane is undoubtedly among the most vast and structurally complex surfaces.

The alveoli of the lung are a part of the respiratory airways which stem from the respiratory bronchioles. These bronchioles contain only a few alveoli integrated in their walls. Along these walls originate the alveolar ducts which in turn hold a great number of alveoli and alveolar sacs[2]. The internal alveolar surface is covered by two types of epithelial cells (type I and type II pneumocytes) which are developmentally related but have drastically distinct morphology and functions. The type I epithelial cells are terminally differentiated and extremely flat, covering about 95% of the alveolar area[3,4]. The organization of their cell organelles leaves vast areas of 'empty' cytosol which makes them permeable to atmospheric oxygen and bodily carbon dioxide. Type I cells originate from the differentiation of type II pneumocytes which in contrast have a cuboidal shape. Although they cover a very small area of the

alveoli, type II alveolar epithelial cells account for about 60% of the pneumocytes in the lung[5]. They have cuboidal shape as well as granulated cytoplasm and are able to produce large amounts of surfactant molecules (e.g. phopsholipids, cholesterol, and proteins such as SP-A, -B, -C, and –D)[6,7].

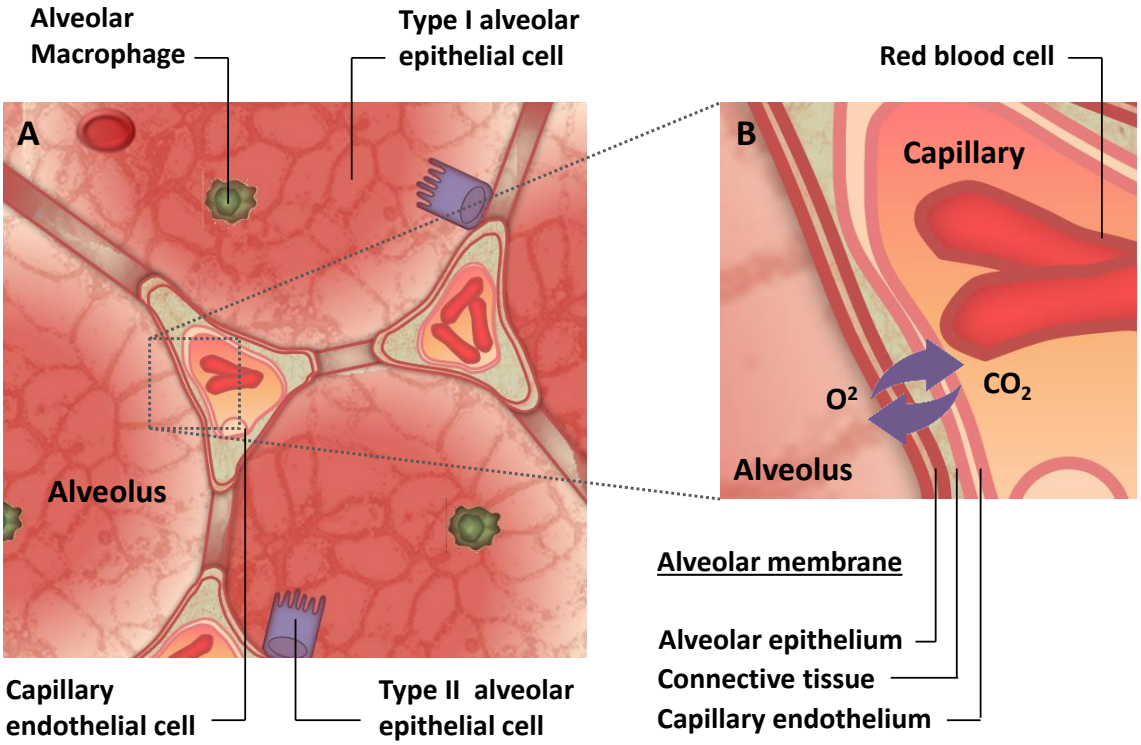

Figure 1: Structure of the alveolus and the alveolar membrane.

The alveolus (A) is the basic respiration unit of the lung. It is lined with type I and type II alveolar epithelial cells and hosts a population of resident alveolar macrophages. The basement membrane of the alveolar epithelium is in close proximity to that of the underlying capillary endothelium thus forming the endo-epithelial alveolar membrane (B). The alveolar membrane is extremely thin in order to allow the proper exchange of oxygen (O^2), carbon dioxide (CO_2) and other gases.

The lung alveoli are backed by an extensive network of capillaries which are in direct proximity to the lung epithelium. The non-fenestrated pulmonary endothelium is a continuous, highly differentiated monolayer with organization similar to that of simple squamous epithelium. The basolateral membranes of the endothelium and the epithelium are in very close proximity. In addition, other cell types such as alveolar macrophages, DCs and fibroblasts are also present in the alveoli[8].

With its area of 75 m^2 and thickness of as little as 0.2 μm this tissue barrier is the biggest surface of the body which is in direct contact with the environment[5]. Since gas exchange is extremely important for the organism's survival, there are a number of defense mechanisms in place which counteract external damaging stimuli. Yet, both infectious and tissue-damaging stimuli can induce inflammatory responses and lung injury.

2. PNEUMOCOCCAL PNEUMONIA

2.1. EPIDEMIOLOGY OF PNEUMONIA AND PNEUMOCOCCAL DISEASE

With records dating as far as medicine itself, bacterial pneumonia is among the oldest diagnosed diseases in human history[9]. The discovery of the causative agent of pneumococcal pneumonia happened in 1881 when Louis Pasteur in France and George Sternberg in the USA simultaneously identified the lancet-shaped bacterium *Streptococcus pneumoniae* in saliva[10]. Then, in 1884 in Berlin, the bacterium was also used by Hans Christian Gram for the establishment of the well-known Gram staining[11]. However, in spite of the long experience we have had with this bacterium and the associated disease, it still continues to be among the leading causes of mortality worldwide. The signature symptoms of pneumonia are a combination of chest pain, fever, trouble breathing and cough[12]. Whereas the most important causative agent of community-acquired bacterial pneumonia is *S. pneumoniae*, other bacterial species such as *Legionella pneumophila, Mycoplasma pneumoniae, Chlamydophila pneumoniae*, *Staphylococcus aureus,* and *Haemophilus influenzae* can also cause this type of infection[12]. Yet, the significance of *S. pneumoniae* infections worldwide is emphasized by the data that pneumococcal pneumonia is among the leading causes of mortality among children under the age of five[13,14]. According to the official data of the WHO for 2012, in low and middle income countries lower respiratory tract infections are in the top three causes of death for the population as a whole (WHO 2012). Moreover, in countries with high HIV-1 prevalence there has been an alarming increase in mortality of young adults related to pneumococcal bacteremia[15]. The risk is equally serious for the elderly and immunocompromised patients.

S. pneumoniae (often referred to as the pneumococcus) is a weakly infective, gram-positive bacterium transmitted via droplets which usually colonizes asymptomatically the upper respiratory tract of humans. However, if the bacterium gets access to the normally sterile lower airways, it can cause pneumonia as well as

otitis media, sepsis and meningitis[16–18]. The outcome of the disease depends on the health status of the individual and the particular serotype. The risk of developing a life-threatening pneumococcal pneumonia is strongly associated with preceding viral infection of the respiratory tract. During influenza outbreaks in particular, influenza virus becomes the principal cause of community-acquired pneumonia (CAP)[19–21]. In addition, respiratory syncytial virus, parainfluenza virus, coronavirus, rhinovirus, adenovirus among others are very often detected in patients with CAP. It is however unclear whether they were the main cause of disease or if they play a role only in the predisposition of the patients to secondary bacterial infections[22–24].

With at least 93 different serotypes, the pneumococcus is a very versatile pathogen[25]. The serotypes have variable propensity to cause disease – whereas serotypes 3, 6 and 19F are associated with high mortality but lower invasiveness, serotypes such as 1 and 7F are more common cause of invasive diseases[26]. The burden of *S.pneumoniae*-associated diseases is counteracted by antibiotic treatment and the introduction of vaccines. A cause for concern is that the global prevalence of antibiotic resistance is increasing. The greatest source of resistance is the pneumococcal colonization in children due to the higher chance of antibiotic use and the longer carriage[27–30]. In line with this, an international study of more than 2100 *S.pneumoniae* isolates from sterile body sites, it was observed that globally 33,3% were resistant to penicillin, 22.9% were resistant to erythromycin, and 16,2% tested resistant against both (with serotypes 19A, 6A, 19F, 14, 6B, 9V and 15A being more likely to be resistant to both)[31]. Interestingly, while the percentages reported for Germany are markedly lower, other nearby European countries such as France and Italy show significantly higher resistance rates. The pattern of susceptibility and geographic distribution varies among serotypes and is often due to antibiotic overuse or low vaccination rates in certain regions[27,30,32–34]. Currently, the existing vaccines are polysaccharide-based. The most commonly used in Germany is the one containing 23 serotypes (PPV23) which however is weakly immunogenic in children under the age of 2 due to their immature immune system. In order to increase immunogenity, vaccines containing capsular polysaccharide conjugated to diphtheria toxoid CRM_{197} were produced (PCVs). Those vaccines however cover a smaller number of serotypes (7, 10, or 13).

2.2. VIRULENCE FACTORS OF *S. PNEUMNIAE*

Studies focusing on genetic evidence suggest that there are two strategies responsible for the success of *S. pneumoniae* as a human pathogen[15,35]. On one hand, there are highly invasive strains which induce rapid disease progression and dissemination in the population. On the other hand, there are also clones defined by the ability to colonize and persist with a minor risk of tissue invasion. To ensure long carriage, the non-invasive phenotype relies on immune evasion strategies (surface adhesions, IgA1 protease) leading to low-level long-lasting transmission. It is highly possible that the differences in pathogenicity are due to variations in gene expression of specific virulence factors[36].

2.2.1. PLY (Pneumolysin)

One of the most important virulence factors of the pneumococcus is the cholesterol-dependent cytolysin (CDC) called pneumolysin (PLY). This is a 53-kD protein with about 20 variants and is present in most clinical isolates of *S.pneumoniae*[17,37]. Like other CDCs, PLY is produced during the log phage of bacterial growth[38]. Yet, what makes it unique is that it does not contain a signal secretion leader sequence and thus cannot be secreted via a standard type II secretion system. Instead, it has been suggested that PLY release is facilitated by the bacterial cell wall hydrolases LytA, LytC and the choline-binding prtein D (CbpD)[39,40]. However, toxin release has also been observed in the absence of autolysis, pointing to the presence of alternative mechanisms [38] .

Upon release in lytic concentrations, PLY is able to bind to cholesterol-rich membranes and forms micropores, which consequently increase in size and can reach up to 35 nm in diameter[41–45]. That kind of membrane damage often leads to the death of the host cells[46–52]. Yet, the response towards PLY is dependent on cell type, dose used and time point examined. Some cell types can also repair their membranes thus avoiding the cytolytic effect of the toxin. For instance it has been shown that after treatment with CDCs, murine macrophages are able to repair their membrane by

removing the damaged regions via endocytosis[53]. Sub-lytic concentrations of PLY are in addition able to activate many defense mechanisms from the innate immune system. For instance, it has been reported that PLY is able to activate the gene expression of chemokines and cytokines (e.g. IL-8, MIP-1β) but also of other proteins involve in inflammatory responses (Caspase-4. Caspase-6, cathepsin E, ICAM-1)[54].

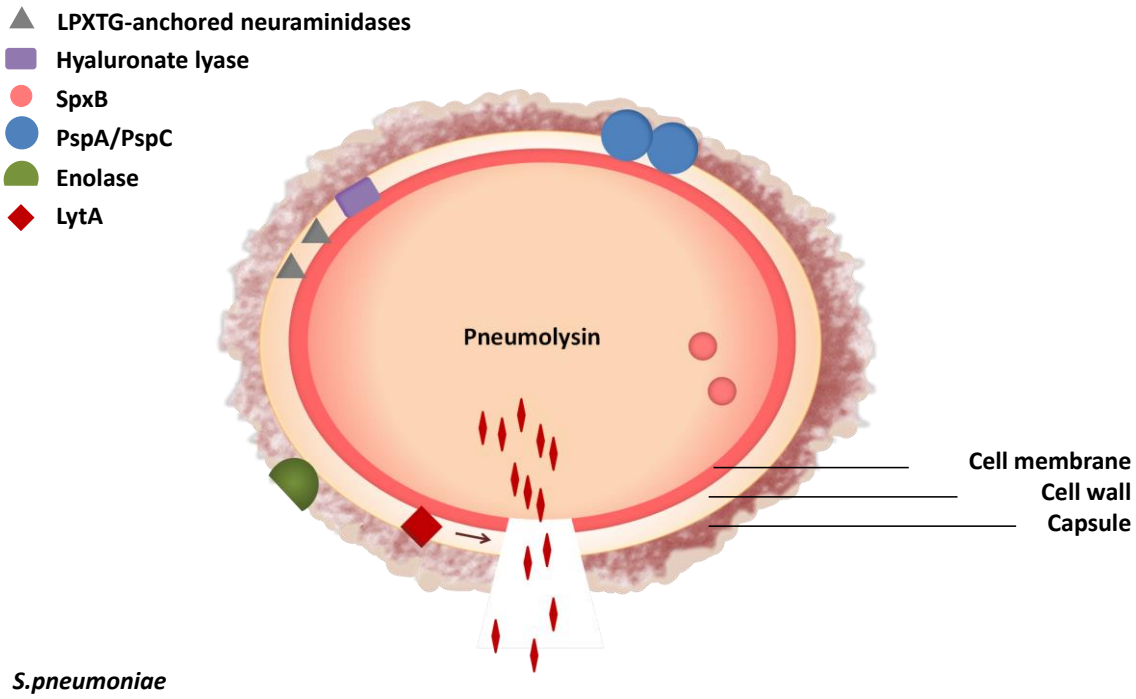

Figure 2: Virulence factors of *S. pneumoniae*

Important virulence factors of the pneumococcus are found in the cytoplasm (PLY, SpxB), the cell wall (neuraminidases, pneumococcal surface proteins (PspA/PspC), hydrolases (LytA) hyaluronate lyase) and the bacterial surface (capsule, enolase).

The role of pneumolysin in the pathogenesis of pneumococcal pneumonia has been highlighted in studies of murine lung infections[55–57]. In *in vivo* infection experiments, PLY-deficient bacteria were shown to have lower colonization capacity, and the infection resulted in increased clearance from the lung combined with significantly longer survival of the infected animals. Moreover, bacteremia was greatly reduced

when compared with WT infection[37,55]. These data point to the role of PLY in lung damage and bacterial invasiveness.

2.2.2. CAPSULE

Another major virulence factor of *S.pneumoniae* is the capsule. Actually, the separation into the vast number of serotypes is based on its reaction with specific antibodies and can be achieved through genetic recombination[58]. The capsule is composed of polysaccharides and is covalently attached to the peptidoglycan of the cell wall[59]. In general, all clinically relevant *S. pneumoniae* strains have a capsule. In contrast, the strains with attenuated virulence tend to be non-encapsulated[60]. The bacterium has been shown to regulate the production of capsular components depending on its needs. During invasion, the capsule envelops the bacterium and prevents its recognition by impairing opsonization whereas during colonization it is able to interfere with mucosciliary clearance[61].

2.2.3. OTHER VIRULENCE FACTORS

S. pneumoniae posseses additionally other virulence factors such as PspA, LPXTG-anchored neuraminiadases, enolase, hyaluronate lyase etc. They carry out different functions in the processes of host-complement interaction and of divalent cation transport in the bacterial cytoplasm[62,63]. In addition, the spxB-encoded pyruvate oxidase of the bacterium has been shown to play a part in pneumococcal infection[64,65]. It has been suggested that hydrogen peroxide produced by its action causes cell death and impairment of mucociliary clearance in vivo[66–69].

Altogether, *S.pneumoniae* is a pathogen that successfully colonizes the upper respiratory tract of the host. Through a range of virulence factors it is able to evade the host innate defense mechanisms and to cause bacterial pneumonia which could progress into life-threatening conditions such as ARDS.

2.3. ACUTE RESPIRATORY DISTRESS SYNDROME (ARDS)

Bacterial and viral pneumonias are the most common causes of the acute respiratory distress syndrome (ARDS). This condition is characterized by injury associated with widespread edema, alveolar permeability and inflammatory changes that are often accompanied or followed by aggressive fibrosis events[70–74]. Among other causes, the syndrome can also occur as a result of sepsis and trauma. Clinically, ARDS is characterized with improper gas exchange short after a known injury of the lung and without a concurrent heart failure[75]. ARDS is associated with mortality rate of 20-50%[76]. The condition is driven by exaggerated and locally unrestricted immune response. ARDS development can be divided into three overlapping phases – (1) an exudative phase, (2) a proliferative phase, and (3) a fibrotic phase[71–73,77]. There is additionally the danger of complications caused by nosocomial bacterial pneumonia or ventilation which further complicate the condition. One of the main and most dangerous symptoms in the exudative and proliferative phases is the damage of the alveolar membrane (diffuse injury of alveolar barrier)[76]. Thus, the identification of innate immune mechanisms which counteract alveolar barrier dysfunction during infections is of enormous importance.

3. THE INNATE IMMUNE SYSTEM

The innate immune system is an ancient and conserved network of defense mechanisms that protects the body against sterile and infectious cues. All anatomical barriers of the body (gut, skin, lung epithelium, etc.) rely on evolutionary conserved pattern recognition receptors (PRRs) that recognize the so-called pathogen-associated molecular patterns (PAMPs) or damage-associated molecular patterns (DAMPs)[78]. In turn, following detection these signals trigger acute inflammatory response which includes the production of pro-inflammatory cytokines, the recruitment of leukocytes and the subsequent activation of the adaptive immune response via antigen presenting cells (APCs)[79,80]. Virtually all cell types of the body with potential for exposure to microbial or danger molecules are equipped with a set of PRRs. In the case of pulmonary infections, it has been shown that resident alveolar macrophages (AMΦs) and dendritic cells (DCs) play an important defensive role. However, it has recently been suggested that lung epithelial and endothelial cells also contribute significantly to the response[81]. The chemokines and cytokines produced from the simultaneous activation of the PRRs on all those cell types work in concert to activate adjacent cells and to attract neutrophils, macrophages and DCs from the interstitial space and the circulation. The transmigration of cells from the vascular system is facilitated by dilation of the vessels as well as the upregulation of adhesion molecules on endothelial cells. The cells recruited to the site of infection then target the pathogen and use a number of potent effector mechanisms (phagocytosis, antimicrobial peptide production, ROS production, neutrophil extracellular traps, etc.) to eradicate it[80,82–84].

3.1. INTERACTIONS WITH THE MICROBIOTA

As a first line of the defense, the innate immune system is responsible for introducing the body to environmental signals while at the same assuring a proper response to the sensed signals [85,86]. The formation of the organism's immune system starts during early development. Even though these early events are still not clearly understood, it is known that metabolites as well as components of the mother immune system (e.g. cytokines and IgA) are transferred via the mother's milk [87,88]. These factors work together to imprint a proper immune response to commensals which would give the basis of both the local and the systemic responses. Thus, it is not surprising that variations of infant microbiota composition can cause stark differences in inflammatory responses at sites other than the gut throughout life [89].

3.2. PATTERN RECOGNITION RECEPTORS (PRRs)

The sensing of microbial and danger molecular patterns is achieved through germline-encoded PRRs[90]. Charles Janeway Jr. first described a model in which the innate immune system serves to not only distinguish self from non-self molecules but also to ensure the proper activation of the adaptive immune system[91]. In the recent years, the importance of pattern recognition for the host immune response has been widely studied and a number of PRR subfamilies with different specificities have been identified[92]. Depending on their structure, PRRs are divided into the Toll-like receptors (TLRs), the C-type lectins (CTLs), the retinoic acid-inducible gene (RIG)-I-like receptors (RLRs), the cytosolic DNA sensor and the nucleotide-binding oligomerization domain (NOD)-like receptors (NLRs). In addition, these families can be separated in to membrane-bound (e.g. TLRs, CTLs) and cytosolic receptors (e.g. NLRs, RLRs, DNA sensors, etc). Yet, independent from their localization and specificities to extracellular and cytoplasmic signals, PRR activation generally causes the induction of proinflammatory gene transcription and to the production of critical inflammatory mediators such as cytokines and interferons (IFNs). Moreover, PRR activation could also initiate cellular processes such as cytokine processing, autophagy and cell death[93–96]. The coordination of transcriptional and non-

transcriptional events downstream of PRR activation is carried out by a network of tightly controlled signal transduction pathways thus ensuring the proper response towards the detected thread[97].

3.2.1. TOLL-LIKE RECEPTORS (TLRs)

TLRs are the most extensively studied group of PRRs. They are type I transmembrane proteins with ectodomains whose interaction with PAMPs is mediated by their leucine-rich repeats (LLRs)[92]. In addition, TLRs possess a transmembrane domain and an intracellular Toll-interleukin 1 receptor (TIR) domain (required for downstream signaling)[92]. TLR stimulation induces the recruitment of the adaptor molecules MyD88 (myeloid differentiation primary response 88), TRIF (TIR-domain-containing adapter-inducing interferon-β), TRAM (TRIF related adaptor molecule), and TIRAP (TIR-containing adaptor protein)[98]. Depending on the differences in the intracellular domain of the TLRs, they are able to interact with particular adaptors in the network. For instance, the signaling adaptor MyD88 is able to interact with all TLRs (except for TLR3) leading to the activation of NFkB (nuclear factor κB) and mitogen-activated protein kinases (MAPK) that in turn initiate the production of proinflammatory cytokines. Alternatively, MyD88 can also work downstream of TLRs7, 8 and 9 causing the production of Type 1 IFNs via the interferon regulatory factor 7 (IRF7). In contrast to MyD88, the signaling adaptor TRIF specifically binds TLR3 and TLR4 but not to other TLR family members leading to the activation of both NFkB and IRF3/7. Finally, TIRAP and TRAM have been shown to act as sorting adaptors which promote the recruitment of MyD88 to TLRs 1, 2, 4, and 6 and of TRIF to TLR4[92].

Currently, ten human and twelve murine TLRs have been identified. TLRs homo- or heterodimerize to activate downstream signal transduction events. TLRs 1, 2, 4, 5, and 6 are primarily present at the cell surface and are specialized in the recognition of microbial pattern molecules[92]. The first characterized family member was TLR4 homodimer which was identified as the receptor for bacterial lipopolysaccharide (LPS)[99]. It was also shown that TLR2/6 and TLR1/2 heterodimers are able to

recognize di- and triacetylated lipopeptides[100] and that TLR5 detects flagellin. In contrast to the plasma membrane-associated TLRs, TLRs 3, 7, 8, and 9 are expressed on endosomal membranes and generally recognize nucleic acids. For instance, TLR3 is specialized in recognizing virus-derived dsRNA whereas TLR9 is required for the response to unmethylated CpG DNA. Finally, TLRs 7 and 8 have been shown to recognize ssRNA but also small synthetic antiviral molecules[97].

3.2.2. C-TYPE LECTIN RECEPTORS (CTLs)

The C-type lectin receptor family is characterized by the presence of C-type lectin-like domain that binds to various carbohydrates in the presence of calcium[101]. To date, there are around 17 different groups of CTLs identified. Even though CTLs can act as opsonins or be involved in cell-cell adhesion, many can also recognize various PAMPs and DAMPs and can act as PRRs. For instance CTL Dectin-1 has been shown to detect β-glucans, whereas the Dectin-2 family members (e.g. Mincle, DCAR, DCIR, Dectin-3, etc) specialize in the recognition of α-mannans[102]. Signal transduction following Dectin-1 stimulation relies on a transcellular hemITAM (modified immunoreceptor tyrosine-based activation motif) and leads to ligand phagocytosis, gene expression and/or cytokine production[103]. In contrast, all Dectin-2 family members except for DCIR have no intracellular domain and thus most of them associate with the ITAM-bearing adaptor FcRγ. Most CTLs signal through spleen tyrosine kinase (Syk) eventually leading to NFkB activation[104].

3.2.3. RIG-I-LIKE RECEPTORS (RLRs)

RLRs are a group of receptors containing a DExD/H box RNA helicase domain which are predominantly involved in the recognition of viral nucleic acids. The family consists of three members: retinoic acid-inducible gene-I (RIG-I), melanoma differentiation gene 5 (MDA5), and laboratory of genetics and physiology 2 (LGP2)[105]. RIG-I, MDA5 and LGP2 are cytosolic receptors that detect foreign RNA features such as 5' triphosphate RNA, long dsRNA, and viral-specific RNA sequences

(such as poly-U)[106]. Both RIG-I and MDA5 bind to the adaptor MAVS (mitochondrial antiviral signaling) via a CARD-CARD domain interaction that results in the activation of IRF3/7 and NFkB and the production of type IFNs and cytokines respectively[105]. Interestingly, LGP2 does not have a CARD domain but it has been proposed to enhance RNA recognition by increasing the initial rate of MDA5-RNA interactions[107].

3.2.4. CYTOSOLIC DNA CENSORS

Another pathway for sensing of cytosolic dsDNA which results in the production of type I IFNs is dependent on the newly discovered cyclicGMP-AMP synthase (cGAS)[108]. Upon activation, cGAS produces the cyclic dinucleotide GMP-AMP (cGAMP) which together with secondary messengers from bacterial origin (e.g. cyclic diguanylate, cyclic diadenylate, etc) is able to activate the so-called stimulator of interferon genes (STING). In turn, stimulation of STING results in IRF3- or NFkB-dependent production of type I IFNs or proinflammatory cytokines, respectively [109–111]. Other cytosolic DNA sensors such as absent in melanoma 2 (AIM2) and probably interferon gamma-inducible protein 16 (IFI16) regulate the production of IL-1β and IL-18 via the formation of the inflammasome complexes. Similar to some NOD-like receptors, this depends on the ability of AIM2 and perhaps IFI16 to initiate Caspase-1 activation which is known to perform the proteolytic cleavage of IL-1β and IL-18[112,113].

3.2.5. NOD-LIKE RECEPTORS (NLRs)

One of the most important family of intracellular PRRs are the NLRs which are characterized by the their nucleotide-binding oligomerization domain (NBD or NOD) and C-terminal LLRs. Originally identified in plants, these molecules were shown to respond to microbial virulence factors and were referred to as disease-resistance genes (R genes)[114–120]. The relationship between mammalian NLRs and plant R genes was first suggested after the cloning of cytoplasmic caspase-recruiting domain 4

(CARD4)/NOD1, which suggested that CARD4/NOD1 can act as a sensor for microbial factors[120–122]. In humans, the NLR family consists of 22 members and at least of 33 members in mice[123]. NLR proteins have a variable N-terminal domain which could contain a CARD, a pyrin (PYD) or a baculoviral inhibitor of apoptosis protein repeat (BIR) domain[123]. Depending on their structure, NLRs are divided into the NLRA, NLRB, NLRC, NLRP and NLRX1 subfamilies. The only member of the NLRA subfamily is the CARD-containing transcription factor CIITA known to induce the transcription of the major histocompatibility complex class II (MHC II)[124]. The NLRB subfamily has been characterized by the presence of a BIR domain and consists of seven NLR apoptosis inhibitory proteins (NAIPs) in mice and one in human. The next group, characterized by the presence of a CARD, is the NLRC one which consists of NOD1, NOD2, NLRC3, NLRC4 and NLRC5. NLRP is the biggest subfamily of NLRs consisting of 14 proteins containing an N-terminal PYD. Finally, the NLRX subfamily has only one family member (NLRX1) which unlike all other NLRs is known to localize to the mitochondria[123,125]. The NLR subfamilies can carry out diverse and important functions in pattern recognition and signal transduction during infection.

3.2.5.1. NOD1 and NOD2

NOD1 and NOD2 are the prototypical members of the NLR family and represent the first group of NLRs. They are composed of C-terminal LLRs, a central NBD domain, and a single (NOD1) or tandem (NOD2) N-terminal CARD domain[97]. Both receptors specialize in the detection of bacterial outer membrane/cell wall components such as the peptidoglycan-derived structures γ-D-glutamyl-m-diaminopimelic acid (iE-DAP) and MDP[126]. Upon ligand recognition, both NOD1 and NOD2 activate NFkB, MAPK, and – in the context of viral infections of some cell types – the MAVS/IRF pathways leading to the production cytokines, antimicrobial peptides and type I IFNs[123,127,128].

3.2.5.2. NLR and other inflammasomes

Unlike NOD1 and NOD2, other NLR family members have been shown to transmit downstream signals via the formation of multiprotein complexes named inflammasomes. Coined in 2002 by Tschopp et al., this term describes a high-molecular weight complex found in the cytosol of immune cells which facilitates the activation of the pro-inflammatory caspase-1[129,130]. Since the publication of this report, intensive work in the field has proven the existence of various types of inflammasomes which sense different PAMPs and DAMPs. In the initial priming step, the detection of a specific stimulus from surface receptors such as the TLRs induces the upregulation of inflammasome-related and other signaling molecules[130]. Subsequently, the inflammasome sensor oligomerizes and recruits the adaptor named apoptosis-associated speck-like protein containing CARD (ASC). Composed of an N-terminal pyrin domain (PYD) and a C-terminal CARD domain, ASC is able to in turn recruit pro-caspase-1. The physical closeness within the complex initiates the proteolytic cleavage and activation of caspase-1 which leads to many downstream responses including the maturation and release of the pro-inflammatory cytokines IL-1β and IL-18, as well as a form of inflammatory cell death called pyroptosis[131,132]. Intensive work on inflammasome function and regulation has shown that it plays a vital role not only in host defense against pathogens but also in neurodegenerative, autoimmune and metabolic diseases[133].

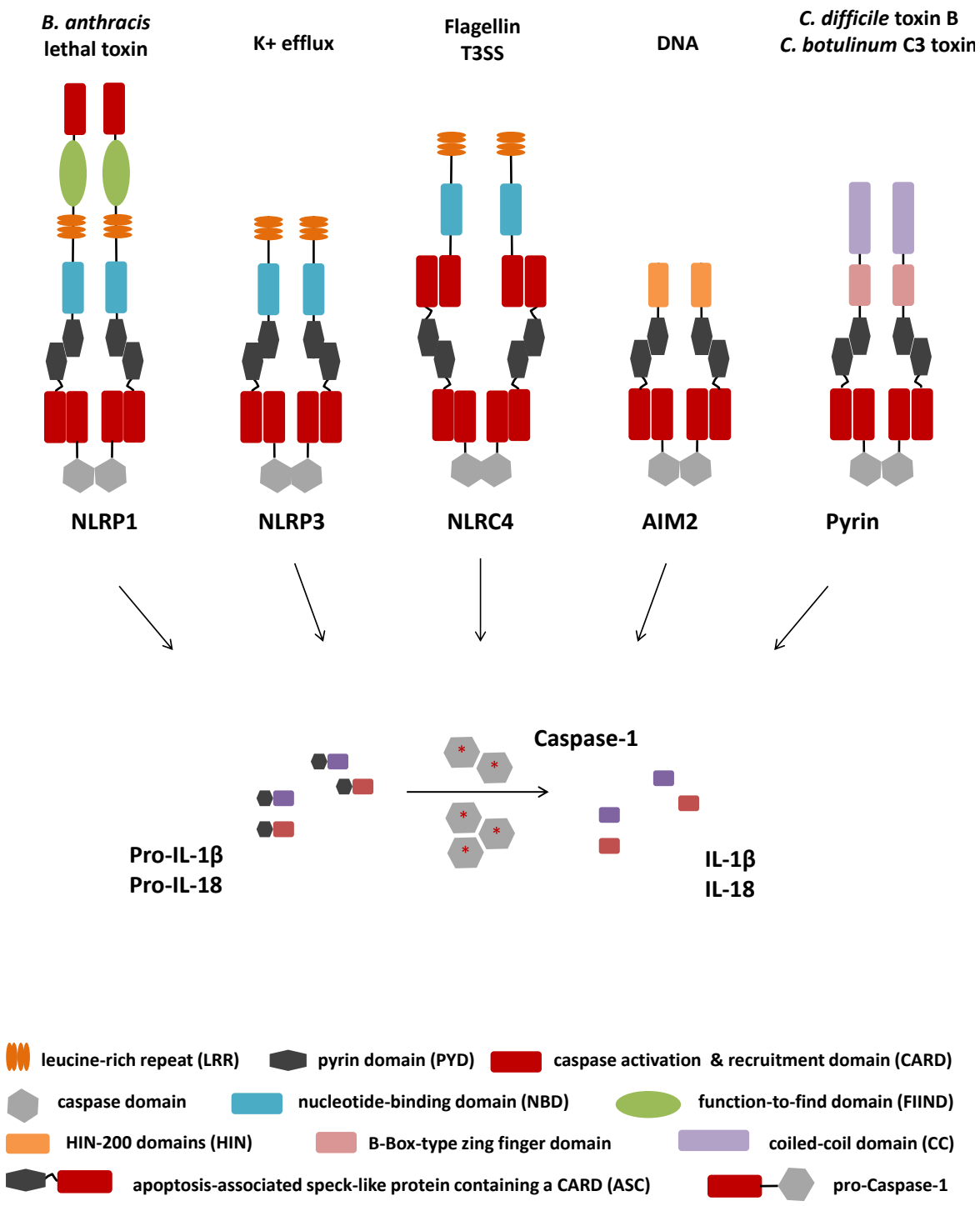

Figure 3: IL-1β/IL-18 production by canonical inflammasome complexes

Canonical inflammasomes contain sensors belonging to the NLR (NLRP1, NLRP3, NLRC4) and the PYHIN (AIM2) protein families which define their ligand specificity. Recently, pyrin also joined the list of sensor proteins that form inflammasomes. Upon activation, the receptors recruit the adaptor protein ASC and the proinflammatory caspase-1 to form a complex. The complex formation in turn triggers proteolytic caspase-1 activation and results e.g. in the release of the inflammasome-dependent cytokines IL-1β/IL-18.

So far, several pattern recognition proteins have been shown to form the so-called classical inflammasomes. Whereas most of them are NLRs such as NLRP1, NLRP3 and NLRC4, there are also complexes formed by pyrin and absent in melanoma 2 (AIM2).

NLRP1 inflammasome

Being the first identified PRR involved in the formation of an inflammasome, NLRP1 has 3 orthologues in mice whereas humans possess only one version of it. The protein is expressed by various cell types such as granulocytes, monocytes, DCs, T cells, B cells, neurons, etc[134] and is composed of a N-terminal PYD, a NBD, LLRs, a function-to-find domain (FIIND) and a C-terminal CARD. The gene however is very polymorphic and in mice two of the variants have been shown to respond to the *Bacillus anthracis* lethal toxin. As a classical A/B type toxin, the *B.anthracis* lethal toxin consists of 4 components (protective antigen, a cell-binding protein, oedema factor, and lethal factor) which act together to from a channel through which the zinc metalloproteinase lethal factor is delivered to the cytosol where it proteolytically inactivates MAPK kinases and the NLRP1B protein itself[135]. NLRP1B cleavage in turn enables the consequent formation of an inflammasome and the activation of caspase-1. Interestingly, it has been reported that during *Toxoplasma gondii* infection murine NLRP1B does not get cleaved but that it is still involved in the resistance against the parasite[136]. Thus, it is currently believed that rodent NLRP1 actually acts as a decoy receptor for the *B. anthracis* lethal factor in a similar way to the proteins produced by some plant resistance (R) genes[137].

NLRC4 inflammasome

NLRC4 is a member of the NLR protein family with a classical structure composed of CARD, NBD and LLR domains[138]. The protein was shown to respond to bacterial flagellin, as well as the rod and needle subunits of bacterial type 3 secretion systems (T3SSs)[139–143]. Yet, subsequent studies determined that in mice the specificity in ligand recognition is dependent on NLR family, apoptosis inhibitory proteins (NAIPs) which act upstream of NLRC4[138]. NAIPs have a structure consisting of a NBD and LLR domains, preceded by three baculovirus inhibitor of apoptosis protein repeat (BIR) domains. Interestingly, ligand recognition was shown to be performed not by the LLRs but rather by the NBD domain of the protein[144]. Thus, flagellin was shown to be recognized by NAIP5 and NAIP6, whereas NAIP1 and NAIP2 recognize respectively the needle and the rod subunits of T3SSs.

AIM2 Inflammasome

Another sensor protein that forms an inflammasome complex is the absent in melanoma 2 (AIM2) protein which is a member of the pyrin and HIN-200 (PYHIN) family [112,113,145]. The gene encoding AIM2 is interferon-inducible and the protein is predominantly expressed in myeloid cells. The AIM2 inflammasome has been shown to specifically detect the presence of DNA in the cytosol. Upon detection of DNA via the HIN-200 domain, AIM2 proteins have been shown to polymerize forming a complex that is able to recruit ASC and caspase-1 thus causing in the production of inflammasome-dependent cytokines[112]. Studies have shown that AIM2 is important in the coordination of host response towards DNA viruses (vaccinia virus, murine cytomegalovirus) as well as with intracellular bacteria (*L. monocytogenes*, *F. tularensis*)[146–148].

Pyrin Inflammasome

The inflammasome containing pyrin as a sensor is the newest member of the inflammasome complexes. In mice, this tripartite motif (TRIM) family member protein consists of PYD, two B-boxes and a coiled-coil domains whereas the human protein variant contains an additional B30.2 domain[129,149]. Recently, the activators of this inflammasome were also uncovered to be bacterial toxins (*C. difficile* toxin B, *C. botulinum* C3 toxin) and effector proteins (*V. parahaemolyticus* VopS, *H. somni* IbpA) which have a disruptive effect on the actin cytoskeleton[149]. Pyrin is believed to specifically detect these changes in cytoskeleton dynamics recognizing the inactivation of the small GTPAse RHOA[149]. Interestingly, it was unable to detect inactivation of other members of the small Rho GTPAse family such as RAC1 and CDC42. Altogether the pyrin inflammasome is suggested to detect pathological disturbances of the actin cytoskeleton of the cell[129].

4. THE NLRP3 INFLAMMASOME

Perhaps the most extensively studied and equally puzzling inflammasome complex is the one containing NLRP3 as a sensor protein. NLRP3 was shown to be expressed in various cell types including DCs, granulocytes, lymphocytes, osteoblasts and even epithelial cells[150,151]. In a study of various murine tissues, it was established that the highest expression of NLRP3 was found in the spleen followed by the lungs[152].

The protein has a classical tripartite structure consisting of PYD, a NBD and LLRs and has been shown to respond to surprisingly broad range of stimuli. Initially, it was reported to sense ATP, nigericin and bacterial toxin such as those derived from *S. aureus* and *L. monocytogenes*[153]. Later, a plethora of stimuli were added to the list including particulate and crystalline matter (alum, asbestos, silica, uric acid crystals), as well as many components of viral, fungal and bacterial origin[154–157]. Subsequent studies however showed that in macrophages the sensing of some of those microbial stimuli actually represented only a priming step and that an additional signal is necessary to activate the release of mature IL-1β and IL-18[85,86,158]. Thus, in this two-step activation model, the first signal is provided by a microbial or sterile stimulus which induces the NFkB-driven upregulation of NLRP3 and pro-Ilβ. The second signal which activates the complex can be delivered by bacterial toxins, ATP, bacterial RNA, crystals, etc[159].

4.1. NLRP3 PRIMING AND PRE-ACTIVATION EVENTS

In most types of murine macrophages, the first signal (priming) is essential for NLRP3 activation, because unlike ASC and caspase-1 NLRP3 expression requires induction. In addition to TLR stimuli, endogenous molecules such as IL-1β and TNF could also act as the first signal and induce gene expression via NFkB activation. This stimulation requires several hours to increase the levels of NLRP3 to the required for proper inflammasome formation and activation[160]. To avoid aberrant activation in some cell types of myeloid origin, there are also reports of cells-specific post-

transcriptional downregulation by miR233. This specific miRNA has been shown to bind to the 3'-UTR of NLRP3 resulting in lower inflammasome activation[161,162].

According to recent reports, it has also become clear that there are also mechanisms at place that regulate inflammasome function at post-translational level[163,164]. In a report by Juliana et al. it was shown that LPS priming of macrophages for as little as 10 min resulted in NLRP3-dependent caspase-1 activation[165]. It was further shown that this is due to a ROS-dependent NLRP3 deubibiquitination carried out by BRCC36 (BRCC3) which is required prior to activation. Other protein modifications such as phosphorylation have also been observed. For instance, it has been shown that sensing of *Candida albicans* via ITAM-containing receptors causes the activation of Syk which in turn lead both to inflammasome formation and to pro-IL-1β transcription[166]. Similarly, the TGF-β-activated kinase 1 (TAK1) has been shown to be required for inflammasome activation induced by cell swelling events[167,168]. Recently, Mishra et al. and Hernandez-Cuellar et al. described a post-translational mechanism induced by nitric oxide (NO) which reduces the damaging effect of prolonged inflammasome activation[169,170]. Intracellular NO produced downstream of type I or type II interferon receptor signaling was shown to cause thiol S-nitrosylation of NLRP3 during *Mycobacterium tuberculosis* infection of macrophages. This modification inhibited the interaction between NLRP3 and ASC thus reducing subsequent caspase-1 activation and cytokine production[169,170]. Altogether, downstream of priming, the function of NLRP3 is strictly regulated on virtually every possible level.

4.2. NLRP3 ACTIVATION

Taking into account the enormous structural diversity of the NLRP3 inflammasome activators, it is inconceivable that NLRP3 is able to sense all of them directly. Thus, it is hypothesized that it actually senses a common endogenous molecule that is induced and/or activated in response to the inflammasome stimuli. Different cellular and molecular mechanisms have been proposed as candidates for this signal including Ca^{2+} signaling, ROS, mitochondrial dysfunction and lysosomal damage but perhaps the most likely common denominator of inflammasome activation is believed to be potassium (K^{+}) efflux[159]. K^{+} efflux was considered because it was observed that like nigericin, low K^{+} can trigger IL-1β production in primed murine macrophages[159,171–173]. Additional studies showed that high extracellular K^{+} can specifically inhibit the activation of the NLRP3 inflamasome but not of AIM2 or NLRC4 inflammasomes[159,174,175]. Moreover, low K^{+} concentrations could actually trigger inflammasome formation in a cell-free experimental system[174] perhaps by causing a conformational change in NLRP3. Importantly, K^{+} efflux was induced as a response to both microbial and sterile NLRP3 inflammasome activators[176].

Ca^{2+} signaling has also been proposed as a possible universal NLRP3 inflammasome activator after it was shown that treatment with the Ca^{2+}-chelator BAPTA blocked IL-1β secretion in macrophages and keratinocytes[53,177–180]. Similar to K^{+} efflux, blocking of Ca^{2+} signaling inhibited NLRP3 inflammasome activation by classical NLRP3 stimuli but had no effect on AIM2 or NLRC4 inflammasome activation[179,180]. However, in a recent study NLRP3 inflammasome activation was found to be independent of increased cytosolic Ca^{2+} concentrations[181]. Moreover, it was shown that BAPTA inhibits NLRP3 independently of its function as an inhibitor of Ca^{2+} signaling. The involvement of Ca^{2+} in inflammasome activation is thus currently unclear[181].

Cytosolic ROS has been implicated as a common activation signal as well[182]. Initially, in studies with inhibitors, intracellular ROS produced via NADPH were believed to activate the NLRP3 inflammasome. However, subsequent experiments with human PBMCs and murine macrophages which lack NADPH activity showed no impairment

of inflammasome activation[183,184]. Therefore, the role of NADPH-dependent ROS needs to be clarified. Others studies have also suggested a role for mitochondrial ROS[164,185]. Tschopp et al. showed that a blockade of mitophagy/autophagy causes the accumulation of damaged ROS-producing mitochondria which in turn promoted inflammasome activation[185]. Additionally, in another report, oxidized mtDNA found in the cytosol of LPS/ATP-treated macrophages has also been proposed to contribute to IL-β/IL-18 secretion[164]. The involvement of other mitochondrial components such as cardiolipin and the adaptor MAVS have also been suggested but further research is required in order to elucidate their contribution[156,182,186–189].

Lysosomal destabilizayion is another cellular process which leads to NLRP3 activation during the intake of particulate matter (e.g. cholesterol crystals)[53]. The lysosomal perturbations were reported to cause cytosolic release of proteases such as CathepsinB leading to inflammasome activation. Yet, particulate matter has also been shown to trigger K^+ efflux but future research will be required to further clarify the involvement of lysosomal leakage independently of potassium changes[176].

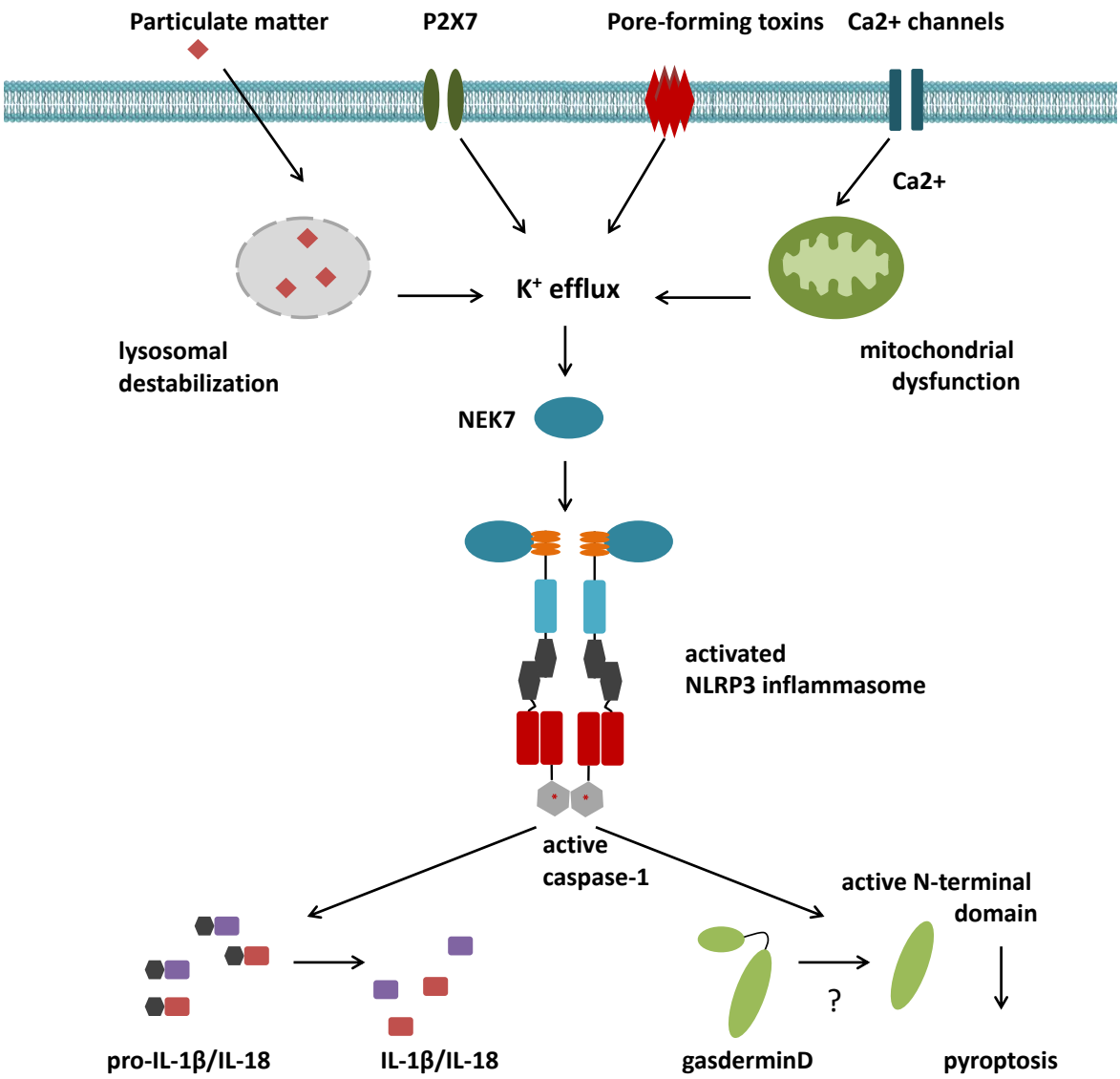

Figure 4: Multiple cellular signal events lead to NLRP3 inflammasome activation

Various stimuli (particulate matter, pore-forming toxins, ATP, etc) have been shown to facilitate inflammasome activation after an initial priming step. K^+ efflux is required for activation and is induced by most inflammasome stimuli. Particulate matter causes lysosomal destabilization resulting in K^+ efflux and the release of cathepsins in the cytosol. Ca^{2+}dependent mitochondrial dysfunction induces the release of mitochondrial ROS and DNA is also proposed be important for activation. Three independent studies identify NEK7 as an inflammasome regulator acting upstream of NLRP3. Inflammasome activation results in caspase-1 activation which leads to release of mature IL-β/IL-18 as well as induction of pyroptosis (possibly via the proteolytic activation of gasdermin D).

4.3. THE NON-CANONICAL INFLAMMASOME PATHWAY

Recently, a non-canonical inflammasome pathway activated specifically by Gram negative bacteria has been described. This pathway is defined by the involvement of murine caspase-11 (human caspase-4) and the induction of cell death[190–193]. In experiments with TLR4-deficient macrophages pointed to the existence of cytosolic receptor for LPS sensing[190,194]. Thus, whereas TLR4 is responsible for extracellular LPS detection, caspase-11 senses cytosolic LPS[131,194]. Interestingly, it was shown that LPS binds directly to the CARD domain of caspase-11 whereby inducing oligomerization and activation of caspase-11[195]. In addition, the downstream substrate of caspase-11 (as well as of caspase-1) was identified to be the protein gasdermin D (GSDMD)[131,132]. Caspase-11 dependent GSDMD cleavage resulted in the production of an N-terminal fragment which promoted pyroptosis by forming pores on cellular membranes[131]. These recent studies propose GSDMD as a major regulator of the immune response against Gram negative bacteria including *Escherichia coli*, *Salmonella typhimurium* and *Shigella flexneri*[190]. The function of GSDMD in in the context of the cannonical inflammasome and the response to gram positive bacteria needs to be further elucidated.

4.4. NLRP3 REGULATION

Several proteins such as the dsRNA-dependent protein kinase (PKR) or guanylate-binding protein 5 (GBP5) have been suggested to regulate NLRP3 inflammasome activation but their actual function is still not fully elucidated[190,194,196]. While it was shown that PKR inhibition causes decreased caspase-1 activation in NLRP1, NLRP3 and NLRC4 inflammasomes, these data could not be reproduced in a more recent study that used the same animals deficient in PKR[196,197]. Similarly, GBP5 was initially shown to specifically promote NLRP3 inflammasome activation but subsequent experiments with independently-generated GBP5-knockout macrophages failed to show the same effect[190,198].

Recently, several independent studies have reported an unexpected and essential role for the NIMA-related kinase 7 (NEK7) as a component of the NLRP3 inflammasome[199–201]. NEK7 was shown to be required for activation with virtually all NLRP3 activators but was found to be dispensable for NLRC4 or AIM2 inflammasome stimuli[199–201]. In addition, it was reported that it binds to the LLR region of NLRP3 and that its kinase activity was not required for the process[199,201]. NEK7 was found to act downstream of K^+ efflux and to regulate NLRP3 oligomerization, ASC speck formation, caspase-1 activation and IL-1β/IL-18 secretion[199]. Interestingly, it was shown that NEK7 was required for caspase-1 activation induced by a gain-of-function NLRP3 variant (R258W) associated with Muckle-Wells syndrome in humans[199]. Moreover, as a member of the NIMA (never in mitosis gene a)-related kinases, NEK7 was also shown to regulate mitotic progression and separation of centrosomes[129]. The interaction between NEK7 and NLRP3 was also reported to be reduced in mitotic cells as compared to that in interphase cells[201]. Thus, it is suggested that NEK7 acts as a switch which regulate the exclusivity of cell division and inflammasome responses[129]. Altogether, NEK7 emerges as an important NLRP3 inflammasome regulator acting downstream of K^+ efflux. Future studies will be necessary to elucidate its overall importance.

In conclusion, the host innate immune system is equipped with a wide range of PRRs which work cooperatively and in distinct modes to sense and protect the organism from microbial and danger signals. Proper recognition of that signal is necessary for the subsequent production of mediators which in turn orchestrate the events which later lead to adaptive immune response initiation.

5. INNATE IMMUNE RECOGNITION OF *S. PNEUMONIAE*

During infection, virtually all groups of PRR are involved in the extra- and intracellular recognition of *S. pneumonia*e components. TLR2 and -9, for instance, were reported to respond to extracellular pneumococcal cell wall lipopeptides and endosomal unmethylated DNA, respectively[202,203]. The importance of TLR and/or IL-1R/IL-18R signaling has been underlined in studies with mice lacking the adaptor protein MyD88. The reports showed dramatically increased susceptibility during pneumococcal infection, associated with impaired cytokine production as well as with enhanced bacterial dissemination and replication[204–206]. The involvement of TLR2 during pneumococcal infection has been hinted in reports where TLR2 deficiency was associated with enhanced bacterial loads and moderately increased susceptibility[207,208]. Interestingly, the mortality of TLR2-deficient animals was further increased in infection experiments with *S. pneumoniae* mutants deficient in PLY[209]. Previously, PLY was suggested to be recognized by TLR4. However, controversial reports about TLR4 function in colonization control and survival have created doubt on its involvement in pneumococcal recognition[210,211]. In line with these data, PLY-dependent cytokine production was shown to be independent of TLR4 but to be rather dependent on NLRP3[212]. Furthermore, pneumococcal DNA sensing by TLR9 contributed to antibacterial defense during lung infection[57,213]. Indeed, *Tlr9*-/- mice showed reduced bacterial clearance and increased mortality, which however was independent of changes in cytokine production[213].

In addition to TLRs, NLR proteins such as NOD2 as well as NLRP3 have also been implicated in innate immune recognition of *S. pneumoniae*. NOD2 was shown to sense pneumococcal peptidoglycan found in the cytosol, leading to NFkB activation and downstream cytokine production[214]. The recognition has been shown to be dependent on PLY released during bacterial phagocytosis and phagosomal degradation[215,216]. Moreover, PLY has been identified as an activation stimulus of the NLRP3 inflammasome and was also suggested to be indirectly involved in the activation of the AIM2 inflammasome by cytosolic DNA[212,217]. NLRP3-deficient animals showed worsened disease outcome and increased lung permeability during pneumococcal

infection[217]. Moreover, experiments with mice deficient in the adaptor ASC (required for e.g. NLRP3 and AIM2 inflammasome formation) showed that these animals were highly susceptible to pneumococcal infection[212,217]. The increase in susceptibility as well as the reduction in IL-1β/IL-18 production was less pronounced in *Nlrp3*-/- as compared to *Asc*-/-[218,219]. This protective role of inflammasome-dependent IL-1β could be explained perhaps by its ability to induce the recruitment and activation of immune cells such as neutrophils and macrophages[220,221].

Excessive activation of the inflammasomes can also cause widespread tissue damage which in turn worsens inflammation and has a detrimental effect on pneumococcal disease progression. For instance, administration of IL-1/IL-18 antagonists during pneumococcal meningitis was shown to result in reduced tissue damage and improved clinical outcome in both *Nlrp3*-/- and *Asc*-/- mice[222]. In addition to AIM2, another pathway for detection of pneumococcal DNA was identified. Cytosolic DNA recognition in macrophages was shown to be dependent on the adaptor STING and interferon regulating factor 3 (IRF3) which lead to the production of type 1 IFNs[57]. Finally, the importance of C-type lectins like SIGN-R1 and Mincle as well as the scavenger receptors MARCO and SR-1has also been reported[223–228].

Altogether, the host immune system relies on various PRRs to detect extra- and intracellular pneumococcal components which results in in downstream signaling events, leading to production of inflammatory mediators and the initiation of antibacterial immunity and inflammation.

6. AIM OF THE STUDY

Bacterial pneumonia is one of the main causes of acute lung injury and acute respiratory distress syndrome. Since alveolar barrier dysruption is central for these life-threatening conditions, it is important to characterize potentially protective mechanisms involved in the the early stages of the disease. The innate immune receptor NLRP3 is best known for its ability to form inflammasomes within hematopoetic cells, to regulate IL-1β/IL-18 production, and to induce pyroptosis in responce to bacterial infection or other insults. However, little is known about the involvement of NLRP3 in pulmonary barrier protection and its function in non-hematopoetic cells such as lung epithelial cells. The aim of this study was therefore to examine the effect of NLRP3 on the alveolar membrane integrity during pneumococcal infection and in response to the pneumoccocal toxin pneumolysin.

I – Results

1. CO-HOUSING OF *NLRP3-/-* AND WT ANIMALS INCREASES SIMILARITY OF GUT MICROBIOTA

Previously, it has been published that the immune responses to respiratory pathogens is influenced by the microbiota and vice versa – that the immune system affects the microbiota[229,230]. Animals lacking ASC, NLRP3 and NLRP6 for example, have been shown to harbor altered intestinal microbial communities, which are dominant and transferable to WT mice during co-housing[231,232]. It has also been demonstrated that the microbiota changes induced by lack of inflammasome components affects the local immune response in the gut[229,233].

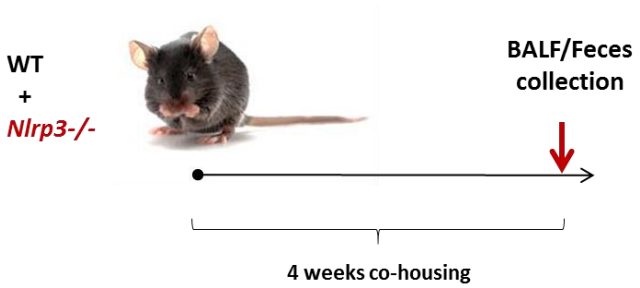

Figure 5: Scheme for microbiota transfer experiment

WT and *Nlrp3-/-* animals were removed from the mother at 4 weeks of age and were housed together for another 4 weeks in a ratio 1:1. At the end of the period, the mice were sacrificed and feces samples were collected from each mouse. n = 5 mice/group

In order to avoid potential effects of differences of the microbiota in WT and *Nlrp3*-/- animals on the immune response and barrier function we co-housed 4 weeks old WT and *Nlrp3*-/- mice for 4 weeks in a 1:1 ratio (Fig. 5). This procedure was recently shown to (partly) equalize the intestinal microbiota[234]. After 4 weeks of co-housing we collected fecal samples and analyzed their microbial composition based on 16S rDNA sequences (Fig 6).

We observed that co-housing caused only minor shifts in the beta diversity in feces as can be seen in the pie chart in Fig. 6A. 80-90% of the total bacteria in feces was composed of Bacteriodales (phylum Bacteriodetes), Lactobaccilales and Clostridiales (phylum Firmicutes) (Appendix, Table A1). Previously, the intestinal microbiota of *Nlrp3*-/- animals have been shown to harbor more *Bacteroidetes* species (*Prevotellacae*) and less members of the genus *Lactobacillus*[231]. In our analysis, we only found low amounts of TM7 and Prevotella species and similar Lactobacilli levels (Appendix, Fig. A1).

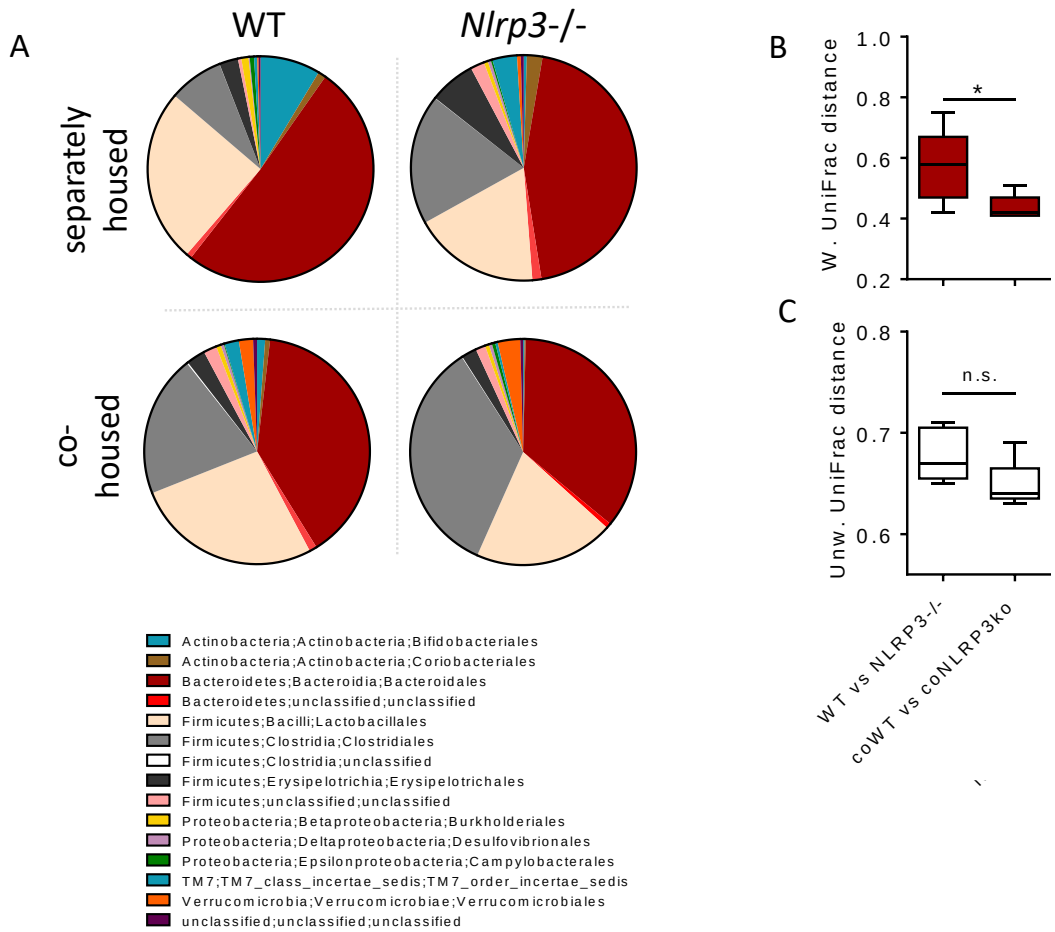

Figure 6: Fecal microbiota composition and microbial community shift upon co-housing of WT and *Nlrp3-/-* mice

(A) Relative abundance of major bacterial orders found in the feces of WT and *Nlrp3-/-* mice. Phylogenetic dissimilarities in fecal microbial communities between separately housed and co-housed animals determined by weighted (B) and unweighted (C) UniFrac distance analysis. (A-C) n = 5 independent animal samples, (B and C) Non-parametric t test. $p < 0.05$ (*); $p < 0.01$ (**); Boxplot whiskers represent interquartile range ± SEM.

Subsequently, we performed Unifrac analysis on the collected data (Fig. 6B-C). Unifrac is an algorithm which measures the phylogenetic distance between sets of taxa in phylogenetic trees. This method describes whether two or more communities have the same structure. As an extension of the standard unweighted Unifrac algorithm there exists also a weighted Unifrac variation which attempts to make a quantitative beta diversity measurement. Our analysis showed no significant

difference in the unweighted comparison of separately housed and co-housed WT and *Nlrp3*-/- animals suggesting that the microbial composition did not change qualitatively. Yet interestingly, co-housing caused changes in the weighted Unifrac analysis, thus suggesting that the relative proportion of different bacterial communities has shifted.

Altogether, co-housing increased the similarity of the microbial communities found in the gut of WT and *Nlrp3*-/- animals. To ensure that we study lung functions independently of microbiota differences, we used co-housed animals for all following *in vivo* experiments.

2. NLRP3 PROTECTS THE LUNG BARRIER DURING *IN VIVO* PNEUMOCCOCAL INFECTION

In order to examine the effect of NLRP3 on the barrier function of the lung during bacterial pneumonia WT and NLRP3-deficient animals were infected intranasally with $5x10^6$ *Streptococcus pneumoniae* Serotype 3 strain PN36 and the inflammatory responses were analyzed 24 h after infection (Fig.7A-E). Prior to preparation, HSA was introduced into the circulation and the ratio of HSA in BALF/blood was used as surrogate marker for damage of the epithelial-endothelial lung barrier (Fig. 7B). In confirmation of previous studies[235,236], both WT and *Nlrp3*-/- mice showed significant increase in alveolar leakage. Importantly, the barrier dysfunction was significantly enhanced in *Nlrp3*-/- as compared to WT animals. Interestingly, we observed no significant differences in bacterial loads in the BALF and blood of WT and *Nlrp3*-/- animals (Fig. 7C, D).

Finally, to test whether the destabilization of the lung barrier function could be due to difference in inflammatory cell recruitment to the lung, we measured by flow cytometry the amount of recruited $CD11b^+Ly6G^+$ cells (as a percentage of all $CD45^+$ cells) but detected no differences (Fig. 7E). Altogether, 24 h p. i. we observed a defect

in the maintenance of the alveolar membrane of *Nlrp3*-deficient animals which was not due to differences in lung bacterial loads, bacterial spreading or neutrophil infiltration.

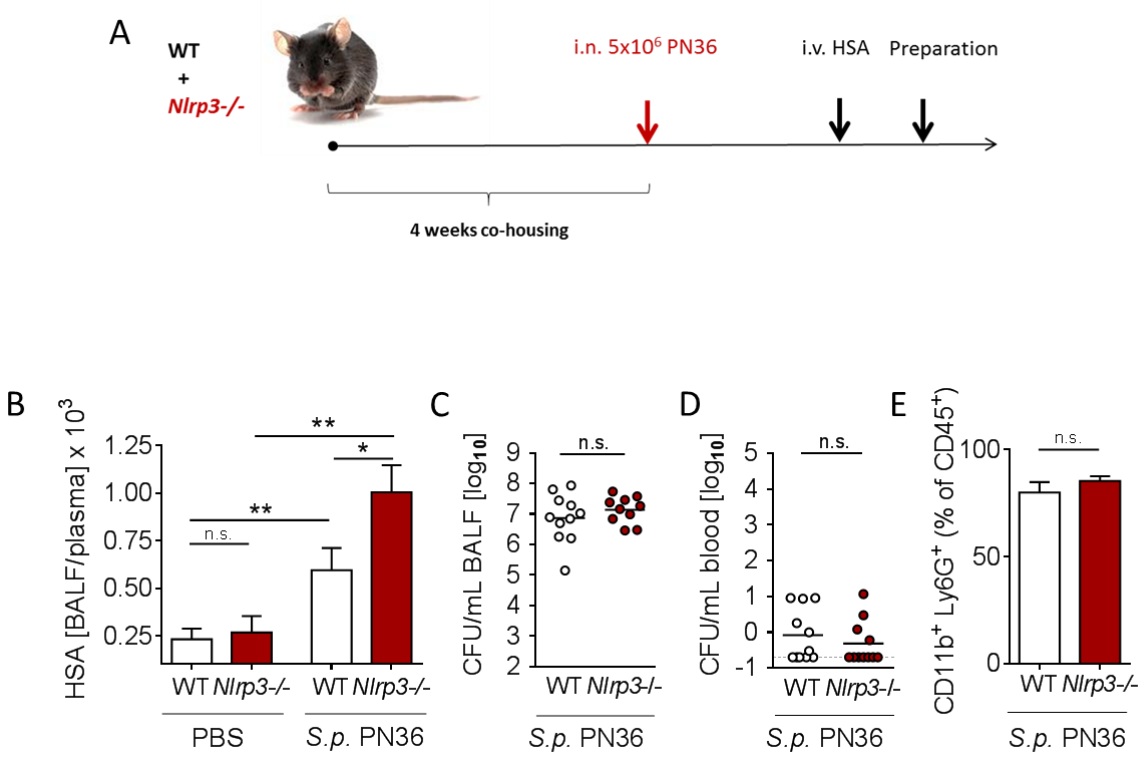

Figure 7: NLRP3 protects the alveolar barrier during *in vivo Streptococcus pneumoniae* infection

8-10 week old female mice were intranasally infected with 5x10⁶ *S. pneumoniae* PN36 for 24 h. (A) Lung permeability was quantified by measuring the HSA BALF/serum ratio after i.v. injection of HSA. Bacterial loads in BALF (B) and blood (C), as well as neutrophil infiltration (E) were measured 24h post infection. Values are given as mean ± SEM; n = 7–11. *$p < 0.05$, **$p < 0.01$, n.s. = not significant.

3. NLRP3 PROTECTS THE LUNG BARRIER DURING TREATMENT WITH AEROZOLYZED PNEUMOLYSIN (PLY) IN ISOLATED MURINE LUNGS

So far, our data suggested a lung-specific function of NLRP3 for barrier protection. Thus, we employed the IPML model which allows to study the effect of the pneumococcal toxin pneumolysin (PLY) on isolated murine lungs (Fig. 8A). PLY is a critical virulence factor of *S. pneumonia* which has been demonstrated to cause lung barrier dysfunction[15,35,62]. Moreover, being a pore-forming toxin, PLY is a well-known activator of the classical NLRP3 inflammasome[17,53,57,217]. We used aerosolized PLY and treated with it lungs of WT and *Nlrp3*-/- animals for 30 min (Fig. 8B). The lungs were perfused, ventilated under negative pressure, and maintained in a chamber at 37°C to achieve conditions close to the physiological ones. To measure PLY-induced permeability, HSA was introduced to the perfusion system and the concentration of HSA that leaked into the broncho-alveolar space was measured by ELISA.

As previously described, PLY caused a very significant increase in alveolar permeability compared to PBS-treatment[237]. Moreover, we observed a greater alveolar leakage in PLY-treated *Nlrp*3-/- lungs as compared to WT. Surprisingly, when examining the lungs of WT and *Asc*-/- animals we did not observe a similar difference in barrier dysfunction (Fig. 8C). To exclude the possibility that the observed effects on the lung barrier are due to a secondary mutation in the mouse strain used, we examined lungs of an independently generated NLRP3 knockout mouse strain (obtained from The Jackson laboratory) in the isolated lung model. Similar to our results shown in Fig. 8A, we found that PLY-induced barrier dysfunction was enhanced in Jax® *Nlrp3*-/- mice (*Nlrp3*-/-J) compared to WT controls (Fig. 8D).

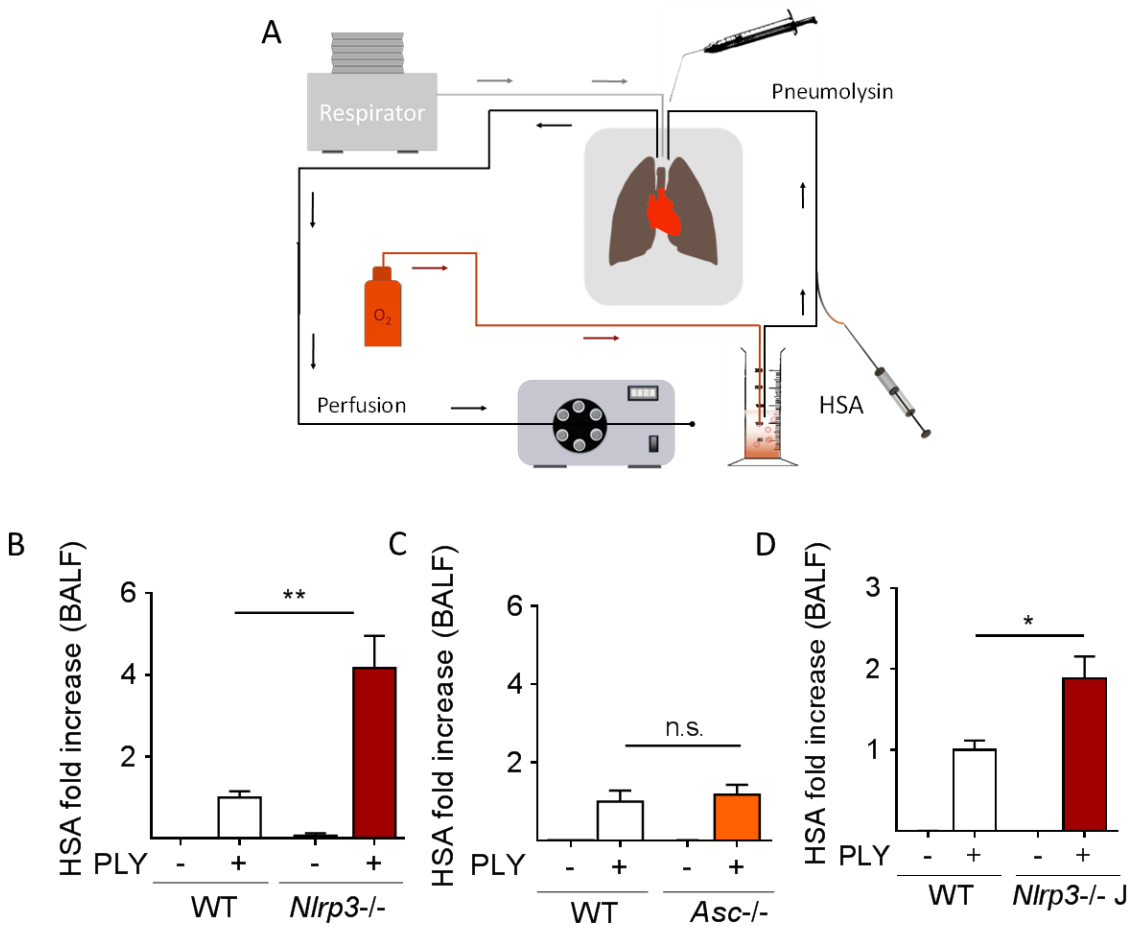

Figure 8: NLRP3 deficiency causes increased alveolar leakage upon PLY treatment *ex vivo*.

(A) Scheme of isolated perfused and ventilated mouse lung model system (IPML). Isolated lungs from WT, *Nlrp3-/-* (B), *Asc-/-* (C), as well as Jax® *Nlrp3-/-* (D) mice were treated intratracheally with PBS or PLY (0.2 µg/lung). Lung permeability was determined 30 min after stimulation by measuring leakage of HSA from the perfusion system to the broncheo-alveolar space. Values are given as mean ± SEM; n = 7–11. *$p < 0.05$, **$p < 0.01$, n.s. = not significant.

Collectively, our data demonstrate that NLRP3 has a protective function in the alveolar membrane maintenance upon pneumolysin treatment which is independent of the inflammasome adaptor ASC.

4. NLRP3 ENHANCES LUNG EPITHELIAL BUT NOT ENDOTHELIAL BARRIER FUNCTION UPON PNEUMOLYSIN TREATMENT

Based on our previous observations, we concluded that the increased pulmonary destabilization in *Nlrp3*-/- animals can be attributed to a cell type/types that are resident in the lung. It is known that the alveolar membrane is composed of epithelial cells which lie in direct proximity to the endothelial cells composing the microvasculature of the lung[238]. In addition, a specialized set of alveolar macrophages roam the alveolar space and are involved in many early infection events. In an attempt to define the alveolar cell type/types responsible for the NLRP3-dependent alveolar membrane stabilization in the knockout animals, we optimized existing methods for isolation of primary endothelial (MLECs) and epithelial (AECs) cells from mouse lungs. We measured purity using CD144 as a specific marker for MLECs and respectively CD326 for AECs. As seen on figure 9A and C, the purity of both cell types was identical in WT and *Nlrp3*-/- (86% for MLECs, 98% for AECs).

To study stability of epithelial and endothelial monolayers, the isolated cells were grown to confluent monolayers on golden electrodes and were analyzed by Electric Cell-substrate Impedance Sensing (ECIS). The system allows for the measurement of the impedance which is calculated from the changes in voltage between the electrodes[239,240]. In turn, the impedance can be separated into monolayer resistance and cell capacitance. Whereas the resistance gives a numerical description of monolayer permeability, the capacitance represents the coverage of the electrode. To determine the difference in MLEC and AEC permeability, WT and *Nlrp3*-/- cells were treated with PLY and resistance was measured continuously for at least 2 hours (Fig. 9C and D). Both cell types showed significant decrease in transcellular electrical resistance immediately after toxin treatment. Interestingly, the endothelial cells showed higher sensitivity to the toxin treatment but no difference between WT and Nlrp3-/- cells. In the case of AEC however, we could observe that the knockout monolayers showed significantly greater drop in resistance.

These data suggested that the cause for the increased alveolar leakage in lungs of NLRP3-deficient animals during PLY treatment or *S. pneumoniae* infection can be attributed to the AEC barrier.

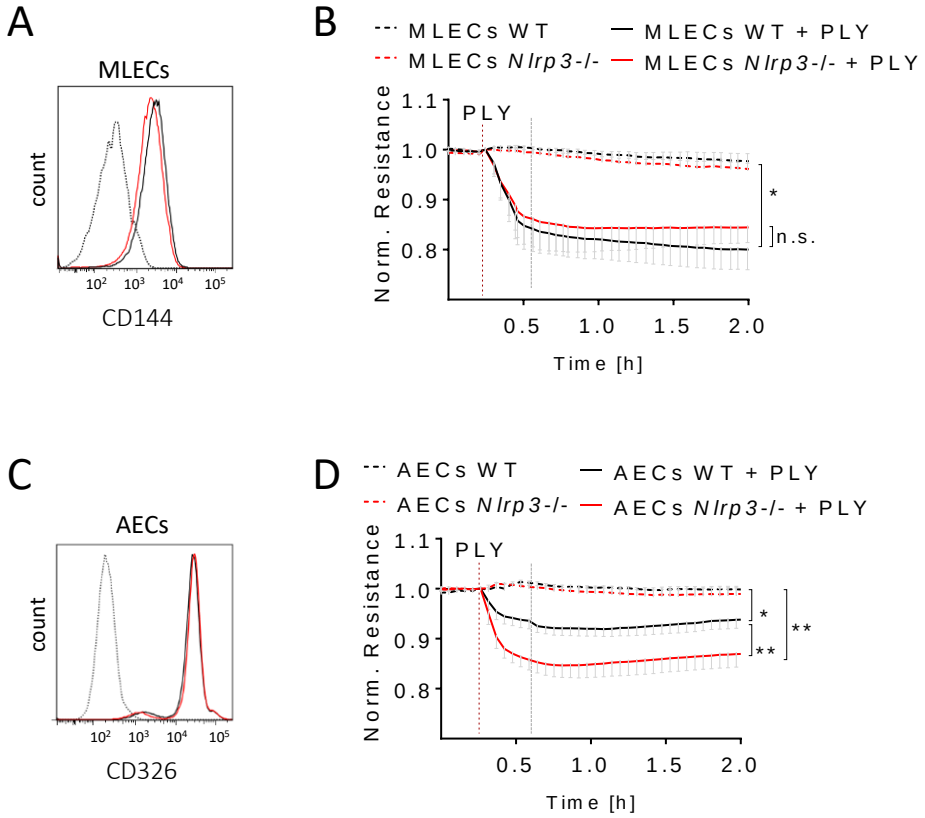

Figure 9: NLRP3 protects the epithelial but not endothelial lung barrier upon PLY treatment

(A) MLECs and AECs from WT (black line) and Nlrp3− /− (red line) mice were isolated and their purities were determined by flow cytometry (A, B). MLECs (C) and AECs (D) were grown on ECIS electrodes. The cell monolayers were treated with 1 µ g/mL PLY and resistance was measured continuously for 2 h at 4000 Hz by ECIS. Values represent a mean of at least 4 independent experiments performed in duplicates and are given as mean ± SEM. Statistical significance of the resistance drop was measured 30 min after PLY stimulation (indicated by grey dotted line). * $p < 0.05$, * * $p < 0.01$, n.s. = not significant.

5. THE PROTECTIVE FUNCTION OF NLRP3 IN LUNG EPITHELIAL CELLS IS INDEPENDENT OF EPITHELIAL CASPASE-1/11 AND CANNOT BE RESCUED BY WILD-TYPE ALVEOLAR MACROPHAGES

Up to now, the NLRP3 protein has been best known for its function as a sensor in the NLRP3 inflammasome complex whose stimulation results in the proteolytic activation of caspase-1[241]. In order to test whether caspase-1 plays a role in PLY-dependent lung epithelial damage, we compared WT and *Casp1/11*-/- AECs in the ECIS system. As seen on Fig. 10A, we observed comparable drop in monolayer resistance upon PLY treatment which pointed to caspase-1-independent function of NLRP3.

In the context of the classical inflammasome, the function of NLRP3 and caspase-1 have been studied predominantly in cells of hematopoietic origin[160]. Our results with isolated AECs presented above already pointed towards an epithelial cell-intrinsic function of NLRP3. However, to further exclude the possibility that small numbers of contaminating alveolar macrophages (AMΦs) were responsible for the NLRP3-dependent epithelial barrier stabilization, we tested whether addition of WT AMΦs to NLRP3-deficient AEC monolayers could rescue the barrier function upon PLY treatment. As expected, we did not see any barrier protective effect of WT AMΦs on the permeability of *Nlrp3*-/- AECs (Fig. 10B), again suggesting that NLRP3 present in the epithelium and not in the macrophages is responsible for the barrier protective effects.

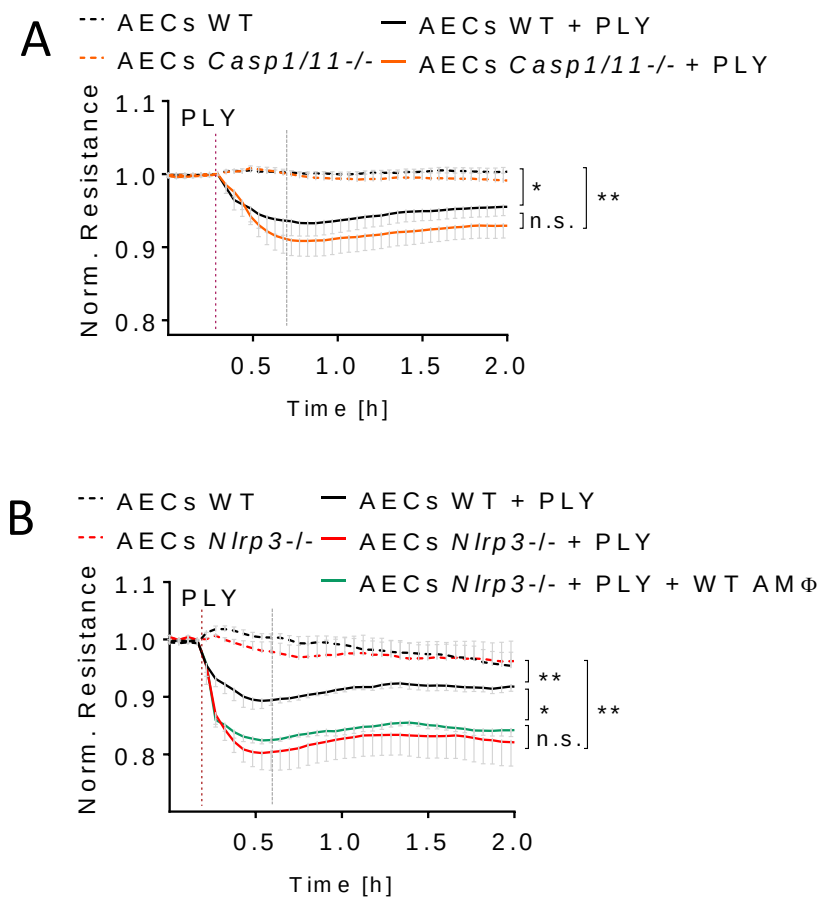

Figure 10: AEC monolayer stability is independent of epithelial caspase1/11 and AMΦ contamination

WT and *Casp1/11-/-* (A), as well as *Nlrp3-/-* AECs co-cultured with WT AMΦ (B) were grown on ECIS electrodes and treated with 1 µg/mL PLY. Resistance was measured continuously for 2 h at 4000 Hz by ECIS. Values represent a mean of at least 3 independent experiments performed in duplicates and are given as mean ± SEM. Statistical significance of the resistance drop was measured 30 min after PLY stimulation (indicated by grey dotted line). * $p < 0.05$, * * $p < 0.01$, n.s. = not significant.

6. NLRP3 PROTECTS THE LUNG DURING *S.PNEUMONIAE* INFECTION INDEPENDENTLY OF THE CYTOKINES IL-1β AND IL-18

Our data suggested an inflammasome-independent function of NLRP3 in the lung barrier protection. However, in order to substantiate this conclusion and since the inflammasome-dependent cytokines have previously been implicated in the regulation of mucosal barriers, we next tested the involvement of IL-1β and IL-18 in the lung barrier protection.[242–244]

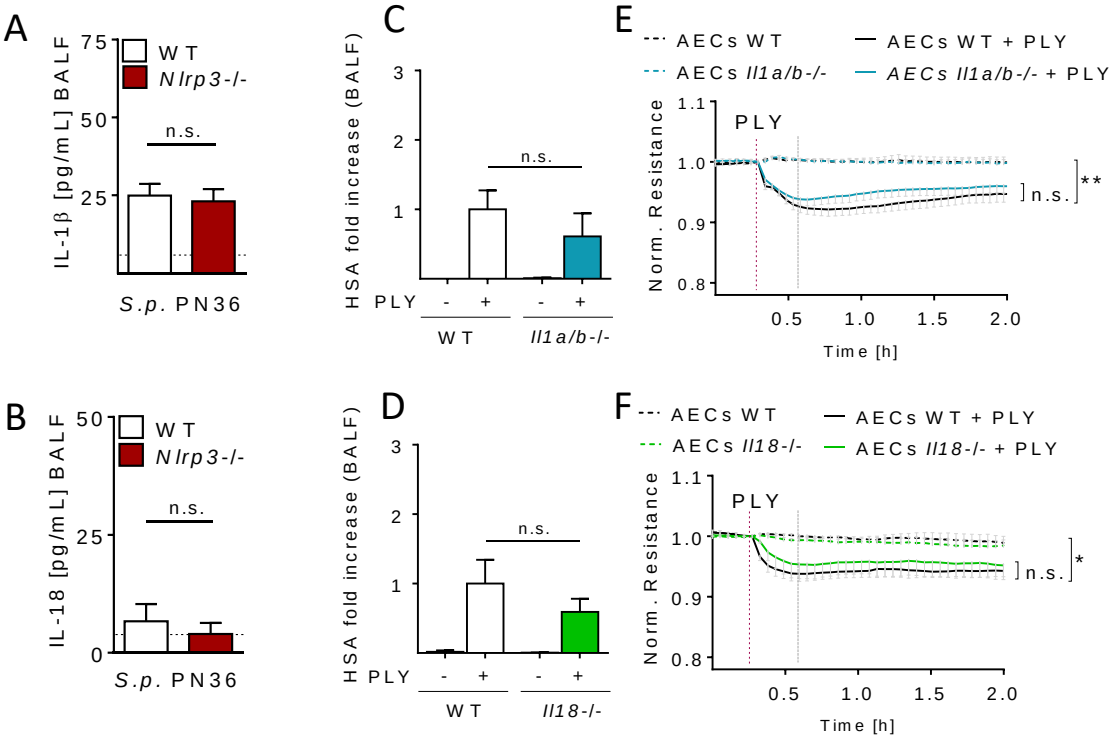

Figure 11: The protective effect of NLRP3 on the alveolar barrier is independent of inflammasome-dependent cytokines.

(A, B). 8-10 week old female mice were intranasally infected with $5x10^6$ *S. pneumoniae* PN36 for 24h. IL-β and IL-18 levels were determined in BALF by ELISA. **(C, D)** Permeability of isolated perfused and ventilated lungs from WT, *Il1a/b-/-* and *Il18-/-* animals was quantified by the HSA ratio in BALF/blood. **(E, F)** AECs grown on gold electrodes were treated with 1 µg/ml PLY and resistance was measured continuously for 2 hours. Values represent a mean of at least 4 independent experiments performed in duplicates and are given as mean ± SEM *p < 0.05, **p < 0.01, n.s. = not significant.

We first measured the concentration of IL-1β and IL-18 in BALF of WT and *Nlrp3*-/- animals infected with *S.pneumoniae* for 24h (Fig. 11 A and B) and found no differences at that time point which is in line with data reported earlier[217].

In an attempt to dissect the specific role of IL-1 family cytokines in alveolar barrier function, we compared isolated lungs from WT, *Ila/b*-/- and *Il-18*-/- animals. Similar to our experiments with *Nlrp3*-/- animals shown above, the lungs were treated with PLY for 30 min and HSA leakage from the circulation was measured. We found that neither IL-1β nor IL-18 had an effect on the barrier function upon PLY treatment (Fig. 11C and D). Finally, isolated primary AEC cells from WT, *Ila/b*-/- and *Il-18*-/- mice were used and monolayer resistance was quantified by the ECIS system. Similar to our results in mice *in vivo* and in IPML *ex vivo* IL-1β and IL-18 did not affect the barrier function of AEC monolayer *in vitro* (Fig. 11 E and F).

Taken together, these data showed clearly demonstrate that NLRP3 protects the lung epithelial barrier independent of the inflammasome-dependent cytokines IL-1β and IL-18.

7. THE EXPRESSION OF ADHESION MOLECULES BY ALVEOLAR EPITHELIAL CELLS IS NOT AFFECTED BY NLRP3

The epithelial monolayer adhesion and stability has previously been shown to be dependent on the expression of adhesion molecules. These molecules regulate not only the cell-cell (e.g. claudins, e-cadherin, occludin, JAM-2, ZO-1) but also the cell-matrix (e.g. integrins α5 and β1) interactions.

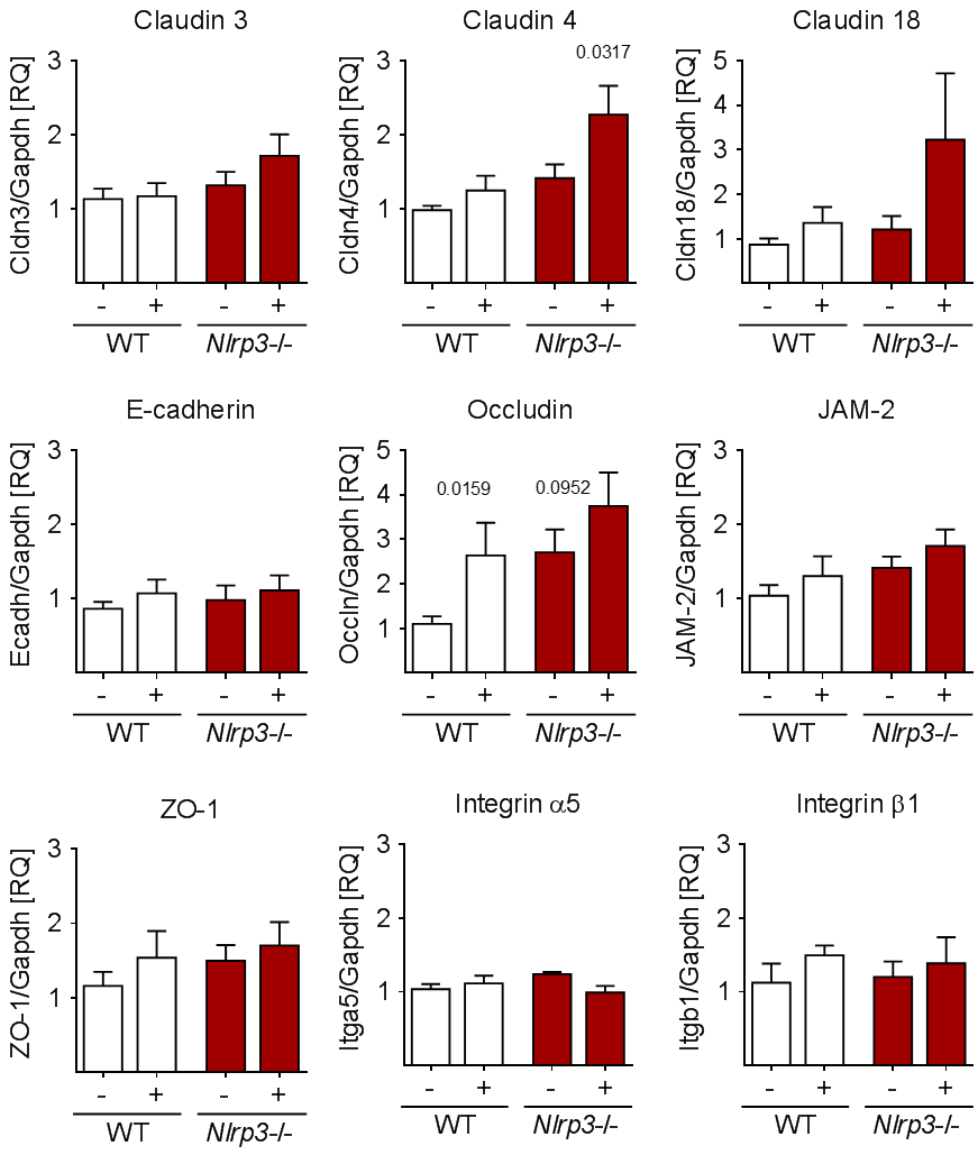

Figure 12: mRNA expression of junctional and basolateral adhesion molecules in AEC is not affected by NLRP3.

Monolayers of WT and *Nlrp3-/-* AECs were left untreated (-) or were treated with PLY(+) for 30 min (as the functional experiment above), and qRT-PCR was performed to analyze the mRNA expression of junctional and basolateral adhesion molecules. Values represent a mean of 5 independent experiments performed in triplicates and are given as mean ± SEM *$p < 0.05$, **$p < 0.01$, n.s. = not significant.

In order to get a hint about mechanisms underlying the protective function of NLRP3 for the lung epithelial barrier, we isolated mRNA from WT and *Nlrp3*-/- AECs and determined relative expression of a number of cell adhesion molecules (Fig. 12). Previous studies have shown that members of the claudin protein family and in particular claudin 4 and 18 play an important role in alveolar permeability to solutes, protein and ions[245–250]. Our data showed no difference in the basal levels of claudins 3, 4 and 18. Similarly, levels of other classical junctional proteins such as e-cadherin, occludin, JAM-2 and ZO-1 were also comparable. Finally, since the AECs were grown on fibronectin-coated wells, we also measured the levels of integrins α5 and β1 (which together act as a receptor for fibronectin binding) but again observed no changes. Altogether, our analysis showed no difference in the basal mRNA expression of these molecules in WT and knockout cells.

8. NLRP3 FACILITATES THE ATTACHMENT OF ALVEOLAR EPITHELIAL CELLS TO THE EXTRACELLULAR MATRIX UPON PNEUMOLYSIN TREATMENT

We next studied in greater detail the defect in epithelial adhesion in the *Nlrp3*-/- AECs. For this purpose, we used a mathematical modeling feature of the ECIS software that is able to discriminate between cell-cell and cell-matrix adhesion. The feature is based on the model of Giaever and Keese[239,240], which assumes that monolayer cells are disc-shaped objects composed of conducting electrolyte inner part and insulating outer membrane. Thus, due to the insulating properties of the plasma membrane, an electrical current passing through the monolayer would have only three possible pathways: 1) between the basolateral cell membrane and the electrode – denoted as the alpha parameter; 2) through the cell-cell junctions – denoted as the Rb parameter; and 3) through the cells (unlikely unless the measurement is done as a very high frequency) - denoted by Cm (Fig. 13A).

Since Cm (or membrane capacitance) is considered to be constant, Rb and alpha can be used to describe the monolayer behavior. Using the ECIS software modeling tool,

we analyzed the change in of these parameters in PLY-treated primary epithelial cells. For simplicity we took the inverted values of the parameters, thus we considered 1/alpha as a measure of AEC basolateral attachment whereas 1/Rb stands for cell-cell junctional stability.

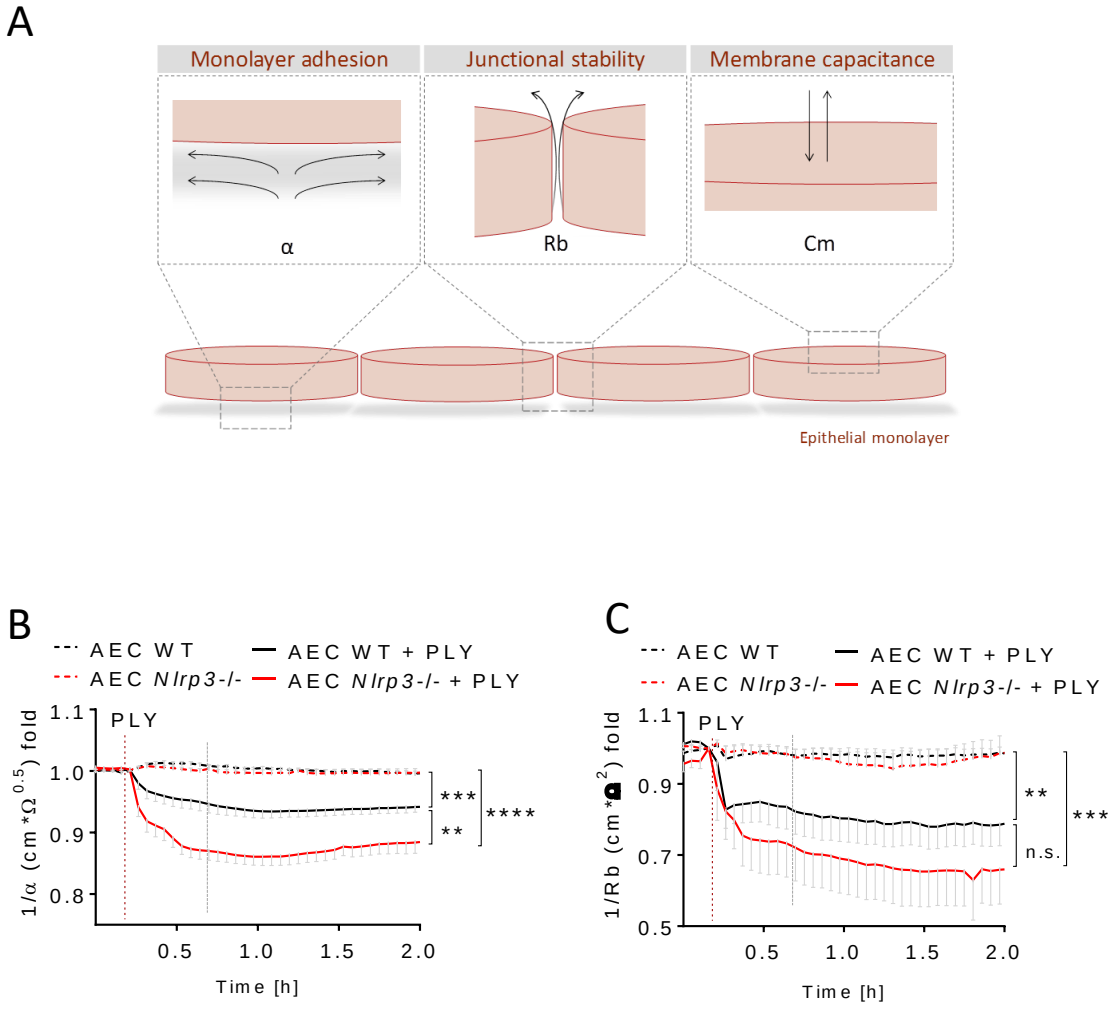

Figure 13: NLRP3 regulates epithelial monolayer quality by influencing cell attachment

(A) Scheme of the components of cell monolayer stability used in the mathematical modeling tool of the ECIS software after. AEC attachment (B), as well as junctional stability (C) upon PLY treatment were determined by the fold change of the alpha (α) and Rb parameters. (B, C) Values represent a mean of ten independent experiments performed in duplicates. Statistical significance was measured 30 min after PLY stimulation (indicated by grey dotted line). All data are given as mean ± SEM *$p < 0.05$, **$p < 0.01$, ***$p < 0.001$, n.s. = not significant.

The modeling revealed that upon toxin treatment, *Nlrp3-/-* AEC monolayers show significantly increased detachment compared to WT cells (Fig. 13 B and C). Interestingly, the junctional stability of both WT and knockout monolayers was comparable. Next, in order to confirm the effect of NLRP3 on the AEC attachment by a complementary method, we performed Total Internal Reflection Fluorescence (TIRF) microscopy (Fig. 14). For this purpose, AECs were grown on glass-bottom slides, labeled with fluorescent membrane dye and treated with PLY. The decrease of mean fluorescence in the 200 nm evanescent field was used as a measure of cell detachment.

Our results again confirm the effect of NLRP3 on AEC adherence, as PLY-dependent detachment was enhanced in NLRP31-deficiency in AEC (Fig. 14). Collectively, our data indicate that NLRP3 protects the lung epithelial barrier by enhancing the basolateral attachment of AECs.

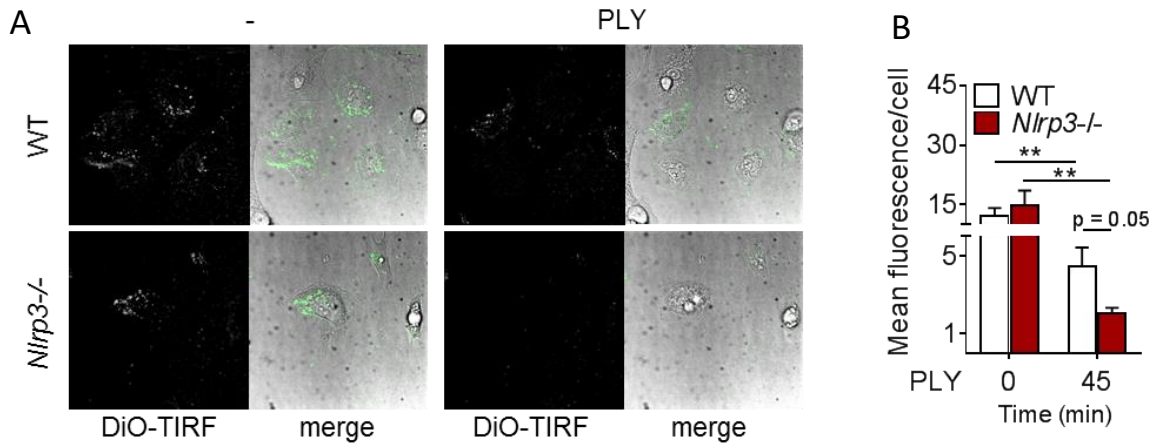

Figure 14: Nlrp3 deficiency in AEC enhances detachment upon PLY treatment

AECs were stained with the membrane dye DiO and subsequently subjected to TIRFM life imaging. Pictures were taken at 30 min after adding medium without (−) and 45 min after changing media containing PLY (1 µg/ml). (A) Representative DiO-TIRF and DIC images are shown. (B) Particle analysis was performed from four fields from two independent experiments and values were normalized to cell numbers and average control values. Data represent the mean of three independent experiments. All data are given as mean ± SEM *$p < 0.05$, **$p < 0.01$, n.s. = not significant.

9. THE FUNCTION OF NLRP3 IN EPITHELIAL BARRIER MAINTENANCE IS NOT DEPENDENT ON DIFFERENCES IN CELL DEATH

Finally, since the classical inflammasome activation is also associated with cell death, the next logical question was whether differences in cell death could explain the increased detachment of NLRP3-deficient AECs[251–253]. We studied this using three different methods for cell death determination (Fig. 15). Under the tested conditions, we observed a moderate increase in apoptotic and/or necrotic epithelial cell death upon PLY treatment which was around 20% higher than in the untreated control cells. However, we did not observe any difference between WT and *Nlrp3-/-* AECs upon PLY treatment. Thus, NLRP3-dependent lung epithelial barrier stabilization seems to be independent of cell death regulation.

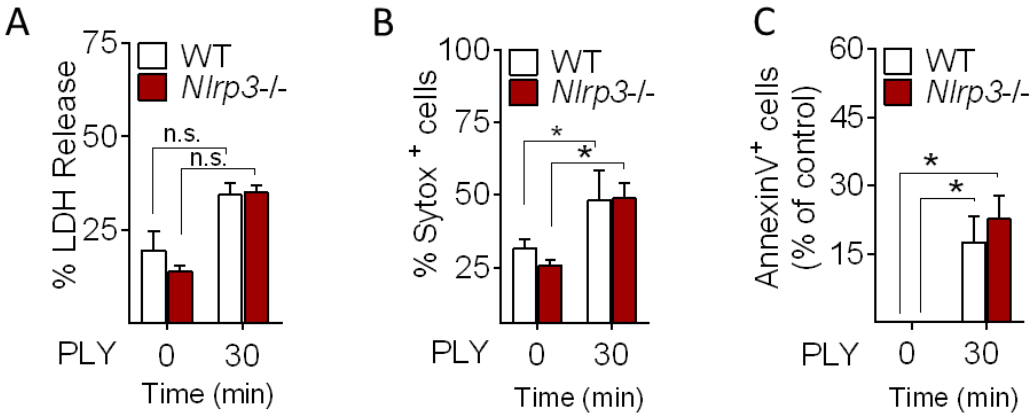

Figure 15: NLRP3-dependent AEC monolayer stabilization does not seem to be due to altered cell death response

Cell death of WT and *Nlrp3-/-* AEC treated for 30 min with PLY (1 µg/ml) was measured by LDH release (A), Sytox staining (B) and AnnexinV staining (C). (A-C) Data represent the mean of three independent experiments. All data are given as mean ± SEM *$p < 0.05$, **$p < 0.01$, n.s. = not significant.

III – Discussion

1. SUMMARY

Bacterial pneumonia caused by *S. pneumoniae* often results in a dangerous destabilization of the alveolar membrane which can even lead to the development of ALI/ARDS. The increased alveolar permeability is associated with barrier dysfunction of the lung epithelial and endothelial cells, as well as with inflammatory cell recruitment. In order to respond appropriately to the threads posed by the bacterium, the host innate immune system has a plethora of detection mechanisms at place. One of the main virulence factors of *S. pneumoniae* responsible for barrier destabilization is pneumolysin (PLY)[217,237]. This pore-forming toxin is sensed by the NLRP3 inflammasome complex[217,254,255]. The function of NLRP3 has been studied extensively in cells of myeloid origin. However, little is known about its functions in epithelial or endothelial cells during infection.

In the current study, we set up to investigate the role of the NLRP3 inflammasome in lung barrier protection during pneumococcal pneumonia. In *in vivo* infection experiments with animals with equalized microbiota, we observed significantly increased alveolar permeability in *Nlrp3*-/- mice as compared to WT. Interestingly, this effect was independent of cell recruitment, lung bacterial loads and bacterial dissemination in the blood. This suggested that the protective function of NLRP3 is localized to the lung and is perhaps independent of cues originating from the circulation. In line with this, subsequent *ex vivo* experiments with PLY-treated murine lungs once again showed greater alveolar leakage in NLRP3- but not in ASC-deficient animals. In order to shed light on the NLRP3-dependent protective effects, we isolated lung epithelial and endothelial cells and studied monolayer permeability in response to PLY. While WT and *Nlrp3*-/- endothelial cells showed comparable response, NLRP3-deficiency affected the lung epithelial monolayers independently of alveolar macrophages. This epithelium-specific NLRP3 function was also

independent of caspase-1/11 and of the inflammasome-related cytokines IL-1β and IL-18. Furthermore, my results suggest that the effect was not due to differences in expression of basolateral and junctional adhesion molecules or cell-cell contact weakening. Instead, through mathematical modeling and TIRF microscopy approaches, we observed that upon PLY treatment, *Nlrp3*-/- epithelial cells presented increased monolayer detachment which was not due to increased cell death.

In conclusion, this study reveals a novel protective role of NLRP3 in alveolar barrier maintenance during pneumococcal pneumonia which is independent of classical inflammasome function.

2. INFLAMMASOMES AND THE MICROBIOTA

In recent years, it was shown that gut microbiota and the immune system mutually shape each other in order to establish stable relationship between the microorganisms and the host[230,233,256–262]. On one hand, the microbiota affects the immune pathways in the intestine, as well as the immune responsiveness at distant body sites. In line with this notion, numerous studies have shown that microbiota depletion results in worse outcome after respiratory bacterial or viral infection[263–268]. Yet on the other hand, the immune system has also been reported to affect the bacterial composition of the gut[269–274]. Previous experiments with *Nlrp3*-/- mice have suggested a protective role of NLRP3 in murine models of colitis or colon cancer[275–277]. However, this phenotype was milder than that observed in *Asc*-/- and *Caspase-1*-/-, suggesting that there is perhaps another inflammasome (e.g. the NLRP6 inflammasome) which could promote gut barrier protection[278,270]. Subsequently, it was discovered that deficiencies in inflammasome components (NLRP3, NLRP6, ASC, IL-18) could cause the outgrowth of pathogenic bacteria resulting in aberrant microbial gut composition which thus leads to disease development[231,271–273,279]. Remarkably, it was also shown that this dysbiotic microbiota could be transferred from knockout to WT animals during co-housing, which in turn lead to transferable disease succeptibility[231,234,280–283]. In order to exclude potential effects of microbiota changes on the lung barrier

function, we therefore housed together WT and *Nlrp3*-/- mice to equalize their microbiota.

We compared the shifts in the microbota of WT and NLRP3-deficient animals via Unifrac distance analysis[284]. This method has been used widely used as an effective distance metric for complex bacterial community examination. Our data showed that co-housing causes significant decrease in gut microbiota variations in WT and *Nlrp3*-/- mice as compared to that of separately housed animals. Previous studies have attributed positive and negative effects of specific bacterial species found in the gut. For instance, some *Lactobacillus* strains were shown to reduce intestinal epithelial permeability by promoting of junctional stability[285]. In line with these data, peptidoglycan-dependent TLR2 signaling strengthened epithelial tight junctions and reduced cell death[286,287]. Moreover, another study has reported that NLRP6-deficient animals have higher levels of the disease-associated TM7 and *Prevotellaceae* species[231]. Yet, our data for WT and *Nlrp3*-/- mice showed virtually unchanged levels of *Lactobacilales* and very low levels of TM7 and *Prevotellaceae*. These variations in the reports are possibly due to differences in the housing conditions of the animals. Altogether, all animals had a normmal gut microbiota dominated by the two major phyla, Bacteroidetes and Firmicutes. However, co-housing indeed resulted in increased similarity of the microbiota composition in WT and *Nlrp3*-/- mice. The use of co-housed mice in our experiments thus reduced the likelihood that the observed differenced in barrier function were caused by variations in the microbiota.

3. NLRP3-DEPENDENT PROTECTION MECHANISMS IN THE LUNG

Having ensured that our test animals have an equalized gut microbiota, we went on further to examine the role of NLRP3 in the lung during *in vivo* pneumococcal pneumonia. A number of previous studies have already highlighted functions of the classical NLRP3 inflammassome in respiratory infections[217,288–293]. The consensus idea that emerges suggests that, due to its central role as innate immune response regulator, the NLRP3 inflammasome activation can have not only deleterious but also protective functions.

3.1. THE PROTECTIVE FUNCTION OF NLRP3 IS INDEPENDENT OF ASC, IL-1β AND IL-18

In this study we confirmed our previously published data showing significantly greater alveolar leakage in *Nlrp3*-/- mice after a 24h infection with $5x10^6$ CFU as compared to their WT counterparts[217]. This protective effect seemed independent of neutrophil recruitment, bacterial killing and tissue dissemination as bacterial numbers in the lung and blood, as well as leukocyte recruitment were similar in WT and knockout mice. Beneficial roles of NLRP3 have been previously reported. For instance, in an infection with group B streptococci (GBS), *Nlrp3*-/-, *Asc*-/-, and *Casp-1*-/- animals were more susceptible to the infection[294]. The activation of the NLRP3 inflammasome in DCs was dependent on the expression of a β-hemolysin and resulted in the production of IL-1β. Similarly, another study showed that NLRP3, ASC and caspase-1 deficiency caused higher susceptibility to *Burkholderia pseudomallei* lung infection attributed again to reduced secretion[295]. However, the above mentioned studies describe cytokine-dependent antibacterial effects rather than barrier function-related mechanisms observed by us in the current work.

The importance of IL-1β but also of IL-18 in the early stages of streptococcal and pneumococcal infections have been pointed out in numerous studies[218–220,296–299]. For instance, IL-1β has been shown to play critical role in the recruitment of neutrophils

and macrophages during infection – a vital early step in the initiation of systemic response to *S. pneumoniae*[300–302]. Il-1β has also been shown to limit *S. pneumoniae* dissemination from the lung via the induction of fibrinogen expression and localized coagulation events[303]. In addition, the other inflammasome-regulated cytokine IL-18 was also reported to play a role mainly in the stimulation of NK cells and the induction of IFN-γ signaling[294,304–308]. IL-18-deficiency was also shown to cause higher susceptibility to pneumococcal pneumonia in mice[218]. Yet, in contrast to these reports, the protective effect of NLRP3 on the barrier function observed by us was independent of the inflammasome-related cytokines. In order to test if the NLRP3-dependent effects were mediated by classical inflammasome components and downstream mediators, we examined permeability in lungs of *Il1a/b*-/-and *Il18*-/- and in epithelial monolayers from *Casp1/11*-/-, *Il1a/b*-/-, *Il18*-/- animals. Our data showed no differences between WT and the compared knockouts in either lung or epithelial barrier functions. Moreover, we compared IL-1β/IL-18 levels in BALF of WT and *Nlrp3*-/- animals 24 h. p.i.. The similar cytokine levels measured in WT and *Nlrp3*-/- animals suggested that perhaps other inflammasome complexes could be also responsible for their induction during pneumococcal infection. In line with this notion, it has previously been shown that AIM2-deficient macrophages produce lower cytokine levels in response to infection pointing to a role of the AIM2 inflammasome in *S.pneumoniae* detection[57,308,309]. Altogether, whereas IL-1β and IL-18 play important role in pneumococcal infection, the data presented here suggest that the protective effect of NLRP3 on the barrier function is independent of their release and of caspase-1/11 action.

In addition to regulating IL-1β and IL-18 production, another characteristic feature of all cannonical inflammasomes is their employment of ASC as adaptor molecule. Since NLRP3 is best known for its role as an inflammasome-forming sensor we went on further to test the response of ASC-deficient animals to PLY in the isolated lung system. Surprisingly, *Asc*-/- lungs responded similarly to the WT ones, suggesting that the role of NLRP3 in guarding the alveolar barrier is independent of the classical inflammasome complex. Interestingly, a few previous studies have also reported ASC- and inflammasome-independent functions of NLRP3[270,310–313]. For instance,

NLRP3 has been shown to contribute to renal ischemia-reperfusion injury independently of ASC, IL-1β and IL-18[310]. Inflammasome-independent NLRP3 was shown to promote the epithelial-mesenchymal transition of kidney epithelial cells via enhanced TGF-β signaling and R-Smad activation[313]. More recently, NLRP3 has also been demonstrated to have an inflammasome-independent function in neutrophils during *F. tularencis* lung infection[270].

Altogether, the results presented by us up to now point to a hitherto unknown protective function of NLRP3 for alveolar barrier function of the lung during pneumococcal pneumonia *in vivo* and during PLY-stimulation *ex vivo*. Importantly, this function independent of the adaptor molecule ASC and of IL-1β/IL-18.

3.2. PLY – A CENTRAL NLRP3 ACTIVATOR

PLY is a major virulence fator of *S. pneumoniae*[37,48,50,56]. Indeed, in rats, PLY-induced lung injury *in vivo* was shown to result in histologic features resembling pneumococcal lung infection[314]. Moreover, we previously observed that early-onset lung injury was primarily associated with the release of PLY[55]. Our lab and others previously showed that PLY activated the NLRP3 inflammasome[254,297,315]. I therefore examined the role of NLRP3 in lung barrier function in PLY-treated isolated lungs. The results described in the present work showed that a 30 min treatment with PLY caused dysfunction whih was significantly enhanced in the lung of *Nlrp3*-/- animals compared to wild-type. Importantly, these results were confirmed in a second independently-bred *Nlrp3*-/- mouse line suggesting that the observed barrier dysfunction is caused by the lack of NLRP3 and not by an unrelated mutation in our knockout mice.

An important issue in the response to pore-forming toxins like PLY is that their action is different dependent on the used dose. Whereas at high lytic concentrations PLY forms large membrane pores and cell death, sublytic concentrations were shown

to affect important signaling events in lung-resident cells[316]. Thus, we calibrated the amount of toxin used in the *ex vivo* and *in vitro* experiments to the theoretical levels released 24h after *S. pneumoniae* infection. For all *in vivo* experiments, we used an infection dose of $5x10^6$ *S. pneumoniae* and observed approx. 1 – $5x10^7$ CFU/ml BALF 24 h p.i.. We do not know the exact amount of PLY which is released *in vivo* but in previous *in vitro* experiments in our department, we have determined that a CFU of approximately $1x10^8$ have a total hemolytic activity of about 250 hemolytic units, which compared to the hemolytic activity of 1.25 µg recombinant PLY. Approximately 10-20% of the pneumococcal hemolytic activity was detected in cell supernatant, which corresponds to the range of concentration of recombinant PLY tested by us. We therefore believe that the PLY concentration in murine lungs 24 h p.i. may well correlate to the PLY doses aerosolized in the isolated lungs.

3.3. EPITHELIAL CELL-INTRINSIC NLRP3 MEDIATES BARRIER FUNCTION

In the following *in vitro* experiments with PLY-treated lung cells we attempted to define the cell type which is affected by NLRP3 deficiency during barrier protective events. I first examined monolayers of primary MLECs from WT and *Nlrp3*-/- animals in the ECIS system and saw no significant difference in their response to PLY. Interestingly, the NLRP3 inflammasome has been attributed an endothelial-intrinsic function in a study of hemorrhagic shock (HS)[317]. HS is a condition known to promote acute lung injury via exaggerated immune response. In this previous study, the authors showed that the detection of extracellular HMGB1 stimulates endothelial NADPH oxidase which leads to ROS production and subsequent NLRP3 inflammasome activation[317]. Yet, data about other endothelial NLRP3 functions are scarce. In contrast, a number of PLY-dependent mechanisms controlling endothelial hyperpermeability have been identified up to date. For instance, studies performed in our department and by others have previously shown that PLY is able to induce Ca^{2+} influx and platelet activating factor (PAF) production which then lead to thromboxane release[318,319]. The increased levels of Ca^{2+} and the binding of

thromboxane to its receptor have also been reported to activate protein kinase C alpha (PKCα)-dependent myosin light chain kinase (MLCK) activation signaling. The resulting phosphorylation of myosin light chain in turn causes actin-myosin cytoskeletal contraction leading to disruption of adherens junctions and to increased permeability[320]. In addition, Rho-kinase signaling, ROS and VE-cadherin reorganization have also been reported to be involved in the PLY-dependent lung endothelial dysfunction[48,55,318].

Since we saw no difference in the response of WT and *Nlrp3*-/- endothelial cells, we went on further and optimized existing methods for AEC isolation. In *in vitro* permeability experiments with AEC monolayers we could observe a significantly increased barrier dysfunction in *Nlrp3*-/- AECs as comparted to WT cells. The purity of the epithelial cultures was of particular importance since it was conceivable that the lack of NLRP3 activation in a small population of contaminating macrophages could have been responsible for the enhanced permeability of *Nlrp3*-/- cells. Macrophages can, for instance, produce ROS, lipid mediators, and cytokines which in turn could have affected the epithelial cells. Indeed, PLY has been previously reported to induce ROS and stimulate NO production and NO-mediated bacterial killing in alveolar macrophages[321–323]. In addition, lipid mediators such as lipoxin A4 and B4 produced by alveolar macrophages could also modulate the epithelial barrier function[324,325]. Finally, small amounts of inflammasome-dependent or -independent cytokines could also influence the behavior of the epithelial monolayers. Thus, to confirm that the observed NLRP3-dependent barrier protection is not due to alveolar macrophage contamination, we performed co-culture experiment with alveolar macrophages and saw virtually no influence of the added cells. This result once again pointed to an epithelial-specific role of NLRP3 for barrier integrity.

3.4. EPITHELIAL BARRIER MAINTENANCE MECHANISMS AND THE ROLE OF NLRP3

Our results up to now prompted us to analyze the various mechanisms of epithelial barrier maintenance and the possible involvement of NLRP3 in them.

There is only a limited number of papers suggesting a role of the NLRP3 in pulmonary epithelium. For instance, Allen et al. showed that the NLRP3 inflammasome played a protective function during IAV infection. The authors reported that infected human airway epithelial cells in culture were able to produce mature IL-1β and that intranasal challenge of *Nlrp3*-/- and *Asc*-/- animals with IAV resulted in increased susceptibility[326]. Moreover, in a study of sterile inflammation in human epithelial line BEAS-2B it was shown that cristobalite silica can induce the activation of a functional NLRP3 inflammasome. This in turn was related to the release of basic fibroblast growth factor (bFGF) and to subsequent fibroblast proliferation[327].

Specific functions of NLRP3 have previously also been analyzed in epithelia found at other body sites such as in the eye, intestine, kidneys, cervix and the skin. For example, *S. aureus* infection of conjuctival goblet cells was shown to induce the expression of inflammasome components and lead to ATP-dependent caspase-1 activation and IL-1β secretion[328]. NLRP3 inflammasome activation might also play an important role in the intestinal epithelium. In infection experiments with *C. rodentium*, *Nlrp3*-/-, *Asc*-/-, *Casp1*-/-, as well as *Nlrc4*-/- animals presented higher bacterial colonization, weight loss, and inflammation as compared to their WT counterparts[329–331]. Further experiments with bone marrow chimera animals showed that surprisingly the protective effect of NLRP3 and NLRC4 against infection was due to their activation in non-hematopoietic cells such as the epithelial cells and not in leukocytes[330,331].

Yet, even though the few above mentioned studies describes NLRP3 functions within non-hematopoetic cells, even less is known about the impact of NLRP3 on the barrier function of epithelial cells. Zaki et al. had reported that in *Nlrp3*-/-, as well as *Asc*-/-

and *Casp1*-/- animals were more susceptible to dextran sodium sulfate (DSS)-induced colitis. This was due to loss of gut epithelial integrity which was caused by lower IL-18 levels[276]. Whereas in this instance the protective role of the inflammasome was due to its classical caspase-1 dependent cytokine production, in a study of renal epithelial injury, the authors presented evidence for a direct function of NLRP3 independent of the inflammasome[332]. In the latter study however, NLRP3 deficiency seemed to be protective during renal injury. Since both of the aforementioned roles of NLRP3 did not fit with our data, we delved deeper into the possible mechanisms of NLRP3-dependent epithelial barrier maintenance.

3.4.1. The role of junctions

Both in health and disease, the dynamic regulation of cell adhesion events, junctional stability, as well as trans- and paracellular ion permeability are among the central determinants of lung epithelial integrity. In search for the possible mechanisms of NLRP3-dependent protective effect in epithelial barrier, we measured gene expression of a number of tight junction adhesion molecules known to be important for monolayer stability. In addition to studying the classical epithelial molecules e-cadherin, occluding, JAM-A and ZO-1, we also measured claudin 3, 4, and 18 which were previously reported to be essential for epithelial barrier function in the lung[333]. In particular, differential expression of claudins was previously shown to play a fundamental role in paracellular permeability[334–336]. Interestingly, claudins from adjacent cells were reported to form small paracellular pores (0.3 nm) which function as un-gated ion channels[337–339]. Moreover, claudins were also shown to influence the transport of macromolecules. Our data however showed no difference in the basal expression of any of the tested molecules. These data were also in line with the mathematical modeling of the Rb parameter (representing junctional permeability) via the ECIS software. Moreover, via confocal microscopy and FACS, we examined some of the major adhesion molecules on PLY-treated WT and *Nlrp3*-/- AECs but could not detect any measurable difference (data not shown). Thus, I concluded that the observed protective function of NLRP3 was perhaps not related to cell-cell junctional stability.

In contract to the Rb which was unaffected by NLRP3, the mathematical modeling of the ECIS data indicated a very significant difference in the cell attachment parameter (alpha). This suggests that the increased permeability of NLRP3-deficient AECs might be attributed to reduced interaction not between adjacent cells but rather between their basal membrane and the extracellular matrix. This prediction was confirmed by TIRF microscopy which we used as means cell attachment analysis. Since AECs were grown on fibronectin-coated wells, we hypothesized that the weaker monolayer attachment can be due to reduced levels of the adhesion molecules responsible for interactions with this matrix protein. The integrin α5β1 is a known receptor for fibronectin and has also been shown to directly interact with the pore-forming toxin α-hemolysin and to even be involved in NLRP3 inflammasome activation[340–342]. However, we did not observe differences in gene expression of integrins α5 and β1 suggesting the involvement of another mechanism. Together, I could show that NLRP3 affects the attachment of AEC monolayers to the extracellular matrix (in particular fibronectin) which might be responsible for the enhanced lung barrier dysfunction of NLRP3-deficient animals in response to *S. pneumoniae* infection or PLY challenge. The molecular mechanisms underlying the NLRP3-mediated increase in adherence of AECs, however, remains to be elucidated.

3.4.2. The role of cell death

This study uncovered a novel inflammasome-independent role of NLRP3 for alveolar epithelial barrier protection in response to PLY treatment. A possible explanation for the enhanced barrier dysfunction in *Nlrp3*-/- epithelial monolayers could have been increased cell death in the NLRP3-deficient as compared to the WT epithelial cells. However, this possibility was ruled out by three independent cell death analysis techniques that did not reveal any difference between *Nlrp3*-/- and WT epithelial cells. Whereas all methods showed an increase of cell death upon PLY treatment, there was virtually no difference in the response of PLY-treated WT and *Nlrp3*-/- cells. Interestingly, whereas the percentage of Sytox® and Annexin V positive cells was significantly higher in PLY-treated cells, the increase in LDH release was not significant at the same time point and toxin dose. These data could potentially be

explained by the different mechanisms of the three methods. Sytox® is a small DNA dye which is able to penetrate even weakly compromised lipid membranes and can be used as a marker of early apoptotic events[343]. Similarly, Annexin V is also a marker for early cell death events by its function as a phosphatidylserine (PS)-binding protein[344]. In normal conditions, PS is located exclusively at the cytoplasmic site of the plasma membrane but upon cell damage, it is exposed to the external cellular environment and can thus be detected. In contract to these two methods, the release of LDH from cells is considered to be a measure of a later cell death events(cytotoxicity and cytolysis)[345]. Due to its size, the release of this cytosolic enzyme requires greater membrane permeabilization related to the formation of larger pores. The fact that in our hands the LDH release was not significantly enhanced in PLY-treated cells showed once more that the used toxin concentration was sublytic and that the primary AECs presented only signs of early apoptosis.

The increase in barrier dysfunction in *Nlrp3*-/- AEC as compared to WT AEC already 30 min after PLY challenge suggests that the observed effect is perhaps due to an early and rapid cellular response, independent of gene expression. Such an event could be due to ion flux, cytoskeleton rearrangements or improper function of a basolateral adhesion molecule.

3.4.3. The role of ions

The earliest consequence of pore formation is undoubtedly the increased permeability of the plasma membrane to ions such as K^+ and Na^+ and the resulting variations in cytoplasmic ion composition[346].

Ion fluctuation is a result of pore-forming toxin action, as well as an activator of the NLRP3 inflammasome. Moreover, it might also be possible that ion flux is involved in the barrier-protecting effects of NLRP3. Interestingly, caspase-1 has been shown to activate sterol regulatory element-binding proteins (SREBPs) – known to play a central role in lipid biogenesis and cell survival[347]. This mechanism could be interesting also in our context, where the lack of NLRP3 could be causing lower

SREBP activation and thus impaired membrane resealing after PLY damage. In contrast, another study of exaggerated activation of SREBP proteins in alveolar epithelial cells was shown to cause pulmonary lipotoxicity[348]. While the increased barrier dysfunction we observed in *Nlrp3*-/- AECs was independent of caspase-1, the difference in permeability could still be caused by deregulated SREBPs or other proteins of the lipogenic pathways. This could result in alteration of the general composition of plasma membranes and to their response to toxins. Indeed, PLY is a cholesterol-binding protein and its activity would possibly be altered by the difference in membrane lipid composition[349–353].

In addition to K^+ efflux, Na^+ (but not Cl^- influx) was shown to correlate with NLRP3 activation[176]. It has been reported that Na+ influx can modulate NLRP3 activity even though it was not a strict requirement for inflammasome activation. A proper ion transport across the epithelium was also shown to be an important component of pulmonary edema resolution caused by conditions such as pneumonia[354,355]. The clearance of alveolar fluid has also been reported to be largely dependent on the Na+ concentration gradient. During the clearance process, Na^+ was shown to be internalized via apical the epithelial sodium channel (ENaC) channels and to be secreted by basolateral Na^+/ K^+ ATPases to the interstitial space[356–360]. Interestingly, cell wall component of the bacterium *Leptospira interrogans* were reported to inhibit the expression and function of the Na^+/ K^+ ATPase pump which in turn led to NLRP3 inflammasome activation[361].

Several hemolytic toxins have been described in *L.interrogans* however the hypothesis that injected or pore-forming hemolysins could play a role needs further elucidation[362–364]. In relation to our results, it is conceivable that *Nlrp3*-/- epithelial cells could also have altered expression or function of basolateral Na^+/ K^+ ATPase which cause deficiencies in their response to PLY. However currently there is no data confirming such a theory.

3.4.4. The role of the cytoskeleton

Another possible way in which NLRP3 could be involved in the stabilization of the barrier function is through modulation of the cytoskeleton of the cell. A study by Misawa et al. showed the involvement of microtubule (MT) dynamics for NLRP3 activation. The authors reported that inhibitors of tubulin polymerization such as colchicine and nocodazole suppressed NLRP3 inflammasome functions in response to nigericin and MSU[365]. They went on to describe a mechanism mediated by dynein in which MTs facilitate the transport of ASC on mitochondria to NLRP3 on the ER in response to NLRP3 inducers. Moreover, they showed that MT-mediated transport was related to α-tubulin acetylation status which was controlled by the acetyltransferase MEC-17 and the deacetylate sirtulin 2. Whereas a number of bacterial toxins have been shown to modulate actin dynamics, not much is known about their ability to affect MT stabilization[366]. Interestingly, Iliev et al. have reported that PLY is able to induce extensive MT stabilization and bundling in cholesterol-dependent but macropore-independent manner[367]. Integrating these data with ours, it is conceivable that the lack of NLRP3 in AECs could be hampering the transport on MTs which in turn could result in a greater destabilization of the cytoskeleton and the overall attachment ability of PLY-treated epithelial cells. Yet, further research is required to prove or disprove the hypothesis of a possible link between PLY-dependent MT stabilization and NLRP3 in the epithelium. The newly identified NLRP3 regulator NEK7 has also been shown to play a role in MT dynamic instability and was shown to phosphorylate α- and β-tubulin *in vitro*[368,369]. In addition, its related family member NEK3 was shown to be involved in MT acetylation[370]. Yet, further experiments with nigericin-treated macrophages showed that NEK7 perhaps does not act upstream of tubulin acetylation[200]. The involvement of MTs in early NLRP3 activation has been hinted, however further research is required to determine its role in epithelial-specific NLRP3 function.

In addition to its effect on MTs, PLY has also been reported to induce the rapid activation of Rho and Rac GTPases known to be central regulators of actin dynamics[371]. Yet, whereas the pyrin inflammasome is emerging as a guardian of the actin cytoskeleton[372–377], barely any studies point to an involvement of actin in the

NLRP3 regulation[378,379]. I also did not observe an apparent difference in actin dynamics in WT and *Nlrp3*-/-AECs (data not shown).

Interestingly, a recent study suggested the involvement of the intermediate filament protein vimentin in NLRP3 signaling in the lung[243]. The study showed that vimentin-deficient animals were protected against lethal LPS challenge, bleomycin-induced acute lung injury and asbestos-related inflammation suggesting an important role of vimentin in systemic inflammatory responses dependent on the NLRP3 inflammasome signaling. Moreover, the authors could show that the regulating effect was due to a direct interaction between vimentin and NLRP3 in macrophages[243]. As an important component of focal adhesions of adherent cells, vimentin is an interesting protein which not only bridges actin and membrane-bound adhesion molecules (e.g. integrins) but is also involved in their recycling from the plasma membrane[380–383]. It has also been shown to be sufficient and required for would repair and remodeling in alveolar epithelial cells[384]. Yet, the involvement of these molecules in the NLRP3-mediated alveolar barrier function requires further investigation.

4. FUTURE EXPERIMENTS

Our current study contributes to the understanding of non-inflammasome functions of the NLRP3 proteins while at the same time leaves a lot of unanswered questions. For instance, it would be interesting to perform an in-depth analysis of the differences in cytoskeletal and basolateral adhesion molecule dynamics in WT and NLRP3-deficient cells. In this way we could examine whether NLRP3 affects, for example, microtubule or intermediate filament localization and function in epithelial cells which could in turn cause the differences in monolayer attachment upon PLY treatment. Moreover, NLRP3 could also affect the trafficking and activation of surface adhesion molecules which could futher influence epithelial barrier function. It would also be interesting to check whether the composition of the lung extracellular matrix in *Nlrp3*-/- animals varies from that of their WT counterparts which could further contribute to the barrier dysfunction observed *in vivo*. Since ion flux seems to be the central activator of NLRP3, it would also be interesting to compare the responsiveness of ion receptors/channels in WT and *Nlrp3*-/- AECs. In addition, to prove the epithelial-specific role of NLRP3 for barrier function during *in vivo* pneumococcal pneumonia, future studies should examine the lung barrier function in bone-marrow chimera animals, as well as with epithelial-specific NLRP3 knockout mice.

5. CONCLUSION

Although the NLRP3 inflammasome is predominantly studied in immune cells, an increasing body of evidence points to additional function of the inflammasome components in cells of non-hematopoietic origin. In the current work, I could show that NLRP3 plays a protective function for the barrier function of the alveolar epithelium during pneumococcal pneumonia and treatment with the bacterial toxin PLY. The NLRP3-mediated barrier protection is independent of the inflammasome complex and of IL-1β and IL-18. Instead, the results presented indicate that NLRP3 enhances the attachment of lung epithelial cells.

In the future, studies of the controlled stimulation of NLRP3 could give rise to therapies focusing on lung barrier stabilization during pneumonia.

IV – Materials and Methods

1. BACTERIAL CULTURE

Streptococcus pneumonia strains D39 and PN36 (NCT7978) were cultured as described previously[217]. Bacteria were stored in glycerol stocks (10%) in THY medium at -80°C. Prior to use, the bacteria were plated on Columbia blood agar plates (containing 5% sheep blood) and were grown at 37°C and 5% CO_2 for 8 h (for strain PN36) and 12h (for strain D39). Single colonies were transferred into THY medium and were grown to an OD = 0.2-0.4 (37°C, 5% CO_2). After reaching the required OD range, the liquid cultures were centrifuged (2700 g, 10 min, 4°C) and resuspended in PBS or an appropriate cell culture medium. Bacterial concentration was calculated assuming that in this OD range OD_{600} = 0.1 corresponds to 1×10^8 CFU/mL.
For *in vitro* experiments, the *S. pneumoniae* serotype 2 strain D39 was used[385,386]. In vivo murine infections were made using the serotype 3 strain PN36. Both strains were kindly provided by Prof. Sven Hammerschmidt (Ernst-Moritz-Arndt-Universität Greifswald, Germany).

2. MICE

Nlrp3-/-, *Asc*-/-, *IL-18*-/- and wild-type (WT) animals were bred in the animal facility of the Charité Universitätsmedizin Berlin - Forschungseinrichtungen für experimentelle Medizin (FEM). *Nlrp3*-/- were originally provided by Prof. Jürg Tschopp (University of Lausanne, Switzerland). *Asc*-/- mice were originally provided by Prof. Vishva Dixit (Genentech, USA) and *IL-18*-/- mice were provided by Dr. Markus Heimesaat (Charite Universitätsmedizin Berlin). *Ila/b*-/- and *Casp1/11*-/-were kindly provided by Bärbel Raupach (Max Planck Institute for Infection Biology, Berlin).

All animal experiments were approved by institutional (Charité – Universitätsmedizin Berlin) and governmental animal welfare committees (LAGeSo Berlin; approval IDs G0177/13, T0013/11, T0014/12). All mice used were on C57BL/6 background, 8 - 10 weeks old and female.

3. MURINE PNEUMOCOCCAL PNEUMONIA MODEL

3.1. INFECTION OF MICE

Infection of mice was performed as described previously[217]. Mice were anesthetized by intraperitoneal (i.p.) injection of 80 mg/kg ketamine and 25 mg/kg xylazine and were transnasally inoculated with 5×10^6 CFU *S. pneumoniae* serotype 3 (PN36; NCTC7978) in 20 µl PBS per mouse. The control groups were treated with 20 µl PBS. Mice were sacrificed 24 h post infection (p.i.). At the end point of the experiment, mice were anesthesized (160 mg/kg ketamine, 75 mg/kg xylazine), heparinized (60 µL 12,500 I.E.) and sacrificed by final blood withdrawal. The blood was centrifuged (1500 g, 10 min, 4°C) and the serum was collected. All samples and organs of interest were collected and used for further analysis or were frozen in liquid nitrogen and stored at -80°C.

3.2. BRONCHO-ALVEOLAR LAVAGE OF MURINE LUNGS

After sacrifice, mice were tracheotomized, ventilated and perfused with sterile 0.9% NaCl via the pulmonary artery for 3 min using an IPML (isolated perfused and ventilated mouse lung) system. Broncho-alveolar lavage (BAL) was performed two times with PBS supplemented with protease inhibitors (1 tablet/10 mL). The two brocho-alveolar lavage fluid (BALF) fractions were centrifuged (425 g, 10 min, 4°C) and the resulting supernatants were collected separately. The two cell pellets were combined and used for cell recruitment analysis.

3.3 DETERMINATION OF BACTERIAL LOADS

Bacterial loads were determined in BALF and blood by preparing serial dilutions (up to 1:10^5) from the first BALF fraction and whole blood. The dilutions ware plated on blood agar plates and incubated (37°C, 5% CO_2) overnight. Colony-forming units (CFUs) were counted on the following day.

3.4 DETERMINATION OF LUNG PERMEABILITY

To estimate lung microvascular leakage, human serum albumin (HSA) (1mg in 75µL) was infused intravenously 1 h before broncho-alveolar lavage. HSA concentration in BALF (a 1:1 mixture of first and second BALF fraction was used) and serum was measured by ELISA according to the manufacturer's instructions, and the HSA BALF/serum ratio was calculated.

3.5 CELL RECRUITMENT IN BALF

Cell pellets from BALF collection were pooled and resuspended in 1 mL sterile PBS. To test for cell recruitment the cells incubated with blocking antibody (anti-CD16/32) and stained using CD11c-FITC (Biolegend), SiglecF-PE (BD bioscience), Ly6C-PerCp (Biolegend), F4/80-APC (Biolegend), CD45-Alexa700 (Biolegend), Ly6G-BV421 (Biolegend) and CD11b-BV510 (Biolegend). $CD45^+CD11b^+Ly6G^+$ cells were considered to be polymorphonuclear neutrophils (PMNs). The relative amount of PMNs was expressed as percentage from the number of BAL cells.

4. ISOLATED PERFUSED AND VENTILATED MOUSE LUNG MODEL (IPML)

Mouse lungs were prepared according to the experimental setup described previously[387]. In short, mice were anesthetized and placed in a 37°C chamber. After laparotomy, sternotomy, and cannulation (left atrium, pulmonary artery), lungs were perfused with electrolyte solution (Serag-Wiessner, Germany) supplemented with sodium bicarbonate. The chamber was closed and the lungs were ventilated and perfused for 20 min to establish baseline conditions. 10 min prior to PLY application, HSA was added to the perfusate. For PLY-stimulation, the chamber was opened and

lungs were treated intratracheally with 0,2 µg toxin/lung. After 30 min of perfusion/ventilation with closed chamber albumin concentration was measured in the BALF after the experiment using an ELISA (Bethyl, US).

5. CELL CULTURE

5.1. ISOLATION OF MURINE ALVEOLAR EPITHELIAL CELLS (AEC)

Alveolar epithelial cell (AEC) isolation was performed as described before[57]. In brief, mice were sacrificed and their lungs were perfused via the pulmonary artery with 20 ml HBSS. Subsequently, 1.5 ml of dispase and 500 µl of low-melting point agarose were introduced into the lung through the trachea. The agarose was allowed to solidify for 2-3 min, the lungs were transferred into 4.5 ml dispase (5 U/ml) and were incubated at room temperature for additional 30 min. This was followed by 10 min of DNase digestion (0.1 mg/ml) in AEC medium (DMEM + 2.5% HEPES + 10% FCS + 4.5 mM L-glutamine + 100 µg/ml Pen/Strep) and thorough homogenization of the lung. The suspension was passed through cell strainers (100 µm and 40 µm) and centrifuged twice (100 g, 8 min, 4°C). The cell pellet was resuspended in 2 ml medium and incubated with biotinylated anti-mouse antibodies anti-CD45, anti-CD31 and anti-CD16/32. For each lung were used 20 µL from each antibody. The incubation was performed at 37°C, 5% CO2 for approximately 30 min. The cell pellets were washed twice with AEC medium without FCS and were then incubated with 75 µL/lung Dynabeads® Biotin Binder for 30 min at RT on an overhead shaker. Following this step, the epithelial cells were separated from the cells bound to the magnetic beads by the use of a DynaMag-Spin magnet system.

The isolated cells were washed with AEC medium and were seeded in fibronectin-coated plates/slides (100 µg/mL, 1h at RT) at a density of 1x10^6 (for ECIS and immunofluorescence) or 5x10^5 cells/mL (for all other experiments). The cells were cultured at 37°C and 5% CO_2 and were allowed to differentiate for about 4-5 days into type 1 AECs. Before use, the cells were washed once with HBSS containing Ca^{+2}/Mg^{+2} and their medium was changed.

5.2. ISOLATION OF MURINE LUNG ENDOTHELIAL CELLS (MLECs)

Animals were sacrificed as described before and the lungs were removed and cut into small pieces (approx. 2 µm). The lung pieces were washed with ice-cold HBSS and were then incubated in 5 mL HBSS supplemented with DNAse (0.5 mg/mL) and Dispase (5U/mL) per lung. The incubation was performed for 1 h at 37°C water bath while shaking. In the meantime, Dynabeads® Sheep Anti-Rat IgG were washed 3 times with 1 mL HBSS containing Ca^{+2}/Mg^{+2} and 0.5% BSA (HBSS/BSA). After washing, the beads were coated with rat anti-mouse CD144 antibody (2,5 µL antibody/12, 5 beads) for 1h at RT on an overhead shaker. To remove unbound antibody, the labeled beads were washed 3 times with HBSS/BSA.

The lung digestion was stopped by adding 5 mL FCS. The solution was vigorously pipetted up and down and was then passed through a cell strainer (70 µm) to produce single-cell suspension. The suspension was washed with HBSS/BSA and centrifuged (500 g, 5 min, RT). The resulting cell pellet was resuspended in 700 µL HBSS and was incubated with the anti-CD144-coated magnetic beads for 30 min at RT on overhead shaker. The bead-bound MLECs were isolated using a DynaMag-Spin magnet system and the supernatant was discarded. The cells were washed 3 times with HBSS/BSA and were then resuspended in endothelial cell medium (Endothelial Cell Growth Medium MV2 + Supplement + 15% FCS + 100 µg/mL Pen/Strep). The isolated cells were plated on fibronectin-coated (100 µg/mL, 1 h at RT) on 35mm culture dishes. The medium was changed after 24h and the cells were splitted in a ratio 1:3 after reaching confluence. Confluent monolayers were detached using Trypsin-EDTA (5 min, 37°C), washed with endothelial medium and incubated on the DynaMag-Spin magnet to remove the cells labeled with magnetic beads. The beads-free cells were then plated on fibronectin coated ECIS arrays (see below). MLECs were cultured at 37°C and 5% CO_2.

5.3. ISOLATION OF ALVEOLAR MACROPHAGES FOR CO-CULTURE

Mice were sacrificed and each lung was lavaged approximately ten times with PBS supplemented with 2 mM EDTA. The collected BALF was pooled together and was centrifuged at 300g for 5 min at 4 °C. The pelleted cells were then resuspended in alveolar macrophage medium (RPMI 1640 + 10% FCS+4,5 mM L-glutamine + 100 µg/mL Pen/Strep). The isolated alveolar cells were added to cultures of differentiated AECs in cell number ratio 1:20. The cells were cultured at 37°C and 5% CO_2 overnight and were used in experiments on the following day.

5.4. PNEUMOLYSIN STIMULATION

Pneumolysin was kindly provided by prof. T. Mitchel (Institute of Microbiology and Infection, Birmingham, UK). For all *in vitro* experiments, the toxin was used at concentration of 1 µg/mL in the respective cell medium.

6. ELECTRIC CELL-SUBSTRATE IMPEDANCE SENSING (ECIS)

6.1. ECIS MONOLAYER RESISTANCE MEASUREMENT

ECIS measurements were performed as described previously[388]. AECs and MLECs were seeded on fibronectin-coated 8W10E+ 8 – well ECIS arrays (gold electrodes) and grown to confluence. Prior to experiments, the medium of the cells was changed and the arrays were set on an ECIS Model 1600R system connected to an incubator (37°C, 5%, CO_2). Normalized resistance values were taken from the measurements at 4000 Hz (64 sec interval) and are presented as the ratio of measured resistance to baseline resistance.

6.2. ECIS MODELING

ECIS software (v1.2.50.0 PC, Applied Biophysics) was used to model specific morphological properties of the monolayer including the barrier function and

attachment to the substratum[239]. In order to mathematically model those properties, the resistance and capacitance of cell-free electrode (1 well of each ECIS experiment) was measured at 4 different AC frequencies (1000 Hz, 4000 Hz, 16 000 Hz and 64 000 Hz). These measurements were used as a reference for estimating the impedance changes attributed to the cell monolayer alone. Using the model of Giaever and Keese, the measured impedance was broken down into three main parameters: Rb – barrier function/junctional stability of the cell layer; α – current flow beneath the cells/monolayer attachment; and Cm – membrane capacitance. Normalized Rb and α values are presented as the ratio of measured parameter to baseline.

7. IMMUNOLOGICAL METHODS

7.1. ELISA

Concentrations of murine IL-1β in BALF were quantified by commercially available sandwich ELISA kit (eBioscience). ELISA was performed according to the instructions of the manufacturer. In short, 96-well flat-bottom plates were incubated with coating antibody (4°C, overnight). The plates were washed two times with washing buffer (PBS containing 0,5% Tween20) and were incubated with blocking solution (assay diluent) for 1h at RT. Following this, standards and undiluted BALF samples were applied and were incubated for 2 h at RT. The plates were then washed 5 times with washing buffer and were incubated with biotinylated detection antibody for 1h at RT. Similarly, murine IL-18 concentration was measured by a specific ELISA (MBL, R&D Systems). In short, the 96-well plates were coated overnight with 0.5 μg/mL anti-mouse IL-18 antibody (MBL) diluted in PBS. The plate was washed and blocked for at least 1 h at RT with 3%BSA in PBS. Standards were prepared with recombinant IL-18 in PBS + 1% BSA (highest standard concentration 1000 pg/mL) and were incubated together with the samples to the plate at RT for 2 h. Following 5 times washing, the plates were incubated with biotinylated detection anti-IL-18 antibody in 1:4000 dilution.

For both IL-1β and IL-18 ELISAs, following the incubation with detection antibody the plates were washed again (5 times) and were incubated in the dark for 30 min with streptavidin-horseradish peroxidase (HRP) at RT. After the incubation was over, the plates were washed 7 times and substrate solution (TMB) was added for 10 min. The reaction was stopped by the addition of 2N H_2O_4 and the optical density was measured in a microplate reader (OD_{450}-Ref:OD_{570}).

7.2. FACS

All flow cytometry data were acquired on FACS CantoII by Dr. Catherine Chaput (Charité Universitätsmedizin Berlin). Gating strategy was processed after exclusion of the doublets. Data were analyzed using the data analysis software, FlowJo (Ashland, OR, USA).

8. MOLECULAR BIOLOGY

8.1. PURIFICATION OF RNA FROM CELLS

RNA was isolated using the "PerfectPure TM RNA Cultured Cell Kit" (5'Prime) according to the manufacturer's instructions. In short, the medium of the cells was removed and they were lysed with 400 µl lysis buffer. The samples were stored at -20°C until further use. The samples were pipetted up and down to assure proper cell lysis and the samples were loaded onto the supplied in the kit purification columns. The columns were centrifuged for 1 min and then washed with 400 µl "Wash 1 solution" per column followed by another centrifugation step (1 min). Next, 50 µL of DNAse solution was added and the columns were incubated at RT. After 15 min of incubation, the columns were washed 2 times with 200µl "DNase wash solution" (1 min) and twice with 200 µl "Wash 2 solution" (1 min; last step 2 min). The RNA was eluted in a new collection tube by adding 50 µl "Elution Solution". All centrifugation steps were carried out at 16 000g/RT. The extracted RNA samples were stored at -80°C.

8.2. RNA REVERSE TRANSCRIPTION TO cDNA

RNA was transcribed to cDNA using High Capacity Reverse Transcription Kit (Applied Biosystems). A mastermix (4.2 µl ddH_2O, 2 µl Reverse Transcription buffer, 2 µl Random Primers, 0.8 µl dNTPs, 1 µl Reverse Transcriptase per reaction) was prepared and 10 µl Mastermix was added to 10 µl purified RNA. The reactions were placed in thermocycler with the following program: 10 min at 25°C, 2 h at 37°C, 5 sec at 85°C. The cDNA samples were diluted with 40 µl ddH_2O and stored at -20°C.

8.3. QUANTITATIVE REAL TIME PCR (qRT PCR)

cDNA samples from epithelial cells were used to measure relative mRNA levels. The mRNA expression was measured using quantitative real time (RT)-PCR. 5 µl of cDNA was added to mastermix containing 10 µl Gene Expression Master Mix (Applied Biosystems), 4 µl ddH_2O and 1 µl Taqman Assay (self-made/probe mix from Applied Biosystems) adding up to a total volume of 20 µl per reaction. Reaction conditions were as follows: 2 min at 50°C, then for 10 min at 95°C followed by 40 amplification cycles (15 sec at 95°C, then 1 min at 60°C). The raw data were evaluated using automatic baseline and automatic Ct and data analysis was done using the $2^{-\Delta\Delta Ct}$ method[389]. *Gapdh* expression was used as an endogenous control for the normalization of the data and the untreated WT control samples were set as 1.

Table 1: Gene expression assays

TaqMan Gene Expression Assays

Target gene	**Assay ID**
Cldn3	Mm00515499_s1
Cldn4	Mm00515514_s1
Cldn18	Mm00517321_m1
Cdh1	Mm01247357_m1
Ocln	Mm00500912_m1

F11r	Mm00554113_m1
Tjp1	Mm01320642_g1
Itga5	Mm01305870_g1
Itgb1	Mm01253229_m1

Self-designed Endogenous Control Primers

Target gene	**Forward and Reverse Primers**	**5'- FAM, 3'- TAMRA probe**
Gapdh	5'- TGT GTC CGT CGT GGA TCT GA 3'- CCT GCT TCA CCA CCT TCT TGA	CCG CCT GGA GAA ACC TGC CAA GTA TG

The self-made gene expression assays were diluted in ddH_2O to concentration 18 nmol/ml (forward and reverse-primer) and 5 nmol/ml (6-FAM-labeled probe).

9. CELL DEATH ASSAYS

9.1. LACTATE DEHYDROGENASE ASSAY

Cellular cytotoxicity and cytolysis were measured with CytoTox 96® (Promega) which is a colorimetric assay detecting the release of lactate dehydrogenase (LDH) in the medium of damaged cells. To quantify cell death, cells were treated with for 3 h with 1 µg/mL PLY (30 min) and cell-free supernatants were collected. The LDH assay was performed according to the manufacturer's protocol. Spontaneous LDH release (control) was measured in the uninfected control supernatants, whereas for maximum LDH release (total) supernatants from Triton X-100- lysed cells was used. In short, 50 µL supernatant was added to 50 µL substrate solution in a 96-well flat bottom plate and the reaction was incubated in the dark (30 min, RT). At the end of the incubation, 50 µL stop solution was added to each well and absorbance was measured

in a plate reader at 490 nm. The percentage of specific LDH release was calculated using the formula:

$\%_{specific} = ((OD_{target} - OD_{control})/(OD_{total} - OD_{control})) \times 100$

9.2. SYTOX STAINING

To measure early cell death events, SYTOX® Orange (Molecular probes, Thermofisher) was used. SYTOX is a nuceic acid stain with very high affinity which does not cross the membranes of living cells. The stain fluoresces in bright orange when excited with 488 nm laser (or any other 450-490 nm source) and this signal is enhanced >500 fold when it is bound to nucleic acids. Monolayers of AECs were pre-incubated with for 10 min with 0.5 µM dye and the increase in fluorescence (F) upon 30 min of 1 µg/mL PLY (30 min) treatment was measured with the help of microplate reader. Excitation was made with 488 nm laser whereas emission was recorded at 530 nm. The percentage SYTOX-positive cells was calculated following the formula:

$\%_{SYTOX^+}$ cells $= ((F_{sample} - F_{baseline})/(F_{total} - F_{baseline})) \times 100$

10. TOTAL INTERNAL REFLECTION FLUORESCENCE MICROSCOPY (TIRFM)

AECs were grown on fibronectin-coated µ-slide 8 well glass bottom slides for 4 days and stained with 5 µl/ml Vybrant DiO cell labeling solution for 10 min at 37 °C prior to the experiment. Life imaging was performed by Dr. Juliane Lippmann (Charité Universitätsmedizin Berlin) with the help of Dr. Thomas Korte in the imaging facility of the Molecular Biophysics group, HU Berlin. Confocal Laser Scanning Microscope (Olympus FV-1000MPE) equipped with a TIRFM upgrade at 37 °C and 5% CO2 using a 63x oil objective and a cooled CCD camera was used. Images were taken at indicated time points and analyzed using FijI by Dr. Juliane Lippmann. Particle analysis was performed from binary images after thresholding (method Isodata). Total intensity of attachment from all detected particles was measured.

11. MICROBIOTA ANALYSIS

Four weeks after birth, female WT and *Nlrp3*-/- mice were housed together in new cages at the animal facility of the Charité Universitätsmedizin Berlin - Forschungseinrichtungen für experimentelle Medizin (FEM) in 1:1 ratio. After four weeks of co-housing, feces and BALF samples were collected from co-housed and separately housed WT and *Nlrp3*-/- mice. In short, feces from each mouse were collected in sterile tubes and then the animals were anesthetized. The mice were then intubated with sterile single-use cannulas and BAL was performed 10 times with 500 µL sterile PBS. The lavage samples were then centrifuged for 10 min at 1500 rpm and the pellet was dissolved in 70% ethanol.

DNA was extracted from each animal and the following analysis of the microbiota was performed by LCG Genomics, Berlin. Beta diversity was calculated via QIIME[390] and Mothur[391]. Shifts in gut and respiratory tract microbiota composition and were calculated by Unifrac Distance analysis[390,392].

12. STATISTICAL ANALYSIS

Data are expressed as mean ± SEM. For comparison of two groups, Mann-Whitney U Test was used. Student t-test was used for the particle analysis of TIRFM data. Data analysis was performed using the Prism software (GraphPad Software, La Jolla, CA). For all statistical analysis, p values < 0.05 were considered significant with $*p < 0.05$, $**p < 0.01$, $***p < 0.001$, $****p < 0.0001$.

13. REAGENTS, ANTIBODIES AND KITS

Table 2: Reagents

Reagent	Manufacturer
Ampuwa® (RNase-free H2O)	Fresenius Kabi
Bacto Twodd Hewitt Broth	BD Biosciences
Bacto Yeast extract	BD Biosciences
Bovine Serum Albumin	Sigma-Aldrich
Columbia Agar + 5% sheep blood	BD Biosciences
Complete protease inhibitor cocktail tablets	Roche
Dispase	BD Biosciences
DMEM high glucose	Gibco
DMSO	Sigma-Aldrich
DNase	Serva
Dynabeads® Biotin Binder	Invitrogen
Dynabeads® Sheep Anti-Rat IgG	Invitrogen
EDTA	Roth
Endothelial Cell Growth Medium MV2 (+ Supplement)	PromoCell
Ethanol	Merck
FCS	PAA
Fibronectin	Sigma-Aldrich
Glycerol	Roth
HBSS	PAA
Heparin	Ratiopharm
HEPES	Biochrom
Human serum albumin	Baxter
Isopropanol	Sigma-Aldrich
SYTOX Orange Nucleic Acid stain	Thermofisher Scientific
Sodium Bicarbonate	Gibco
Ketamine (Ketavet)	Sigma-Aldrich
L-glutamine	PAA
Low-melt agarose	Bio-Rad
LPS	Alexa Biochemicals
NaCl (0.9%)	B. Braun
PBS	Gibco
Penicillin/Streptomycin	PAA
Perfusion solution	Serag-Wiessner

RPMI 1640	Gibco
RBC Lysis Buffer 10X	BioLegend
TaqMan® Gene Expression Master Mix	Applied Biosystems
Trypsin-EDTA	Sigma
Tween®-20	Sigma-Aldrich
Vybrant DiO cell labeling solution	Thermofisher
Xylazine (Rompun 2%)	Bayer

Table 3: Antibodies

Antibody	Manufacturer
biotinylated rat anti-mouse CD45	BD Pharmingen
biotinylated rat anti-mouse CD31	BD Pharmingen
biotinylated rat anti-mouse CD16/32	BD Pharmingen
biotinylated rat anti-mouse CD144	BD Pharmingen
anti-mouse CD326-BV421	Biolegend
anti-mouse CD144-Alex647	Biolegend
anti-mouse CD11c-FITC	Biolegend
anti-mouse SiglecF-PE	BD Pharmigen
anti-mouse Ly6C-PerCp	Biolegend
anti-mouse F4/80-APC	Biolegend
anti-mouse CD45-Alexa700	Biolegend
anti-mouse Ly6G-BV421	Biolegend
anti-mouse CD11b-BV510	Biolegend

Table 4: Kits

Kit	Manufacturer
APC Annexin V Apoptosis Detection Kit with 7-AAD	Biolegend
CytoTox® 96 Assay	Promega
Human Albumin ELISA Quantitation Set	Biomol
Mouse IL-1 beta ELISA Ready-SET-Go!®	EBioscience
Mouse TNF alpha ELISA Ready-SET-Go!®	EBioscience
PerfectPure RNA Cultured Cell Kit	5 PRIME
PerfectTaq™ Plus DNA Polymerase Kit	5 PRIME

13. INSTRUMENTS AND CONSUMMABLES

Table 5: Consumables

Consumable	Manufacturer
Cell strainers (100 µm, 70 µm, 40 µm)	BD Biosciences
Cell culture tubes	Falcon
Cuvettes	Thermo Scientific
8-well ECIS Cultureware™ electrode arrays 8W10E+	Ibidi
ELISA plates	Thermo Scientific
Inoculation Loops	Sarstedt
MicroAmp™ Optical 96-Well Reaction Plates	Applied Biosystems
µSlides 8-Well slides	Ibidi
Serological pipets	Thermo Scientific
Sterile filters	Millipore

Table 6: Instruments

Instrument	Manufacturer
ABI 7300 Real-Time PCR System	Applied Biosystems
BD FACSCanto™	BD Biosciences
Centrifuges	Thermo scientific
Confocal Laser Scanning Microscope FV-1000MPE	Olympus
ECIS Model 1600R	Applied Biophysics
FilterMax F3 Multi-Mode Microplate Reader	Molecular Devices, USA)
Heracell™ 240i CO2 Incubator	Thermo scientific
High pressure syringe (Model No.FMJ-250)	Penn-Century, Inc
Intratracheal Aerosolizer (Model No. IA-IC SIN 2054)	Penn-Century, Inc
Isolated perfused and ventilated mouse lung (IPML) system	Hugo Sachs Elektronik Havard Apparatus
Microcentrifuge 5417R	Eppendorf
Microscope LSM 780	Carl-Zeiss
NanoDrop 2000c	Thermo Scientific
pH Meter 766 Calimatic	Knick
PTC-200 Peltier Thermal cycler	MJ Research
Vortex Mixer VV 3	VW R

V – Appendix

ADDITIONAL DATA

<u>Figure A1</u>: Quantitative changes of gut microbiota in WT and *Nlrp3-/-* mice upon co-housing

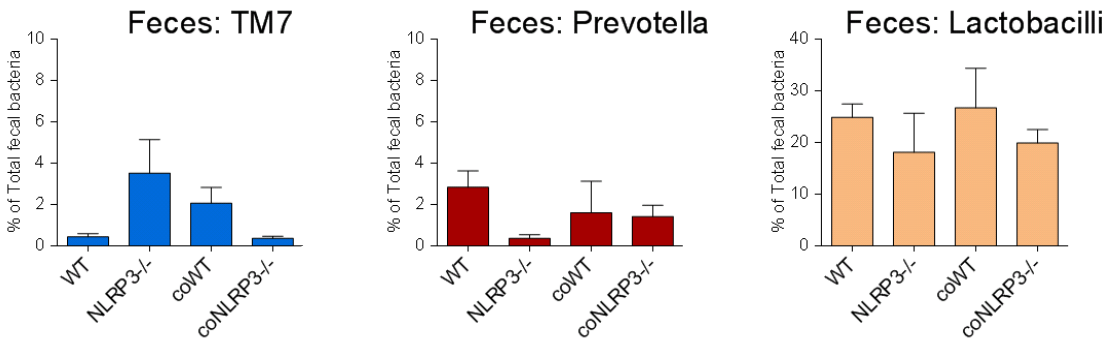

<u>Table A1</u>: Gut microbiota composition changes of WT and *Nlrp3-/-* mice upon co-housing

	WT	NLRP3ko	coWT	coNLRP3ko
Actinobacteria;Actinobacteria;Bifidobacteriales	8,60%	0,44%	1,16%	0,20%
Actinobacteria;Actinobacteria;Coriobacteriales	1,12%	2,24%	0,70%	0,18%
Bacteroidetes;Bacteroidia;Bacteroidales	50,74%	44,66%	39,28%	35,48%
Bacteroidetes;unclassified;unclassified	0,76%	1,30%	1,08%	0,72%
Firmicutes;Bacilli;Lactobacillales	24,88%	18,10%	26,70%	19,92%
Firmicutes;Clostridia;Clostridiales	7,78%	18,62%	20,34%	34,12%
Firmicutes;Clostridia;unclassified	0,02%	0,04%	0,16%	0,08%
Firmicutes;Erysipelotrichia;Erysipelotrichales	2,68%	6,60%	2,72%	2,16%
Firmicutes;unclassified;unclassified	0,48%	1,98%	1,88%	1,40%
Proteobacteria;Betaproteobacteria;Burkholderiales	1,04%	0,58%	0,68%	0,56%
Proteobacteria;Deltaproteobacteria;Desulfovibrionales	0,16%	0,44%	0,44%	0,44%
Proteobacteria;Epsilonproteobacteria;Campylobacterales	0,62%	0,24%	0,12%	0,48%
TM7;TM7_class_incertaesedis;TM7_order_incertae_sedis	0,44%	3,52%	2,06%	0,36%
Verrucomicrobia;Verrucomicrobiae;Verrucomicrobiales	0,20%	0,54%	2,04%	3,22%
unclassified;unclassified;unclassified	0,28%	0,42%	0,56%	0,40%

LIST OF ABBREVIATIONS

6-FAM	6-Carboxyfluorescein
ASC	apoptosis-associated speck-like protein containing a card
ARDS	acute respiratory distress syndrome
ALI	acute lung injury
AMΦ	alveolar macrophage
APC	antigen presenting cell
ATP	adenosine triphosphate
BAL	broncho-alveolar lavage
BMM	bone marrov-derived macrophage
CARD	caspase recruitment domain
CAP	community-aquired pneumonia
CDC	cholesterol-dependent cytolysin
cDNA	complementary deoxyribonucleic acid
CFU	colony-forming unit
cGAMP	cyclic GMP-AMP
cGAS	cyclic GMP-AMP synthase
CLR	C -type lectin receptors
CpG	cytidine-phosphateguanosine DNA sequence
DAMP	damage-associated molecular pattern
DC	dendritic cell
DMEM	Dulbecco's Modified Eagle Medium
DMSO	dimethyl sulfoxide
DNA	deoxyribonucleic acid
EDTA	ethylenediaminetetraacetic acid
ELISA	enzyme-linked immunosorbent assay
FACS	fluorescence-activated cell sorting
FcRγ	Fc receptor γ chain
FCS	fetal calf serum
GAPDH	glyceraldehydes-3-phosphate dehydrogenase
GTPAse	guanosine triphosphate hydrolase
HBSS	Hank's Balanced Salt Solution
HEPES	4-(2-hydroxyethyl)-1-piperazi-neethanesulfonic acid
HIV-1	human immunodeficiency virus 1
HMGB1	high-mobility-groupprotein
HRP	horseradish peroxidase
IgA	imunnoglobulin A
IFN	interferon
IL	interleukin
IL-1R	interleukin-1 receptor
IRF	interferon regulatory factor
ICAM1	intercellular adhesion molecule 1
ITAM	immunoreceptor tyrosinebased activation motif
ITIM	immunorecept or tyrosine-based inhibition motif
LDH	lactate dehydrogenase
LLR	leucine-rich repeat
LPS	lipopolysaccharide
LTA	lipoteichoic acid
LXPTG	Leu-Pro-any-Thr-Gly motif
MAPK	mitogen-activated protein kinases
MCP1	monocyte chemotactic protein 1
MIP-1β	macrophage inflammatory protein 1-beta
MOI	multiplicity of infection
mRNA	messenger ribonucleic acid
MVEC	microvascular endothelial cell
MyD88	myeloid differentiation primary response 88
n. s.	not significant
NADPH	nicotinamide adenine dinucleotide phosphate
NETs	neutrophil extracellular traps
NIMA	never in mitosis A
NF-κB	nuclear factor ‚kappa-light-chain-enhancer' of activated B-cells
NK cell	natural killer cell
NLR	NOD-like receptors
NLRP3	NOD-like receptor family, pyrin domain containing 3

NOD	nucleotide-binding oligomerization domain
p.i.	post infection
PAMP	pathogen-associated molecular pattern
PBS	phosphate-buffered saline
Pen/Strep	Penicillin/Streptomycin
PLY	pneumolysin
PMN	polymorphonuclear neutrophil
PRR	pattern recognition receptors
PYD	pyrin domain
RIG-I	retinoic acid-inducible gene-I
RIPK	receptor-interacting protein kinase
RLRs	RIG-I-like receptors
RNA	ribonucleic acid
ROS	reactive oxygen species
RT-PCR	real-time polymerase chain reaction
SIRS	systemic inflammatory response syndrome
WT	wild-type
S.p.	*Streptococcus pneumonia*
SP	surfactant proteins
SpxB	pyruvate oxidase encoded by spxB
ssRNA	single-stranded dsRNA
STING	stimulator of IFN genes
Syk	spleen tyrosine kinase
TAMRA	5-carboxytetramethylrhodamine
TIR	Toll/interleukin-1 receptor
TIRAP	TIR-containing adaptor protein
TLR	Toll-like receptors
TNF	tumor necrosis factor
TRAM	TRIF-related adaptor molecule
TRIF	TIR-domain-containing adapter-inducing interferon-β
UTR	untranslated region
WHO	World Health Organization

LIST OF FIGURES

LIST OF TABLES

SUMMARY

The sensing of pathogens via the innate immune system is carried out by a plethora of pattern recognition receptors (PRRs). Their proper activation and signaling plays a vital role for the protection of the lung against invading microorganisms. The bacterium *Streptococcus pneumoniae* is the main causative agent of community-acquired pneumonia throughout the world. The condition often progresses to more serious lung injury characterized by life-threatening alveolar leakage due to barrier dysfunction. In the current study, we set out to study the potential involvement of the innate immune sensor NLRP3 for the alveolar barrier function maintenance.

Best known for its ability to form inflammasomes and to regulate the production of Il-1β and IL-18, the role of NLRP3 has been widely studied in cells of myeloid origin. Our data demonstrate that in a model of *S.pneumoniae*-induced pneumonia, NLRP3 facilitates the integrity of the alveolar barrier. Moreover, NLRP3 was shown to play a protective function *ex vivo* experiments with isolated, perfused and ventilated murine lungs as well as *in vitro* studies with primary lung cells treated with the purified bacterial toxin pneumolysin (PLY). Interestingly, we reveal that the beneficial effect of NLRP3 on the lung barrier is independent of the classical inflammasome function and of the inflammasome-dependent cytokines IL-1β and IL-18. We show that NLRP3 improves the integrity of alveolar epithelial cell (AEC) monolayers *in vitro* by promoting cellular adherence to the extracellular matrix.

In summary, this work uncovers a hitherto unknown function of the NLRP3 protein which is involved in epithelial barrier function and is independent of the inflammasome.

ZUSAMMENFASSUNG

Pathogene werden vom angeborenen Immunsystem über eine Vielzahl an „pattern recognition“-Rezeptoren (PRRs) erkannt. Deren angemessene Aktivierung und Signalweiterleitung sind essentiell, um die Lunge vor eindringenden Mikroorganismen zu schützen. Das Bakterium *Streptococcus pneumoniae* ist weltweit der Hauptverursacher von ambulant erworbener Pneumonie. Der Verlauf einer solchen Lungenentzündung geht oft mit der Entstehung von schweren Schädigungen der Lunge einher, die durch lebensbedrohliche alveolare Durchlässigkeit, aufgrund von Barriere-Dysfunktion gekennzeichnet ist. Das Ziel der vorliegenden Arbeit war es, die potentielle Beteiligung des angeborenen Immun-Sensors NLRP3 an der Erhaltung der alveolaren Barriere-Funktion zu untersuchen.

Die Rolle von NLRP3, welches bekannt ist durch seine Fähigkeit, Inflammasome zu bilden und die Produktion von Il-1β und IL-18 zu regulieren, wurde weitgehend in Zellen mit myeloider Herkunft untersucht. Unsere Daten zeigen, dass NLRP3 in einem Modell der *S. pneumoniae*-induzierten Pneumonie die Integrität der alveolaren Barriere unterstützt. Außerdem konnte gezeigt werden, dass NLRP3 sowohl in *ex vivo* Experimenten mit isolierten, perfundierten und ventilierten murinen Lungen, als auch in *in vitro* Experimenten mit primären, Pneumolysin (PLY)-behandelten Lungenzellen eine protektive Funktion hat. Interessanterweise stellte sich heraus, dass der vorteilhafte Effekt von NLRP3 auf die Lungenbarriere unabhängig von der klassischen Inflammasom-Aktivität und der Inflammasom-abhängigen Zytokine IL-1β und IL-18 ist. Wir konnten zeigen, dass NLRP3 die Integrität der alveolaren Epithelzell (AEC)-Schicht *in vitro* durch die Unterstützung der zellulären Adhärenz an die extrazelluläre Matrix verbessert.

Zusammenfassend deckt diese Arbeit eine bisher unbekannte Funktion des NLRP3 Proteins auf, welche an der epithelialen Barriere-Funktion beteiligt ist, unabhängig vom Inflammasom.

For reasons of data protection, the curriculum vitae is not published in the electronic version

For reasons of data protection, the curriculum vitae is not published in the electronic version

VI – Bibliography

1. Charles A Janeway, J., Travers, P., Walport, M. & Shlomchik, M. J. The front line of host defense. (2001).
2. Rhoades, R. and D. R. B. Medical Physiology: Principles for Clinical Medicine. *ippincott Williams & Wilkins* 258–266 (1982).
3. Jones, G. S., Miles, P. R., Lantz, R. C., Hinton, D. E. & Castranova, V. Ionic content and regulation of cellular volume in rat alveolar type II cells. *J. Appl. Physiol.* **53,** (1982).
4. Donald M. Haies, Joan Gil, and E. R. W. Morphometric Study of Rat Lung Cells I. Numerical and Dimensional Characteristics of Parenchymal Cell Population. *Am. Rev. Respir. Dis.* **123,** (1980).
5. James D. Crapo, Stephen L. Young, Evan K. Fram, Kent E. Pinkerton, Brenda E. Barry, and R. O. C. Morphometric Characteristics of Cells in the Alveolar Region of Mammalian Lungs. *Am. Rev. Respir. Dis.* **128,** (1983).
6. King, R. J. Pulmonary surfactant. *J. Appl. Physiol.* **53,** (1982).
7. Griese, M. Pulmonary surfactant in health and human lung diseases: state of the art. *Eur. Respir. J.* **13,** 1455 (1999).
8. Kim, C. F. B. *et al.* Identification of Bronchioalveolar Stem Cells in Normal Lung and Lung Cancer. *Cell* **121,** 823–835 (2005).
9. Pope, F. M. The importance of pneumonia as a cause of death. *Br. Med. J.* **1,** 1363 (1911).
10. Henrichsen, J. Typing of Streptococcus pneumoniae: past, present, and future. *Am. J. Med.* **107,** 50–54 (1999).
11. Lanzendörfer, C., Lanzendörfer, R. & Schardelmann, H. Entzündliche Erkrankungen und Aids. *Inn. Med.* (1998).
12. Musher, D. M. & Thorner, A. R. Community-Acquired Pneumonia. *N. Engl. J. Med.* **371,** 1619–1628 (2014).
13. Walker, C., Rudan, I., Liu, L., Nair, H. & Theodoratou, E. Global burden of childhood pneumonia and diarrhoea. *Lancet* (2013).
14. World Health Organization. Pneumonia. Fact Sheet. (2013).
15. Kadioglu, A., Weiser, J. N., Paton, J. C. & Andrew, P. W. The role of Streptococcus pneumoniae virulence factors in host respiratory colonization and disease. *Nat. Rev. Microbiol.* **6,** 288–301 (2008).
16. Daniels, C. C., Rogers, P. D. & Shelton, C. M. A Review of Pneumococcal Vaccines: Current Polysaccharide Vaccine Recommendations and Future Protein Antigens. *J. Pediatr. Pharmacol. Ther.* **21,** 27–35
17. Barnett, T. C. *et al.* Streptococcal toxins: role in pathogenesis and disease. *Cell. Microbiol.* **17,** 1721–41 (2015).
18. Kim, L., McGee, L., Tomczyk, S. & Beall, B. Biological and Epidemiological Features of Antibiotic-Resistant Streptococcus pneumoniae in Pre- and Post-Conjugate Vaccine Eras: a United States Perspective. *Clin. Microbiol. Rev.* **29,** 525–52 (2016).
19. Louie, J., Jean, C., Chen, T., Park, S. & Ueki, R. Bacterial coinfections in lung tissue specimens from fatal cases of 2009 pandemic influenza A (H1N1)-United States, May-August 2009. *Morb. Mortal.* (2009).
20. Severe methicillin-resistant Staphylococcus aureus community-acquired pneumonia associated with influenza--Louisiana and Georgia, December 2006-January. *MMWR. Morb.* (2007).
21. Sheng, Z., Chertow, D. & Ambroggio, X. Autopsy series of 68 cases dying before and during the 1918 influenza pandemic peak. *Proc.* (2011).
22. Johansson, N. & Kalin, M. Etiology of community-acquired pneumonia: increased microbiological yield with new diagnostic methods. *Clin. Infect.* (2010).
23. Oosterheert, J. & Loon, A. Van. Impact of rapid detection of viral and atypical bacterial pathogens by real-time polymerase chain reaction for patients with lower respiratory tract

infection. *Clin. Infect.* (2005).
24. Pavia, A. What is the role of respiratory viruses in community-acquired pneumonia?: What is the best therapy for influenza and other viral causes of community-acquired. *Infect. Dis. Clin. North Am.* (2013).
25. Song, J.-H., Dagan, R., Klugman, K. P. & Fritzell, B. The relationship between pneumococcal serotypes and antibiotic resistance. *Vaccine* **30,** 2728–2737 (2012).
26. Sandgren, A., Sjöström, K. & Liljequist, B. Effect of clonal and serotype-specific properties on the invasive capacity of Streptococcus pneumoniae. *J. Infect.* (2004).
27. Fenoll, A., Granizo, J. & Aguilar, L. Temporal trends of invasive Streptococcus pneumoniae serotypes and antimicrobial resistance patterns in Spain from 1979 to 2007. *J. Clin.* (2009).
28. Dagan, R. & Klugman, K. Impact of conjugate pneumococcal vaccines on antibiotic resistance. *Lancet Infect. Dis.* (2008).
29. Högberg, L., Geli, P. & Ringberg, H. Age-and serogroup-related differences in observed durations of nasopharyngeal carriage of penicillin-resistant pneumococci. *J. Clin.* (2007).
30. Song, J., Jung, S., Ko, K., Kim, N. & Son, J. High prevalence of antimicrobial resistance among clinical Streptococcus pneumoniae isolates in Asia (an ANSORP study). *Antimicrob. agents* (2004).
31. Hackel, M. *et al.* Serotype prevalence and antibiotic resistance in Streptococcus pneumoniae clinical isolates among global populations. *Vaccine* **31,** 4881–4887 (2013).
32. Farrell, D. & Klugman, K. Increased antimicrobial resistance among nonvaccine serotypes of Streptococcus pneumoniae in the pediatric population after the introduction of 7-valent. *Pediatr. Infect.* (2007).
33. Imöhl, M., Reinert, R. & Linden, M. van der. Regional differences in serotype distribution, pneumococcal vaccine coverage, and antimicrobial resistance of invasive pneumococcal disease among German. *Int. J. Med.* (2010).
34. Reinert, R. & Linden, M. Van der. Molecular epidemiology of penicillin-non-susceptible Streptococcus pneumoniae isolates from children with invasive pneumococcal disease in Germany. *Clin. Microbiol.* (2007).
35. Mitchell, A. M. & Mitchell, T. J. Streptococcus pneumoniae: virulence factors and variation. *Clin. Microbiol. Infect.* **16,** 411–418 (2010).
36. Throup, J., Koretke, K. & Bryant, A. A genomic analysis of two-component signal transduction in Streptococcus pneumoniae. *Molecular* (2000).
37. Maus, U. A. *et al.* Pneumolysin-induced lung injury is independent of leukocyte trafficking into the alveolar space. *J. Immunol.* (2004). doi:citeulike-article-id:10470671
38. Bryant, J. C. *et al.* Pyruvate oxidase of Streptococcus pneumoniae contributes to pneumolysin release. *BMC Microbiol.* **16,** 271 (2016).
39. Price, K. & Camilli, A. Pneumolysin localizes to the cell wall of Streptococcus pneumoniae. *J. Bacteriol.* (2009).
40. Balachandran, P., Hollingshead, S. & Paton, J. The autolytic enzyme LytA of Streptococcus pneumoniae is not responsible for releasing pneumolysin. *J.* (2001).
41. Dalla Serra, M., Tejuca Martínez, M., Serra, M. & Martínez, M. in *eLS* (John Wiley & Sons, Ltd, 2011). doi:10.1002/9780470015902.a0002655.pub2
42. Tweten, R., Parker, M. & Johnson, A. The cholesterol-dependent cytolysins. *Pore-Forming Toxins* (2001).
43. Alouf, J. Cholesterol-binding cytolytic protein toxins. *Int. J. Med. Microbiol.* (2000).
44. Saunders, F., Mitchell, T. & Walker, J. Pneumolysin, the thiol-activated toxin of Streptococcus pneumoniae, does not require a thiol group for in vitro activity. *Infect.* (1989).
45. Tweten, R. Cholesterol-dependent cytolysins, a family of versatile pore-forming toxins. *Infect. Immun.* (2005).
46. Schmeck, B. *et al.* Streptococcus pneumoniae-induced caspase 6-dependent apoptosis in lung epithelium. *Infect. Immun.* **72,** 4940–7 (2004).
47. Schmeck, B. *et al.* Streptococcus pneumoniae-Induced Caspase 6-Dependent Apoptosis in Lung Epithelium. *Infect. Immun.* **72,** 4940–4947 (2004).
48. Zysk, G. *et al.* Pneumolysin Is the Main Inducer of Cytotoxicity to Brain Microvascular Endothelial Cells Caused by Streptococcus pneumoniae. *Infect. Immun.* **69,** 845–852 (2001).
49. Zahlten, J. *et al.* TLR2- and nucleotide-binding oligomerization domain 2-dependent Krüppel-like factor 2 expression downregulates NF-kappa B-related gene expression. *J. Immunol.* (2010). doi:10.4049/jimmunol.0901798

50. Rubins, J., Duane, P. & Clawson, D. Toxicity of pneumolysin to pulmonary alveolar epithelial cells. *Infect.* (1993).
51. GonzÃ¡lez-Juarbe, N. *et al.* Pore-Forming Toxins Induce Macrophage Necroptosis during Acute Bacterial Pneumonia. *PLOS Pathog.* **11,** e1005337 (2015).
52. Braun, J. S. *et al.* Pneumococcal pneumolysin and H2O2 mediate brain cell apoptosis during meningitis. *J. Clin. Invest.* **109,** 19–27 (2002).
53. Chu, J., Thomas, L., Watkins, S., Franchi, L. & Núnez, G. Cholesterol-dependent cytolysins induce rapid release of mature IL-1ß from murine macrophages in a NLRP3 inflammasome and cathepsin B-dependent. *Biol* (2009).
54. Rogers, P. D. *et al.* Pneumolysin-dependent and -independent gene expression identified by cDNA microarray analysis of THP-1 human mononuclear cells stimulated by Streptococcus pneumoniae. *Infect. Immun.* **71,** 2087–94 (2003).
55. Witzenrath, M. *et al.* Role of pneumolysin for the development of acute lung injury in pneumococcal pneumonia. *Crit. Care Med.* (2006). doi:10.1097/01.CCM.0000220496.48295.A9
56. Rubins, J., Charboneau, D. & Paton, J. Dual function of pneumolysin in the early pathogenesis of murine pneumococcal pneumonia. *J. Clin.* (1995).
57. Koppe, U. *et al.* Streptococcus pneumoniae stimulates a STING- and IFN regulatory factor 3-dependent type I IFN production in macrophages, which regulates RANTES production in macrophages, cocultured alveolar epithelial cells, and mouse lungs. *J. Immunol.* **188,** 811–7 (2012).
58. Coffey, T., Enright, M. & Daniels, M. Recombinational exchanges at the capsular polysaccharide biosynthetic locus lead to frequent serotype changes among natural isolates of Streptococcus. *Molecular* (1998).
59. Sørensen, U., Henrichsen, J., Chen, H. & Szu, S. Covalent linkage between the capsular polysaccharide and the cell wall peptidoglycan of Streptococcus pneumoniae revealed by immunochemical methods. *Microb. Pathog.* (1990).
60. Watson, D. & Musher, D. Interruption of capsule production in Streptococcus pneumonia serotype 3 by insertion of transposon Tn916. *Infect. Immun.* (1990).
61. Hyams, C., Camberlein, E., Cohen, J. & Bax, K. The Streptococcus pneumoniae capsule inhibits complement activity and neutrophil phagocytosis by multiple mechanisms. *Infect.* (2010).
62. Jedrzejas, M. Pneumococcal virulence factors: structure and function. *Microbiol. Mol. Biol. Rev.* (2001).
63. Poll, T. van der & Opal, S. Pathogenesis, treatment, and prevention of pneumococcal pneumonia. *Lancet* (2009).
64. Pericone, C., Park, S. & Imlay, J. Factors contributing to hydrogen peroxide resistance in Streptococcus pneumoniae include pyruvate oxidase (SpxB) and avoidance of the toxic effects of the Fenton. *J. Bacteriol.* (2003).
65. Pesakhov, S., Benisty, R., Sikron, N. & Cohen, Z. Effect of hydrogen peroxide production and the Fenton reaction on membrane composition of Streptococcus pneumoniae. *Biophys. Acta (BBA …* (2007).
66. Feldman, C., Anderson, R., Cockeran, R. & Mitchell, T. The effects of pneumolysin and hydrogen peroxide, alone and in combination, on human ciliated epithelium in vitro. *Respiratory* (2002).
67. Kobayashi, K., Salathé, M. & Pratt, M. Mechanism of hydrogen peroxide-induced inhibition of sheep airway cilia. *Am. J.* (1992).
68. Relative roles of pneumolysin and hydrogen peroxide from Streptococcus pneumoniae in inhibition of ependymal ciliary beat frequency. *Infect.* (2000).
69. Okahashi, N., Nakata, M., Sumitomo, T. & Terao, Y. Hydrogen peroxide produced by oral streptococci induces macrophage cell death. *PLoS* (2013).
70. Bellingan, G. J. The pulmonary physician in critical care * 6: The pathogenesis of ALI/ARDS. *Thorax* **57,** 540–546 (2002).
71. Monnet, X. *et al.* Assessing pulmonary permeability by transpulmonary thermodilution allows differentiation of hydrostatic pulmonary edema from ALI/ARDS. *Intensive Care Med.* **33,** 448–53 (2007).
72. Frenzel, J. *et al.* Outcome prediction in pneumonia induced ALI/ARDS by clinical features and peptide patterns of BALF determined by mass spectrometry. *PLoS One* **6,** e25544 (2011).
73. Schutte, H. *et al.* Bronchoalveolar and systemic cytokine profiles in patients with ARDS,

severe pneumonia and cardiogenic pulmonary oedema. *Eur. Respir. J.* **9,** 1858–1867 (1996).
74. Wheeler, A. P. & Bernard, G. R. Acute lung injury and the acute respiratory distress syndrome: a clinical review. *Lancet (London, England)* **369,** 1553–64 (2007).
75. Slevogt, H. *et al.* CEACAM1 inhibits Toll-like receptor 2-triggered antibacterial responses of human pulmonary epithelial cells. *Nat. Immunol.* (2008). doi:10.1038/ni.1661
76. Martin, G. S. *et al.* A randomized, controlled trial of furosemide with or without albumin in hypoproteinemic patients with acute lung injury. *Crit. Care Med.* **33,** 1681–7 (2005).
77. Medford, A. R. L. & Millar, A. B. Vascular endothelial growth factor (VEGF) in acute lung injury (ALI) and acute respiratory distress syndrome (ARDS): paradox or paradigm? *Thorax* **61,** 621–6 (2006).
78. Bianchi, M. DAMPs, PAMPs and alarmins: all we need to know about danger. *J. Leukoc. Biol.* (2007).
79. Janeway, C. A. & Medzhitov, R. Innate immune recognition. *Annu. Rev. Immunol.* **20,** 197–216 (2002).
80. Vance, R., Isberg, R. & Portnoy, D. Patterns of pathogenesis: discrimination of pathogenic and nonpathogenic microbes by the innate immune system. *Cell Host Microbe* (2009).
81. Opitz, B., Laak, V. van & Eitel, J. Innate immune recognition in infectious and noninfectious diseases of the lung. *Am. J.* (2010).
82. Kumar, S., Ingle, H. & Prasad, D. Recognition of bacterial infection by innate immune sensors. *Crit. Rev.* (2013).
83. Chaplin, D. Overview of the immune response. *J. Allergy Clin. Immunol.* (2010).
84. Kolaczkowska, E. & Kubes, P. Neutrophil recruitment and function in health and inflammation. *Nat. Rev. Immunol.* (2013).
85. Bauernfeind, F., Horvath, G. & Stutz, A. Cutting edge: NF-κB activating pattern recognition and cytokine receptors license NLRP3 inflammasome activation by regulating NLRP3 expression. *J.* (2009). at
86. Franchi, L., Eigenbrod, T. & Núñez, G. Cutting edge: TNF-α mediates sensitization to ATP and silica via the NLRP3 inflammasome in the absence of microbial stimulation. *J. Immunol.* (2009).
87. Marcobal, A. *et al.* Consumption of Human Milk Oligosaccharides by Gut-Related Microbes. *J. Agric. Food Chem.* **58,** 5334–5340 (2010).
88. Marcobal, A. & Sonnenburg, J. L. Human milk oligosaccharide consumption by intestinal microbiota. *Clin. Microbiol. Infect.* **18 Suppl 4,** 12–5 (2012).
89. Perez, P. F. *et al.* Bacterial Imprinting of the Neonatal Immune System: Lessons From Maternal Cells? *Pediatrics* **119,** (2007).
90. Kumar, H., Kawai, T. & Akira, S. Pathogen recognition by the innate immune system. *Int. Rev. Immunol.* (2011).
91. Janeway, C. Approaching the asymptote? Evolution and revolution in immunology. *Cold Spring Harb. Symp. Quant.* (1989).
92. Kawai, T. & Akira, S. The role of pattern-recognition receptors in innate immunity: update on Toll-like receptors. *Nat. Immunol.* **11,** 373–384 (2010).
93. Medzhitov, R. & Horng, T. Transcriptional control of the inflammatory response. *Nat. Rev. Immunol.* (2009).
94. Deretic, V., Saitoh, T. & Akira, S. Autophagy in infection, inflammation and immunity. *Nat. Rev. Immunol.* (2013).
95. Lamkanfi, M. & Dixit, V. Mechanisms and functions of inflammasomes. *Cell* (2014).
96. Drummond, R. & Brown, G. The role of Dectin-1 in the host defence against fungal infections. *Curr. Opin. Microbiol.* (2011).
97. Brubaker, S. W., Bonham, K. S., Zanoni, I. & Kagan, J. C. Innate immune pattern recognition: a cell biological perspective. *Annu. Rev. Immunol.* **33,** 257–90 (2015).
98. O'Neill, L. & Bowie, A. The family of five: TIR-domain-containing adaptors in Toll-like receptor signalling. *Nat. Rev. Immunol.* (2007).
99. Poltorak, A., He, X., Smirnova, I. & Liu, M. Defective LPS signaling in C3H/HeJ and C57BL/10ScCr mice: mutations in Tlr4 gene. (1998).
100. Masahiro, Yamamoto Sato, Shintaro Hemmi, Hiroaki Sanjo, Hideki Uematsu, Satoshi Kaisho, Tsuneyasu Hoshino, Katsuaki Takeuchi, Osamu Kobayashi, Masaya Fujita, Takashi Takeda, Kiyoshi & Akira, S. Essential role for TIRAP in activation of the signalling cascade shared by TLR2 and TLR4. *Nature* (2002).

101. Zelensky, A. & Gready, J. The C-type lectin-like domain superfamily. *Febs J.* (2005).
102. Saijo, S. *et al.* Dectin-2 Recognition of α-Mannans and Induction of Th17 Cell Differentiation Is Essential for Host Defense against Candida albicans. *Immunity* **32,** 681–691 (2010).
103. Rogers, N. C. *et al.* Syk-Dependent Cytokine Induction by Dectin-1 Reveals a Novel Pattern Recognition Pathway for C Type Lectins. *Immunity* **22,** 507–517 (2005).
104. Sancho, D. & Sousa, C. e. Signaling by myeloid C-type lectin receptors in immunity and homeostasis. *Annu. Rev. Immunol.* (2012).
105. Wu, J. & Chen, Z. Innate immune sensing and signaling of cytosolic nucleic acids. *Annu. Rev. Immunol.* (2014).
106. Yoneyama, M., Kikuchi, M., Natsukawa, T. & Shinobu, N. The RNA helicase RIG-I has an essential function in double-stranded RNA-induced innate antiviral responses. *Nature* (2004).
107. Bruns, A. M., Leser, G. P., Lamb, R. A. & Horvath, C. M. The Innate Immune Sensor LGP2 Activates Antiviral Signaling by Regulating MDA5-RNA Interaction and Filament Assembly. *Mol. Cell* **55,** 771–781 (2014).
108. Li, X.-D. *et al.* Pivotal Roles of cGAS-cGAMP Signaling in Antiviral Defense and Immune Adjuvant Effects. *Science (80-.).* **341,** (2013).
109. Sun, L., Wu, J., Du, F., Chen, X. & Chen, Z. Cyclic GMP-AMP synthase is a cytosolic DNA sensor that activates the type I interferon pathway. *Science (80-.).* (2013).
110. Wu, J. *et al.* Cyclic GMP-AMP is an endogenous second messenger in innate immune signaling by cytosolic DNA. *Science (80-.).* (2013).
111. Burdette, D., Monroe, K., Sotelo-Troha, K. & Iwig, J. STING is a direct innate immune sensor of cyclic di-GMP. *Nature* (2011).
112. Hornung, V., Ablasser, A. & Charrel-Dennis, M. AIM2 recognizes cytosolic dsDNA and forms a caspase-1-activating inflammasome with ASC. *Nature* (2009).
113. Roberts, T., Idris, A., Dunn, J. & Kelly, G. HIN-200 proteins regulate caspase activation in response to foreign cytoplasmic DNA. (2009).
114. Medzhitov, R. & Janeway, C. Innate immunity: the virtues of a nonclonal system of recognition. *Cell* (1997).
115. Takeda, K., Kaisho, T. & Akira, S. Toll-like receptors. *Annu. Rev. Immunol.* (2003).
116. Inohara, N. & Nuñez, G. NODs: intracellular proteins involved in inflammation and apoptosis. *Nat. Rev. Immunol.* (2003).
117. Kobayashi, K., Eynon, E. & Flavell, R. Intracellular debugging. *Nat. Immunol.* (2003).
118. Belkhadir, Y., Subramaniam, R. & Dangl, J. Plant disease resistance protein signaling: NBS–LRR proteins and their partners. *Curr. Opin. Plant Biol.* (2004).
119. Leister, D. Tandem and segmental gene duplication and recombination in the evolution of plant disease resistance genes. *Trends Genet.* (2004).
120. Wilmanski, J. M., Petnicki-Ocwieja, T. & Kobayashi, K. S. NLR proteins: integral members of innate immunity and mediators of inflammatory diseases. *J. Leukoc. Biol.* **83,** 13–30 (2008).
121. Bertin, J., Nir, W., Fischer, C. & Tayber, O. Human CARD4 protein is a novel CED-4/Apaf-1 cell death family member that activates NF-κB. *J. Biol.* (1999).
122. Inohara, N., Koseki, T., Peso, L. del, Hu, Y. & Yee, C. Nod1, an Apaf-1-like activator of caspase-9 and nuclear factor-κB. *J. Biol.* (1999).
123. Chen, G., Shaw, M. & Kim, Y. NOD-like receptors: role in innate immunity and inflammatory disease. *Annu. Rev.* (2009).
124. Zika, E. & Ting, J. Epigenetic control of MHC-II: interplay between CIITA and histone-modifying enzymes. *Curr. Opin. Immunol.* (2005).
125. Schroder, K. & Tschopp, J. The Inflammasomes. *Cell* **140,** 821–832 (2010).
126. Correa, R., Milutinovic, S. & Reed, J. Roles of NOD1 (NLRC1) and NOD2 (NLRC2) in innate immunity and inflammatory diseases. *Biosci. Rep.* (2012).
127. Watanabe, T., Asano, N. & Fichtner-Feigl, S. NOD1 contributes to mouse host defense against Helicobacter pylori via induction of type I IFN and activation of the ISGF3 signaling pathway. *J.* (2010).
128. Sabbah, A., Harnack, R., Frohlich, V. & Tominaga, K. Activation of innate immune antiviral responses by Nod2. *Nature* (2009).
129. Broz, P. & Dixit, V. M. Inflammasomes: mechanism of assembly, regulation and signalling. *Nat. Rev. Immunol.* **16,** 407–420 (2016).
130. Martinon, F., Burns, K. & Tschopp, J. The Inflammasome. *Mol. Cell* **10,** 417–426 (2002).
131. Kayagaki, N. *et al.* Caspase-11 cleaves gasdermin D for non-canonical inflammasome signalling.

Nature **526,** 666–71 (2015).
132. Shi, J. *et al.* Cleavage of GSDMD by inflammatory caspases determines pyroptotic cell death. *Nature* (2015).
133. Moltke, J. von, Ayres, J. & Kofoed, E. Recognition of bacteria by inflammasomes. *Annu. Rev.* (2013).
134. Masters, S. L. *et al.* NLRP1 inflammasome activation induces pyroptosis of hematopoietic progenitor cells. *Immunity* **37,** 1009–23 (2012).
135. Boyden, E. & Dietrich, W. Nalp1b controls mouse macrophage susceptibility to anthrax lethal toxin. *Nat. Genet.* (2006).
136. Ewald, S. & Chavarria-Smith, J. NLRP1 is an inflammasome sensor for Toxoplasma gondii. *Infect.* (2014).
137. Franchi, L., Eigenbrod, T. & Muñoz-Planillo, R. The inflammasome: a caspase-1-activation platform that regulates immune responses and disease pathogenesis. *Nature* (2009).
138. Man, S. M. & Kanneganti, T.-D. Regulation of inflammasome activation. *Immunol. Rev.* **265,** 6–21 (2015).
139. Zhao, Y. *et al.* The NLRC4 inflammasome receptors for bacterial flagellin and type III secretion apparatus. *Nature* (2011).
140. Miao, E., Mao, D. & Yudkovsky, N. Innate immune detection of the type III secretion apparatus through the NLRC4 inflammasome. *Proc.* (2010).
141. Franchi, L., Amer, A. & Body-Malapel, M. Cytosolic flagellin requires Ipaf for activation of caspase-1 and interleukin 1β in salmonella-infected macrophages. *Nature* (2006).
142. Miao, E., Alpuche-Aranda, C., Dors, M. & Clark, A. Cytoplasmic flagellin activates caspase-1 and secretion of interleukin 1β via Ipaf. *Nature* (2006).
143. Mariathasan, S., Newton, K., Monack, D. & Vucic, D. Differential activation of the inflammasome by caspase-1 adaptors ASC and Ipaf. *Nature* (2004).
144. Tenthorey, J., Kofoed, E., Daugherty, M. & Malik, H. Molecular basis for specific recognition of bacterial ligands by NAIP/NLRC4 inflammasomes. *Mol. Cell* (2014).
145. Fernandes-Alnemri, T., Yu, J., Datta, P. & Wu, J. AIM2 activates the inflammasome and cell death in response to cytoplasmic DNA. *Nature* (2009).
146. Rathinam, V., Jiang, Z., Waggoner, S. & Sharma, S. The AIM2 inflammasome is essential for host defense against cytosolic bacteria and DNA viruses. *Nature* (2010).
147. Fernandes-Alnemri, T., Yu, J. & Juliana, C. The AIM2 inflammasome is critical for innate immunity to Francisella tularensis. *Nature* (2010).
148. Jones, J., Kayagaki, N. & Broz, P. Absent in melanoma 2 is required for innate immune recognition of Francisella tularensis. *Proc.* (2010).
149. Xu, H. *et al.* Innate immune sensing of bacterial modifications of Rho GTPases by the Pyrin inflammasome. *Nature* (2014).
150. Man, S. M. & Kanneganti, T.-D. Converging roles of caspases in inflammasome activation, cell death and innate immunity. *Nat. Rev. Immunol.* **16,** 7–21 (2016).
151. Dagenais, M., Skeldon, A. & Saleh, M. The inflammasome: in memory of Dr. Jurg Tschopp. *Cell Death Differ.* **19,** 5–12 (2012).
152. Guarda, G., Zenger, M. & Yazdi, A. Differential expression of NLRP3 among hematopoietic cells. *J.* (2011).
153. Mariathasan, S. *et al.* Cryopyrin activates the inflammasome in response to toxins and ATP. *Nature* **440,** 228–232 (2006).
154. Latz, E., Xiao, T. & Stutz, A. Activation and regulation of the inflammasomes. *Nat. Rev. Immunol.* (2013).
155. Sha, W., Mitoma, H. & Hanabuchi, S. Human NLRP3 inflammasome senses multiple types of bacterial RNAs. *Proc.* (2014).
156. Franchi, L., Eigenbrod, T. & Muñoz-Planillo, R. Cytosolic double-stranded RNA activates the NLRP3 inflammasome via MAVS-induced membrane permeabilization and K+ efflux. *J.* (2014).
157. Dowling, J. & O'Neill, L. Biochemical regulation of the inflammasome. *Crit. Rev. Biochem.* (2012).
158. Harder, J., Franchi, L. & Muñoz-Planillo, R. Activation of the Nlrp3 inflammasome by Streptococcus pyogenes requires streptolysin O and NF-κB activation but proceeds independently of TLR signaling and P2X7. *J.* (2009).
159. He, Y., Hara, H. & Núñez, G. Mechanism and Regulation of NLRP3 Inflammasome

Activation. *Trends Biochem. Sci.* **41,** 1012–1021 (2016).
160. De Nardo, D., De Nardo, C. M. & Latz, E. New Insights into Mechanisms Controlling the NLRP3 Inflammasome and Its Role in Lung Disease. *Am. J. Pathol.* **184,** 42–54 (2014).
161. Bauernfeind, F., Rieger, A. & Schildberg, F. NLRP3 inflammasome activity is negatively controlled by miR-223. *J.* (2012).
162. Haneklaus, M. *et al.* Cutting Edge: miR-223 and EBV miR-BART15 Regulate the NLRP3 Inflammasome and IL-1 Production. *J. Immunol.* **189,** 3795–3799 (2012).
163. Wen, H. *et al.* Fatty acid-induced NLRP3-ASC inflammasome activation interferes with insulin signaling. *Nature* (2011).
164. Nakahira, K., Haspel, J., Rathinam, V. & Lee, S. Autophagy proteins regulate innate immune responses by inhibiting the release of mitochondrial DNA mediated by the NALP3 inflammasome. *Nature* (2011).
165. Juliana, C., Fernandes-Alnemri, T. & Kang, S. Non-transcriptional priming and deubiquitination regulate NLRP3 inflammasome activation. *J. Biol.* (2012).
166. Gross, O., Poeck, H., Bscheider, M. & Dostert, C. Syk kinase signalling couples to the Nlrp3 inflammasome for anti-fungal host defence. *Nature* (2009).
167. Gong, Y. *et al.* Chemical probing reveals insights into the signaling mechanism of inflammasome activation. *Cell Res.* (2010).
168. Compan, V., Baroja-Mazo, A. & López-Castejón, G. Cell volume regulation modulates NLRP3 inflammasome activation. *Immunity* (2012).
169. Mishra, B., Rathinam, V. & Martens, G. Nitric oxide controls the immunopathology of tuberculosis by inhibiting NLRP3 inflammasome-dependent processing of IL-1. *Nature* (2013).
170. Hernandez-Cuellar, E. *et al.* Cutting Edge: Nitric Oxide Inhibits the NLRP3 Inflammasome. *J. Immunol.* **189,** 5113–5117 (2012).
171. Perregaux, D. & Gabel, C. Interleukin-1 beta maturation and release in response to ATP and nigericin. Evidence that potassium depletion mediated by these agents is a necessary and common. *J. Biol. Chem.* (1994).
172. Piccini, A., Carta, S., Tassi, S. & Lasiglié, D. ATP is released by monocytes stimulated with pathogen-sensing receptor ligands and induces IL-1β and IL-18 secretion in an autocrine way. *Proc.* (2008).
173. Muñoz-Planillo, R., Kuffa, P., Martínez-Colón, G. & Smith, B. K+ efflux is the common trigger of NLRP3 inflammasome activation by bacterial toxins and particulate matter. *Immunity* (2013).
174. Petrilli, V., Papin, S., Dostert, C. & Mayor, A. Activation of the NALP3 inflammasome is triggered by low intracellular potassium concentration. *Cell Death* (2007).
175. Franchi, L., Kanneganti, T. & Dubyak, G. Differential requirement of P2X7 receptor and intracellular K+ for caspase-1 activation induced by intracellular and extracellular bacteria. *J. Biol.* (2007).
176. Muñoz-Planillo, R. *et al.* K+ Efflux Is the Common Trigger of NLRP3 Inflammasome Activation by Bacterial Toxins and Particulate Matter. *Immunity* **38,** 1142–1153 (2013).
177. Feldmeyer, L., Keller, M., Niklaus, G., Hohl, D. & Werner, S. The inflammasome mediates UVB-induced activation and secretion of interleukin-1β by keratinocytes. *Curr. Biol.* (2007).
178. Brough, D., Feuvre, R. LE & Wheeler, R. Ca2+ stores and Ca2+ entry differentially contribute to the release of IL-1β and IL-1α from murine macrophages. *J.* (2003).
179. Lee, G., Subramanian, N., Kim, A. & Aksentijevich, I. The calcium-sensing receptor regulates the NLRP3 inflammasome through Ca2+ and cAMP. *Nature* (2012).
180. Murakami, T., Ockinger, J., Yu, J. & Byles, V. Critical role for calcium mobilization in activation of the NLRP3 inflammasome. *Proc.* (2012).
181. Katsnelson, M., Rucker, L. & Russo, H. K+ efflux agonists induce NLRP3 inflammasome activation independently of Ca2+ signaling. *J.* (2015).
182. Allam, R., Lawlor, K., Yu, E. & Mildenhall, A. Mitochondrial apoptosis is dispensable for NLRP3 inflammasome activation but non-apoptotic caspase-8 is required for inflammasome priming. *EMBO* (2014).
183. Latz, E. NOX-free inflammasome activation. *Blood* **116,** (2010).
184. van Bruggen, R. *et al.* Human NLRP3 inflammasome activation is Nox1-4 independent. *Blood* **115,** (2010).
185. Zhou, R., Yazdi, A. S., Menu, P. & Tschopp, J. A role for mitochondria in NLRP3 inflammasome activation. *Nature* **469,** 221–225 (2011).

186. Iyer, S. *et al.* Mitochondrial cardiolipin is required for Nlrp3 inflammasome activation. *Immunity* (2013).
187. Subramanian, N., Natarajan, K., Clatworthy, M. & Wang, Z. The adaptor MAVS promotes NLRP3 mitochondrial localization and inflammasome activation. *Cell* (2013).
188. Park, S., Juliana, C., Hong, S. & Datta, P. The mitochondrial antiviral protein MAVS associates with NLRP3 and regulates its inflammasome activity. *J.* (2013).
189. Ermler, M., Traylor, Z., Patel, K., Schattgen, S. & Vanaja, S. Rift Valley fever virus infection induces activation of the NLRP3 inflammasome. *Virology* (2014).
190. Kayagaki, N., Wong, M., Stowe, I. & Ramani, S. Noncanonical inflammasome activation by intracellular LPS independent of TLR4. (2013).
191. Rathinam, V., Vanaja, S., Waggoner, L. & Sokolovska, A. TRIF licenses caspase-11-dependent NLRP3 inflammasome activation by gram-negative bacteria. *Cell* (2012).
192. Kayagaki, N. *et al.* Non-canonical inflammasome activation targets caspase-11. *Nature* **479,** 117–121 (2011).
193. Faucheu, C. *et al.* A novel human protease similar to the interleukin-1 beta converting enzyme induces apoptosis in transfected cells. *EMBO J.* **14,** 1914–22 (1995).
194. Hagar, J., Powell, D., Aachoui, Y. & Ernst, R. Cytoplasmic LPS activates caspase-11: implications in TLR4-independent endotoxic shock. *Science (80-.).* (2013).
195. Infect. Immun.-2011-Shinji-2215-23.
196. He, Y., Franchi, L. & Núñez, G. The protein kinase PKR is critical for LPS-induced iNOS production but dispensable for inflammasome activation in macrophages. *Eur. J. Immunol.* (2013).
197. Lu, B. *et al.* Novel role of PKR in inflammasome activation and HMGB1 release. *Nature* (2012).
198. Shenoy, A., Wellington, D., Kumar, P. & Kassa, H. GBP5 promotes NLRP3 inflammasome assembly and immunity in mammals. (2012).
199. He, Y., Zeng, M. Y., Yang, D., Motro, B. & Núñez, G. NEK7 is an essential mediator of NLRP3 activation downstream of potassium efflux. *Nature* **530,** 354–357 (2016).
200. Schmid-Burgk, J., Chauhan, D. & Schmidt, T. A genome-wide CRISPR (clustered regularly interspaced short palindromic repeats) screen identifies NEK7 as an essential component of NLRP3 inflammasome. *J. Biol.* (2016).
201. Shi, H. *et al.* NLRP3 activation and mitosis are mutually exclusive events coordinated by NEK7, a new inflammasome component. *Nature* (2015).
202. Koppe, U., Suttorp, N. & Opitz, B. Recognition of Streptococcus pneumoniae by the innate immune system. *Cell. Microbiol.* (2012).
203. Rabes, A., Suttorp, N. & Opitz, B. Inflammasomes in Pneumococcal Infection: Innate Immune Sensing and Bacterial Evasion Strategies. *Inflammasome Signal. Bact.* (2016).
204. Casanova, J. & Abel, L. Human TLRs and IL-1Rs in host defense: natural insights from evolutionary, epidemiological, and clinical genetics. *Annu. Rev.* (2011).
205. Albiger, B., Sandgren, A. & Katsuragi, H. Myeloid differentiation factor 88-dependent signalling controls bacterial growth during colonization and systemic pneumococcal disease in mice. *Cellular* (2005).
206. Koedel, U., Rupprecht, T., Angele, B. & Heesemann, J. MyD88 is required for mounting a robust host immune response to Streptococcus pneumoniae in the CNS. *Brain* (2004).
207. Rossum, A. van & Lysenko, E. Host and bacterial factors contributing to the clearance of colonization by Streptococcus pneumoniae in a murine model. *Infect.* (2005).
208. Echchannaoui, H., Frei, K. & Schnell, C. Toll-like receptor 2–deficient mice are highly susceptible to Streptococcus pneumoniae meningitis because of reduced bacterial clearing and enhanced inflammation. *J. Infect.* (2002).
209. Dessing, M., Florquin, S. & Paton, J. Toll-like receptor 2 contributes to antibacterial defence against pneumolysin-deficient pneumococci. *Cellular* (2008).
210. Malley, R., Henneke, P. & Morse, S. Recognition of pneumolysin by Toll-like receptor 4 confers resistance to pneumococcal infection. *Proc.* (2003).
211. Branger, J., Knapp, S., Weijer, S. & Leemans, J. Role of Toll-like receptor 4 in gram-positive and gram-negative pneumonia in mice. *Infect.* (2004).
212. McNeela, E., Burke, Á., Neill, D. & Baxter, C. Pneumolysin activates the NLRP3 inflammasome and promotes proinflammatory cytokines independently of TLR4. *PLoS* (2010).
213. Albiger, B., Dahlberg, S. & Sandgren, A. Toll-like receptor 9 acts at an early stage in host

defence against pneumococcal infection. *Cellular* (2007).
214. Opitz, B., Püschel, A., Schmeck, B. & Hocke, A. Nucleotide-binding oligomerization domain proteins are innate immune receptors for internalized Streptococcus pneumoniae. *J. Biol.* (2004).
215. Davis, B. K., Wen, H. & Ting, J. P.-Y. The inflammasome NLRs in immunity, inflammation, and associated diseases. *Annu. Rev. Immunol.* **29,** 707–35 (2011).
216. Koppe, U., Högner, K., Doehn, J. & Müller, H. Streptococcus pneumoniae stimulates a STING-and IFN regulatory factor 3-dependent type I IFN production in macrophages, which regulates RANTES production in. *J.* (2012).
217. Witzenrath, M. *et al.* The NLRP3 inflammasome is differentially activated by pneumolysin variants and contributes to host defense in pneumococcal pneumonia. *J. Immunol.* **187,** 434–440 (2011).
218. Lauw, F., Branger, J. & Florquin, S. IL-18 improves the early antimicrobial host response to pneumococcal pneumonia. *J.* (2002).
219. Kafka, D., Ling, E., Feldman, G. & Benharroch, D. Contribution of IL-1 to resistance to Streptococcus pneumoniae infection. *International* (2008).
220. Lemon, J., Miller, M. & Weiser, J. Sensing of interleukin-1 cytokines during Streptococcus pneumoniae colonization contributes to macrophage recruitment and bacterial clearance. *Infect. Immun.* (2015).
221. Marriott, H., Gascoyne, K., Gowda, R. & Geary, I. Interleukin-1β regulates CXCL8 release and influences disease outcome in response to Streptococcus pneumoniae, defining intercellular cooperation between. *Infect.* (2012).
222. Hoegen, T., Tremel, N., Klein, M. & Angele, B. The NLRP3 inflammasome contributes to brain injury in pneumococcal meningitis and is activated through ATP-dependent lysosomal cathepsin B release. *J.* (2011).
223. Kang, Y., Do, Y., Lee, H., Park, S. & Cheong, C. A dominant complement fixation pathway for pneumococcal polysaccharides initiated by SIGN-R1 interacting with C1q. *Cell* (2006).
224. Kang, Y.-S. *et al.* The C-type lectin SIGN-R1 mediates uptake of the capsular polysaccharide of Streptococcus pneumoniae in the marginal zone of mouse spleen. *Proc. Natl. Acad. Sci. U. S. A.* **101,** 215–20 (2004).
225. Arredouani, M., Yang, Z., Ning, Y. & Qin, G. The scavenger receptor MARCO is required for lung defense against pneumococcal pneumonia and inhaled particles. *J.* (2004).
226. Arredouani, M., Yang, Z., Imrich, A. & Ning, Y. The macrophage scavenger receptor SR-AI/II and lung defense against pneumococci and particles. *Am. J.* (2006).
227. Rabes, A. *et al.* The C-Type Lectin Receptor Mincle Binds to Streptococcus pneumoniae but Plays a Limited Role in the Anti-Pneumococcal Innate Immune Response. *PLoS One* **10,** e0117022 (2015).
228. Behler-Janbeck, F. *et al.* C-type Lectin Mincle Recognizes Glucosyl-diacylglycerol of Streptococcus pneumoniae and Plays a Protective Role in Pneumococcal Pneumonia. *PLOS Pathog.* **12,** e1006038 (2016).
229. Clarke, T. B. *et al.* Recognition of peptidoglycan from the microbiota by Nod1 enhances systemic innate immunity. *Nat. Med.* **16,** 228–31 (2010).
230. Belkaid, Y. & Hand, T. W. Role of the microbiota in immunity and inflammation. *Cell* **157,** 121–41 (2014).
231. Elinav, E. *et al.* NLRP6 inflammasome regulates colonic microbial ecology and risk for colitis. *Cell* **145,** 745–57 (2011).
232. Henao-Mejia, J., Elinav, E., Jin, C., Hao, L. & Mehal, W. Inflammasome-mediated dysbiosis regulates progression of NAFLD and obesity. *Nature* (2012).
233. Belkaid, Y. & Hand, T. W. Role of the Microbiota in Immunity and Inflammation. *Cell* **157,** 121–141 (2014).
234. Henao-Mejia, J. *et al.* Inflammasome-mediated dysbiosis regulates progression of NAFLD and obesity. *Nature* **482,** 179–85 (2012).
235. Domon, H. *et al.* Streptococcus pneumoniae disrupts pulmonary immune defence via elastase release following pneumolysin-dependent neutrophil lysis. *Sci. Rep.* **6,** 38013 (2016).
236. Witzenrath - 2011 - The NLRP3 Inflammasome Is Differentially Activated by Pneumolysin Variants and Contributes to Host Defense in Pneumococcal Pneumonia.
237. Witzenrath, M. *et al.* Role of pneumolysin for the development of acute lung injury in pneumococcal pneumonia. *Crit. Care Med.* **34,** 1947–54 (2006).

238. Weibel, E. R. & Gil, J. Electron microscopic demonstration of an extracellular duplex lining layer of alveoli. *Respir. Physiol.* **4,** 42–57 (1968).
239. Giaever, I. & Keese, C. Micromotion of mammalian cells measured electrically. *Natl. Acad. Sci.* (1991).
240. Szulcek, R., Bogaard, H. J. & van Nieuw Amerongen, G. P. Electric cell-substrate impedance sensing for the quantification of endothelial proliferation, barrier function, and motility. *J. Vis. Exp.* (2014). doi:10.3791/51300
241. He, Y., Hara, H. & Núñez, G. Mechanism and Regulation of NLRP3 Inflammasome Activation. *Trends Biochem. Sci.* (2016). doi:10.1016/j.tibs.2016.09.002
242. Al-Sadi, R., Ye, D., Said, H. M. & Ma, T. Y. IL-1β-Induced Increase in Intestinal Epithelial Tight Junction Permeability Is Mediated by MEKK-1 Activation of Canonical NF-κB Pathway. *Am. J. Pathol.* **177,** 2310–2322 (2010).
243. dos Santos, G. *et al.* Vimentin regulates activation of the NLRP3 inflammasome. *Nat. Commun.* **6,** 6574 (2015).
244. LaRock, C. N. *et al.* IL-1β is an innate immune sensor of microbial proteolysis. *Sci. Immunol.* **1,** (2016).
245. Mrsny, R., Brown, G., Gerner-Smidt, K. & Buret, A. A key claudin extracellular loop domain is critical for epithelial barrier integrity. *Am. J.* (2008).
246. Schneeberger, E. Claudins form ion-selective channels in the paracellular pathway. Focus on "Claudin extracellular domains determine paracellular charge selectively and. *Am. J. Physiol.* (2003).
247. Wright, E. M. *et al.* Effects of pH and polyvalent cations on the selective permeability of gall-bladder epithelium to monovalent ions. *Biochim. Biophys. Acta* **163,** 57–74 (1968).
248. Alexandre, M., Jeansonne, B. & Renegar, R. The first extracellular domain of claudin-7 affects paracellular Cl− permeability. *Biochem.* (2007).
249. Itallie, C. Van & Fanning, A. Reversal of charge selectivity in cation or anion-selective epithelial lines by expression of different claudins. *Am. J.* (2003).
250. Itallie, C. Van & Rahner, C. Regulated expression of claudin-4 decreases paracellular conductance through a selective decrease in sodium permeability. *J. Clin.* (2001).
251. Martinon, F., Mayor, A. & Tschopp, J. The inflammasomes: guardians of the body. *Annu. Rev. Immunol.* (2009).
252. Bryant, C. & Fitzgerald, K. Molecular mechanisms involved in inflammasome activation. *Trends Cell Biol.* (2009).
253. Bergsbaken, T., Fink, S. & Cookson, B. Pyroptosis: host cell death and inflammation. *Nat. Rev. Microbiol.* (2009).
254. McNeela, E., Burke, Á., Neill, D. & Baxter, C. Pneumolysin activates the NLRP3 inflammasome and promotes proinflammatory cytokines independently of TLR4. *PLoS* (2010).
255. Karmakar, M., Katsnelson, M. & Malak, H. Neutrophil IL-1β processing induced by pneumolysin is mediated by the NLRP3/ASC inflammasome and caspase-1 activation and is dependent on K+ efflux. *J.* (2015).
256. Ruane, D. *et al.* Microbiota regulate the ability of lung dendritic cells to induce IgA class-switch recombination and generate protective gastrointestinal immune responses. *J. Exp. Med.* (2015).
257. Stanley, D., Geier, M. S., Chen, H., Hughes, R. J. & Moore, R. J. Comparison of fecal and cecal microbiotas reveals qualitative similarities but quantitative differences. *BMC Microbiol.* **15,** 51 (2015).
258. Samuelson, D. R., Welsh, D. A. & Shellito, J. E. Regulation of lung immunity and host defense by the intestinal microbiota. *Front. Microbiol.* **6,** 1085 (2015).
259. Kubinak, J. L. *et al.* MyD88 signaling in T cells directs IgA-mediated control of the microbiota to promote health. *Cell Host Microbe* **17,** 153–63 (2015).
260. Kamada, N., Seo, S.-U., Chen, G. Y. & Núñez, G. Role of the gut microbiota in immunity and inflammatory disease. *Nat. Rev. Immunol.* **13,** 321–335 (2013).
261. Budden, K. F. *et al.* Emerging pathogenic links between microbiota and the gut–lung axis. *Nat. Rev. Microbiol.* **15,** 55–63 (2016).
262. Sze, M. A. *et al.* Changes in the Bacterial Microbiota in Gut, Blood, and Lungs following Acute LPS Instillation into Mice Lungs. *PLoS One* **9,** e111228 (2014).
263. Budden, K., Gellatly, S. & Wood, D. Emerging pathogenic links between microbiota and the gut-lung axis. *Nat. Rev.* (2016).

264. Schuijt, T., Lankelma, J., Scicluna, B. & Melo, F. e. The gut microbiota plays a protective role in the host defence against pneumococcal pneumonia. *Gut* (2016).
265. Fagundes, C., Amaral, F. & Vieira, A. Transient TLR activation restores inflammatory response and ability to control pulmonary bacterial infection in germfree mice. *J.* (2012).
266. Chen, L., Chen, P. & Hsu, C. Commensal microflora contribute to host defense against Escherichia coli pneumonia through Toll-like receptors. *Shock* (2011).
267. Ichinohe, T., Pang, I. & Kumamoto, Y. Microbiota regulates immune defense against respiratory tract influenza A virus infection. *Proc.* (2011).
268. Wu, S. *et al.* Microbiota regulates the TLR7 signaling pathway against respiratory tract influenza A virus infection. *Current* (2013).
269. Elinav, E., Strowig, T., Henao-Mejia, J. & Flavell, R. A. Regulation of the antimicrobial response by NLR proteins. *Immunity* **34,** 665–79 (2011).
270. Periasamy, S. *et al.* Inflammasome-Independent NLRP3 Restriction of a Protective Early Neutrophil Response to Pulmonary Tularemia. *PLOS Pathog.* **12,** e1006059 (2016).
271. Chen, G., Liu, M., Wang, F. & Bertin, J. A functional role for Nlrp6 in intestinal inflammation and tumorigenesis. *J.* (2011).
272. Wlodarska, M., Thaiss, C., Nowarski, R. & Henao-Mejia, J. NLRP6 inflammasome orchestrates the colonic host-microbial interface by regulating goblet cell mucus secretion. *Cell* (2014).
273. Hu, B., Elinav, E., Huber, S. & Strowig, T. Microbiota-induced activation of epithelial IL-6 signaling links inflammasome-driven inflammation with transmissible cancer. *Proc.* (2013).
274. Ther Adv Respir Dis-2015-Hosseinian-1753465815586335.
275. Macia, L., Tan, J., Vieira, A., Leach, K. & Stanley, D. Metabolite-sensing receptors GPR43 and GPR109A facilitate dietary fibre-induced gut homeostasis through regulation of the inflammasome. *Nature* (2015).
276. Zaki, M., Boyd, K., Vogel, P., Kastan, M. & Lamkanfi, M. The NLRP3 inflammasome protects against loss of epithelial integrity and mortality during experimental colitis. *Immunity* (2010).
277. Hirota, S., Ng, J., Lueng, A. & Khajah, M. NLRP3 inflammasome plays a key role in the regulation of intestinal homeostasis. *Inflamm. bowel* (2011).
278. Sellin, M. E., Maslowski, K. M., Maloy, K. J. & Hardt, W.-D. Inflammasomes of the intestinal epithelium. *Trends Immunol.* **36,** 442–50 (2015).
279. Sun, Y., Zhang, M., Chen, C., Gillilland, M. & Sun, X. Stress-induced corticotropin-releasing hormone-mediated NLRP6 inflammasome inhibition and transmissible enteritis in mice. *Gastroenterology* (2013).
280. Levy, M., Thaiss, C., Zeevi, D. & Dohnalova, L. Microbiota-modulated metabolites shape the intestinal microenvironment by regulating NLRP6 inflammasome signaling. *Cell* (2015).
281. Couturier-Maillard, A. & Secher, T. NOD2-mediated dysbiosis predisposes mice to transmissible colitis and colorectal cancer. *J.* (2013).
282. Garrett, W., Lord, G., Punit, S. & Lugo-Villarino, G. Communicable ulcerative colitis induced by T-bet deficiency in the innate immune system. *Cell* (2007).
283. Ivanov, I., Atarashi, K., Manel, N., Brodie, E. & Shima, T. Induction of intestinal Th17 cells by segmented filamentous bacteria. *Cell* (2009).
284. Lozupone, C., Lladser, M. E., Knights, D., Stombaugh, J. & Knight, R. UniFrac: an effective distance metric for microbial community comparison. *ISME J.* **5,** 169–72 (2011).
285. Lutgendorff, F. & Akkermans, L. The role of microbiota and probiotics in stress-induced gastrointestinal damage. *Curr. Mol.* (2008).
286. Cario, E., Gerken, G. & Podolsky, D. Toll-like receptor 2 controls mucosal inflammation by regulating epithelial barrier function. *Gastroenterology* (2007).
287. Rakoff-Nahoum, S., Paglino, J. & Eslami-Varzaneh, F. Recognition of commensal microflora by toll-like receptors is required for intestinal homeostasis. *Cell* (2004).
288. Thomas, P. G. *et al.* The intracellular sensor NLRP3 mediates key innate and healing responses to influenza A virus via the regulation of caspase-1. *Immunity* **30,** 566–75 (2009).
289. Hassane, M. *et al.* Neutrophilic NLRP3 inflammasome-dependent IL-1β secretion regulates the γδT17 cell response in respiratory bacterial infections. *Mucosal Immunol.* (2017). doi:10.1038/mi.2016.113
290. Peeters, P. M. *et al.* Silica-induced NLRP3 inflammasome activation in vitro and in rat lungs. *Part. Fibre Toxicol.* **11,** 58 (2014).
291. Kuipers, M. T. *et al.* Ventilator-induced lung injury is mediated by the NLRP3 inflammasome.

Anesthesiology **116,** 1104–15 (2012).
292. Rabes, Anne; Suttorp, N. O. B. in *Inflammasome Signaling and Bacterial Infections* 215–227 (Springer International Publishing, 2016).
293. Kim, S. R. *et al.* NLRP3 inflammasome activation by mitochondrial ROS in bronchial epithelial cells is required for allergic inflammation. *Cell Death Dis.* **5,** e1498 (2014).
294. Costa, A., Gupta, R., Signorino, G. & Malara, A. Activation of the NLRP3 inflammasome by group B streptococci. *J.* (2012).
295. Ceballos-Olvera, I., Sahoo, M., Miller, M. A., Barrio, L. del & Re, F. Inflammasome-dependent Pyroptosis and IL-18 Protect against Burkholderia pseudomallei Lung Infection while IL-1β Is Deleterious. *PLoS Pathog.* **7,** e1002452 (2011).
296. Rijneveld, A., Florquin, S. & Branger, J. TNF-α compensates for the impaired host defense of IL-1 type I receptor-deficient mice during pneumococcal pneumonia. *J.* (2001).
297. Karmakar, M., Katsnelson, M. & Malak, H. Neutrophil IL-1β processing induced by pneumolysin is mediated by the NLRP3/ASC inflammasome and caspase-1 activation and is dependent on K+ efflux. *J.* (2015).
298. Hsu, L. *et al.* IL-1□-driven neutrophilia preserves antibacterial defense in the absence of the kinase IKKb. *Nature*
299. Biondo, C., Mancuso, G., Midiri, A. & Signorino, G. The interleukin-1β/CXCL1/2/neutrophil axis mediates host protection against group B streptococcal infection. *Infect.* (2014).
300. Garvy, B. & Harmsen, A. The importance of neutrophils in resistance to pneumococcal pneumonia in adult and neonatal mice. *Inflammation* (1996).
301. Craig, A., Mai, J., Cai, S. & Jeyaseelan, S. Neutrophil recruitment to the lungs during bacterial pneumonia. *Infect. Immun.* (2009).
302. Jones, M., Simms, B. & Lupa, M. Lung NF-κB activation and neutrophil recruitment require IL-1 and TNF receptor signaling during pneumococcal pneumonia. *J.* (2005).
303. Yang, H., Ko, H., Yang, J. & Kim, J. Interleukin-1 promotes coagulation which is necessary for protective immunity in the lung against Streptococcus pneumoniae infection. *J. Infect.* (2012).
304. Lin, A., Beasley, F., Keller, N., Hollands, A. & Urbano, R. A group A Streptococcus ADP-ribosyltransferase toxin stimulates a protective interleukin 1β-dependent macrophage immune response. *MBio* (2015).
305. Mitchell, A., Yau, B., McQuillan, J. & Ball, H. Inflammasome-dependent IFN-γ drives pathogenesis in Streptococcus pneumoniae meningitis. *J.* (2012).
306. LaRock, C. N. & Cookson, B. T. Burning Down the House: Cellular Actions during Pyroptosis. *PLoS Pathog.* **9,** e1003793 (2013).
307. Miettinen, M., Matikainen, S. & Vuopio-Varkila, J. Lactobacilli and streptococci induce interleukin-12 (IL-12), IL-18, and gamma interferon production in human peripheral blood mononuclear cells. *Infect.* (1998).
308. Fang, R., Hara, H. & Sakai, S. Type I interferon signaling regulates activation of the absent in melanoma 2 inflammasome during Streptococcus pneumoniae infection. *Infect.* (2014).
309. Fang, R., Tsuchiya, K., Kawamura, I. & Shen, Y. Critical roles of ASC inflammasomes in caspase-1 activation and host innate resistance to Streptococcus pneumoniae infection. *J.* (2011).
310. Shigeoka, A. A. *et al.* An Inflammasome-Independent Role for Epithelial-Expressed Nlrp3 in Renal Ischemia-Reperfusion Injury. *J. Immunol.* **185,** 6277–6285 (2010).
311. Pulskens, W. P. *et al.* Nlrp3 prevents early renal interstitial edema and vascular permeability in unilateral ureteral obstruction. *PLoS One* **9,** e85775 (2014).
312. Wang, H. *et al.* Inflammasome-independent NLRP3 is required for epithelial-mesenchymal transition in colon cancer cells. *Exp. Cell Res.* **342,** 184–192 (2016).
313. Wang, W. *et al.* Inflammasome-independent NLRP3 augments TGF-β signaling in kidney epithelium. *J. Immunol.* **190,** 1239–49 (2013).
314. Feldman, C., Munro, N. & Jeffery, P. Pneumolysin induces the salient histologic features of pneumococcal infection in the rat lung in vivo. *Am J Respir Cell* (1991).
315. Mitchell, T. J. *et al.* The NLRP3 Inflammasome Is Differentially. doi:10.4049/jimmunol.1003143
316. Marriott, H. M., Mitchell, T. J. & Dockrell, D. H. Pneumolysin: A Double-Edged Sword During the Host-Pathogen Interaction.
317. Xiang, M. *et al.* Hemorrhagic Shock Activation of NLRP3 Inflammasome in Lung Endothelial

Cells. *J. Immunol.* **187,** (2011).
318. Lucas, R., Yang, G. & Gorshkov, B. Protein kinase C-α and arginase I mediate pneumolysin-induced pulmonary endothelial hyperpermeability. *Respir. cell …* (2012).
319. Witzenrath, M., Gutbier, B. & Owen, J. Role of platelet-activating factor in pneumolysin-induced acute lung injury. *Crit. care* (2007).
320. Shen, Q., Rigor, R. & Pivetti, C. Myosin light chain kinase in microvascular endothelial barrier function. *Cardiovascular* (2010).
321. Marriott, H., Ali, F., Read, R., Mitchell, T. & Whyte, M. Nitric oxide levels regulate macrophage commitment to apoptosis or necrosis during pneumococcal infection. *FASEB J.* (2004).
322. Braun, J., Novak, R., Gao, G. & Murray, P. Pneumolysin, a protein toxin of Streptococcus pneumoniae, induces nitric oxide production from macrophages. *Infect.* (1999).
323. Orman, K. & Shenep, J. Pneumococci stimulate the production of the inducible nitric oxide synthase and nitric oxide by murine macrophages. *J. Infect.* (1998).
324. Bonnans, C. & Levy, B. D. Lipid Mediators as Agonists for the Resolution of Acute Lung Inflammation and Injury. *Am. J. Respir. Cell Mol. Biol.* **36,** 201–205 (2007).
325. Shigematsu, M. *et al.* Leukotriene B4 receptor type 2 protects against pneumolysin-dependent acute lung injury. *Sci. Rep.* **6,** 34560 (2016).
326. Allen, I. C. *et al.* The NLRP3 inflammasome mediates in vivo innate immunity to influenza A virus through recognition of viral RNA. *Immunity* **30,** 556–65 (2009).
327. Peeters, P. M., Perkins, T. N., M Wouters, E. F., Mossman, B. T. & Reynaert, N. L. Silica induces NLRP3 inflammasome activation in human lung epithelial cells. doi:10.1186/1743-8977-10-3
328. McGilligan, V. E. *et al.* Staphylococcus aureus Activates the NLRP3 Inflammasome in Human and Rat Conjunctival Goblet Cells. *PLoS One* **8,** e74010 (2013).
329. Liu, Z., Zaki, M., Vogel, P., Gurung, P. & Finlay, B. Role of inflammasomes in host defense against Citrobacter rodentium infection. *J. Biol.* (2012).
330. Song-Zhao, G., Srinivasan, N., Pott, J. & Baban, D. Nlrp3 activation in the intestinal epithelium protects against a mucosal pathogen. *Mucosal* (2014).
331. Nordlander, S., Pott, J. & Maloy, K. NLRC4 expression in intestinal epithelial cells mediates protection against an enteric pathogen. *Mucosal Immunol.* (2014).
332. Shigeoka, A. A. *et al.* An inflammasome-independent role for epithelial-expressed Nlrp3 in renal ischemia-reperfusion injury. *J. Immunol.* **185,** 6277–85 (2010).
333. LaFemina, M. & Rokkam, D. Keratinocyte growth factor enhances barrier function without altering claudin expression in primary alveolar epithelial cells. *Am. J.* (2010).
334. Shen, L., Weber, C. & Turner, J. The tight junction protein complex undergoes rapid and continuous molecular remodeling at steady state. *J. Cell Biol.* (2008).
335. Shen, L., Weber, C., Raleigh, D. & Yu, D. Tight junction pore and leak pathways: a dynamic duo. *Annu. Rev.* (2011).
336. Furuse, M., Sasaki, H. & Fujimoto, K. A single gene product, claudin-1 or-2, reconstitutes tight junction strands and recruits occludin in fibroblasts. *J. cell* (1998).
337. Van Itallie, C. M. *et al.* The density of small tight junction pores varies among cell types and is increased by expression of claudin-2. *J. Cell Sci.* **121,** 298–305 (2008).
338. Shen, L., Weber, C. R., Raleigh, D. R., Yu, D. & Turner, J. R. Tight Junction Pore and Leak Pathways: A Dynamic Duo. *Annu. Rev. Physiol.* **73,** 283–309 (2011).
339. Li, J., Zhuo, M., Pei, L., Rajagopal, M. & Alan, S. Comprehensive cysteine-scanning mutagenesis reveals claudin-2 pore-lining residues with different intrapore locations. *J. Biol. Chem.* (2014).
340. Goldmann, O., Tuchscherr, L., Rohde, M. & Medina, E. α-hemolysin enhances *Staphylococcus aureus* internalization and survival within mast cells by modulating the expression of β1 integrin. *Cell. Microbiol.* (2015). doi:10.1111/cmi.12550
341. Dube, P. H., Thinwa, J., Segovia, J. A. & Bose, S. Epithelial Cells Inflammasome Activation in Intestinal Integrin-Mediated First Signal for Integrin-Mediated First Signal for Inflammasome Activation in Intestinal Epithelial Cells. *J. Immunol.* **193,** 1373–1382 (2014).
342. Jun, H.-K., Lee, S.-H., Lee, H.-R. & Choi, B.-K. Integrin α5β1 activates the NLRP3 inflammasome by direct interaction with a bacterial surface protein. *Immunity* **36,** 755–68 (2012).
343. Frey, T. Nucleic acid dyes for detection of apoptosis in live cells. *Cytometry* **21,** 265–274 (1995).

344. Koopman, G., Reutelingsperger, C. & Kuijten, G. Annexin V for flow cytometric detection of phosphatidylserine expression on B cells undergoing apoptosis. *Blood* (1994).
345. Mosmann, T. Rapid colorimetric assay for cellular growth and survival: application to proliferation and cytotoxicity assays. *J. Immunol. Methods* (1983).
346. Aroian, R. & van der Goot, F. Pore-forming toxins and cellular non-immune defenses (CNIDs). *Curr. Opin. Microbiol.* **10,** 57–61 (2007).
347. Gurcel, L., Abrami, L., Girardin, S. & Tschopp, J. Caspase-1 activation of lipid metabolic pathways in response to bacterial pore-forming toxins promotes cell survival. *Cell* (2006).
348. Plantier, L. *et al.* Activation of sterol-response element-binding proteins (SREBP) in alveolar type II cells enhances lipogenesis causing pulmonary lipotoxicity. *J. Biol. Chem.* **287,** 10099–114 (2012).
349. Nelson, L., Johnson, A. & London, E. How Interaction of Perfringolysin O with Membranes Is Controlled by Sterol Structure, Lipid Structure, and Physiological Low pH INSIGHTS INTO THE ORIGIN OF. *J. Biol. Chem.* (2008).
350. Rottem, S., Cole, R., Habig, W. & Barile, M. Structural characteristics of tetanolysin and its binding to lipid vesicles. *J.* (1982).
351. Flanagan, J. J., Tweten, R. K., Johnson, A. E. & Heuck, A. P. Cholesterol Exposure at the Membrane Surface Is Necessary and Sufficient to Trigger Perfringolysin O Binding. *Biochemistry* **48,** 3977–3987 (2009).
352. Heuck, A., Hotze, E., Tweten, R. & Johnson, A. Mechanism of membrane insertion of a multimeric β-barrel protein: perfringolysin O creates a pore using ordered and coupled conformational changes. *Mol. Cell* (2000).
353. Shatursky, O. *et al.* The Mechanism of Membrane Insertion for a Cholesterol-Dependent Cytolysin. *Cell* **99,** 293–299 (1999).
354. Schonherr, R., Hilger, M., Broer, S., Benz, R. & Braun, V. Interaction of Serratia marcescens hemolysin (ShlA) with artificial and erythrocyte membranes. Demonstration of the formation of aqueous multistate channels. *Eur. J. Biochem.* **223,** 655–663 (1994).
355. Saka, H., Bidinost, C., Sola, C., Carranza, P. & Collino, C. Vibrio cholerae cytolysin is essential for high enterotoxicity and apoptosis induction produced by a cholera toxin gene-negative V. cholerae non-O1, non-O139 strain. *Microbial* (2008).
356. Mosser, E. M. & Rest, R. F. The Bacillus anthracis cholesterol-dependent cytolysin, Anthrolysin O, kills human neutrophils, monocytes and macrophages. *BMC Microbiol.* **6,** 56 (2006).
357. Haug, T. M. *et al.* Formation of Very Large Conductance Channels by Bacillus cereus Nhe in Vero and GH4 Cells Identifies NheA + B as the Inherent Pore-Forming Structure. *J. Membr. Biol.* **237,** 1–11 (2010).
358. Stenfors Arnesen, L. P., Fagerlund, A. & Granum, P. E. From soil to gut: *Bacillus cereus* and its food poisoning toxins. *FEMS Microbiol. Rev.* **32,** 579–606 (2008).
359. Pauchet, Y. *et al.* Effects of a mosquitocidal toxin on a mammalian epithelial cell line expressing its target receptor. *Cell. Microbiol.* **7,** 1335–1344 (2005).
360. Cooper, K. K. & Songer, J. G. Virulence of Clostridium perfringens in an experimental model of poultry necrotic enteritis. *Vet. Microbiol.* **142,** 323–328 (2010).
361. Lacroix-Lamande, S. *et al.* Downregulation of the Na/K-ATPase Pump by Leptospiral Glycolipoprotein Activates the NLRP3 Inflammasome. *J. Immunol.* **188,** 2805–2814 (2012).
362. Zhang, Y., Geng, Y., Yang, J., Guo, X. & Zhao, G. Cytotoxic activity and probable apoptotic effect of Sph2, a sphigomyelinase hemolysin from Leptospira interrogans strain Lai. *BMB Rep* (2008).
363. Lee, S. *et al.* Identification and partial characterization of a novel hemolysin from Leptospira interrogans serovar lai. *Gene* (2000).
364. Lee, S., Kim, S., Park, S. & Kim, M. Cytotoxic activities of Leptospira interrogans hemolysin SphH as a pore-forming protein on mammalian cells. *Infect. Immun.* (2002).
365. Misawa, T. *et al.* Microtubule-driven spatial arrangement of mitochondria promotes activation of the NLRP3 inflammasome. *Nat. Immunol.* **14,** 454–460 (2013).
366. Fiorentini, C., Falzano, L., Travaglione, S. & Fabbri, A. Hijacking Rho GTPases by protein toxins and apoptosis: molecular strategies of pathogenic bacteria. *Cell Death Differ.* **10,** 147–152 (2003).
367. Iliev, A. I. *et al.* Rapid microtubule bundling and stabilization by the *Streptococcus pneumoniae* neurotoxin pneumolysin in a cholesterol-dependent, non-lytic and Src-kinase dependent

manner inhibits intracellular trafficking. *Mol. Microbiol.* **71,** 461–477 (2009).
368. Cohen, S., Aizer, A., Shav-Tal, Y., Yanai, A. & Motro, B. Nek7 kinase accelerates microtubule dynamic instability. *Biochim. Biophys. Acta - Mol. Cell Res.* **1833,** 1104–1113 (2013).
369. O'Regan, L. & Fry, A. The Nek6 and Nek7 protein kinases are required for robust mitotic spindle formation and cytokinesis. *Mol. Cell. Biol.* (2009).
370. Chang, J., Baloh, R. & Milbrandt, J. The NIMA-family kinase Nek3 regulates microtubule acetylation in neurons. *J. Cell Sci.* (2009).
371. Iliev, A., Djannatian, J. & Nau, R. Cholesterol-dependent actin remodeling via RhoA and Rac1 activation by the Streptococcus pneumoniae toxin pneumolysin. *Proc.* (2007).
372. Chung, L., Park, Y., Zheng, Y., Brodsky, I. & Hearing, P. The Yersinia virulence factor YopM hijacks host kinases to inhibit type III effector-triggered activation of the pyrin inflammasome. *Cell Host Microbe* (2016).
373. Ratner, D., Orning, M., Proulx, M. & Wang, D. The Yersinia pestis Effector YopM Inhibits Pyrin Inflammasome Activation. *PLoS* (2016).
374. Park, Y., Wood, G., Kastner, D. & Chae, J. Pyrin inflammasome activation and RhoA signaling in the autoinflammatory diseases FMF and HIDS. *Nat. Immunol.* (2016).
375. Manukyan, G. & Aminov, R. Update on pyrin functions and mechanisms of familial Mediterranean fever. *Front. Microbiol.* (2016).
376. Aubert, D. *et al.* A Burkholderia type VI effector deamidates Rho GTPases to activate the pyrin inflammasome and trigger inflammation. *Cell host* (2016).
377. Dorfleutner, A. & Stehlik, C. A dRAStic RHOAdblock of Pyrin inflammasome activation. *Nat. Immunol.* (2016).
378. Eitel, J., Meixenberger, K., Laak, C. van & Orlovski, C. Rac1 regulates the NLRP3 inflammasome which mediates IL-1beta production in Chlamydophila pneumoniae infected human mononuclear cells. *PLoS One* (2012).
379. Conley, S., Abais-Battad, J., Yuan, X. & Zhang, Q. Contribution of guanine nucleotide exchange factor Vav2 to NLRP3 inflammasome activation in mouse podocytes during hyperhomocysteinemia. *Free Radic. Biol.* (2017).
380. Kim, H. *et al.* Filamin A is required for vimentin-mediated cell adhesion and spreading. *Am. J. Physiol. Cell Physiol.* **298,** C221-36 (2010).
381. Kim, H. *et al.* Regulation of cell adhesion to collagen via β1 integrins is dependent on interactions of filamin A with vimentin and protein kinase C epsilon. *Exp. Cell Res.* **316,** 1829–1844 (2010).
382. Bhattacharya, R. *et al.* Recruitment of vimentin to the cell surface by 3 integrin and plectin mediates adhesion strength. *J. Cell Sci.* **122,** 1390–1400 (2009).
383. Pittet, J.-F. *et al.* HMGB1 Accelerates Alveolar Epithelial Repair via an IL- 1b-and avb6 Integrin-dependent Activation of TGF-b1. (2013). doi:10.1371/journal.pone.0063907
384. Rogel, M. R. *et al.* Vimentin is sufficient and required for wound repair and remodeling in alveolar epithelial cells. *FASEB J.* **25,** 3873–83 (2011).
385. Szymanski, K., Toennies, M. & Becher, A. Streptococcus pneumoniae-induced regulation of cyclooxygenase-2 in human lung tissue. *European* (2012).
386. Schmeck, B., Zahlten, J., Moog, K. & Laak, V. Van. Streptococcus pneumoniae-induced p38 MAPK-dependent phosphorylation of RelA at the interleukin-8 promotor. *J. Biol.* (2004).
387. Seybold, J. *et al.* Tumor necrosis factor-α-dependent expression of phosphodiesterase 2: Role in endothelial hyperpermeability. *Blood* (2005). doi:10.1182/blood-2004-07-2729
388. I.H. Heijink, S.M. Brandenburg, D.S. Postma, and A. J. M. van O. Cigarette smoke impairs airway epithelial barrier function and cell–cell contact recovery. *Eur Respir J* 419–428 (2012).
389. Reimand, J., Arak, T., Adler, P. & Kolberg, L. g: Profiler—a web server for functional interpretation of gene lists (2016 update). *Nucleic acids* (2016).
390. Caporaso, J. G. *et al.* QIIME allows analysis of high-throughput community sequencing data. *Nat. Methods* **7,** 335–6 (2010).
391. Schloss, P. D. *et al.* Introducing mothur: Open-source, platform-independent, community-supported software for describing and comparing microbial communities. *Appl. Environ. Microbiol.* (2009). doi:10.1128/AEM.01541-09
392. Gregory Caporaso, J. *et al.* QIIME allows analysis of high-throughput community sequencing data. *Nat. Publ. Gr.* **7,** (2010).